UNIVERSITY OF PADOVA
FACULTY OF ENGINEERING
Department of Management and Engineering
Doctoral School in Mechatronics and Product Innovation Engineering
Cycle XXXII

EVOLUTION OF CONDITION MONITORING FROM IN-LINE MAINTENANCE TO INDUSTRIAL DESIGN

A dissertation submitted in partial fulfillment of the requirements for the degree of Doctor of Philosophy in Mechatronics and Product Innovation Engineering

Prof. Giovanni Antonio Longo, Chair of the School
Prof. Daria Battini, Course Coordinator
Prof. Aldo Rossi, Candidate's Supervisor

Ph.D. Candidate: ALBERTO CHIARELLO

November 26, 2019

Ai miei genitori,
alla mia famiglia
ed ai nuovi arrivati.

Sempre caro mi fu quest'ermo colle,
E questa siepe, che da tanta parte
Dell'ultimo orizzonte il guardo esclude.
Ma sedendo e mirando, interminati
Spazi di là da quella, e sovrumani
Silenzi, e profondissima quïete
Io nel pensier mi fingo, ove per poco
Il cor non si spaura. E come il vento
Odo stormir tra queste piante, io quello
Infinito silenzio a questa voce
Vo comparando: e mi sovvien l'eterno,
E le morte stagioni, e la presente
E viva, e il suon di lei. Così tra questa
Immensità s'annega il pensier mio:
E il naufragar m'è dolce in questo mare.

— G. Leopardi, "L'Infinito"

ABSTRACT

In these years the concept of Industry 4.0 has acquired an important role in industrial development, proposing solutions to support all business areas. This paradigm revolutionises the concept of automation, planning and optimisation, proposing intelligent systems based on information extracted from data coming from innumerable sources.
In this context, condition monitoring has emerged as an innovative approach to reliability and maintenance.

This research aims to expand the common definition of condition monitoring as it limits the potential that this approach can offer, demonstrating with practical examples the possibility of exploiting these concepts for the study of processes, the design innovation and the quality control. The proposed solutions and the results obtained will be presented in this work, showing how their integration can influence multiple application levels.

Initially the implementation of the monitoring system for an industrial process will be illustrated, showing how the data obtained would allow a more detailed interpretation of the operation of the mechanical system and of the events that occurred.

In the field of automatic machines, condition monitoring is used almost exclusively for applications that exhibit rotational motions at constant speed. During this work, it will be described how similar techniques are more generally applicable to stochastic cyclostationary processes, demonstrating their effectiveness during the study of the degradation of a component.

The potential of condition monitoring can also be used for product innovation, as it was possible to demonstrate even during the study conducted to compare a new component model with that already present in industrial solutions.

Finally, the development of new technologies has also been included in the fields of application for which it is possible to implement the condition monitoring approach. In the study related to this proposal, it will be shown how this approach can interface with different types of data, including those coming from vision systems, becoming part of the functional systems of the process and integrating with quality control.

Keywords: Industry 4.0, condition monitoring, reliability, maintenance, data acquisition, data analysis, design innovation, filling machines, test rigs

SOMMARIO

In questi anni il concetto di Industria 4.0 ha acquisito un ruolo importante nello sviluppo industriale, proponendo soluzioni a supporto di tutte le aree di business. Questo paradigma rivoluziona il concetto di automazione, pianificazione ed ottimizzazione, proponendo sistemi intelligenti basati sulle informazioni estrapolate da dati provenienti da innumerevoli fonti.
In questo contesto, è emerso il monitoraggio delle condizioni come un approccio innovativo all'affidabilità e alla manutenzione.

Questa ricerca mira ad espandere la comune definizione di monitoraggio delle condizioni in quanto limitante rispetto al potenziale offerto da questo approccio, dimostrando con esempi pratici la possibilità di impiegare questi concetti per lo studio di processi, per l'innovazione progettuale e per il controllo qualità. Le soluzioni proposte ed i risultati ottenuti saranno presentati, dimostrando come la loro integrazione possa influenzare diversi livelli applicativi.

Inizialmente verrà riportata l'implementazione del sistema di monitoraggio di un processo industriale, mostrando come i dati ottenuti consentissero un'interpretazione più dettagliata del funzionamento del sistema meccanico e degli eventi che si venivano a verificare.

Nel campo delle macchine automatiche, il monitoraggio delle condizioni viene quasi esclusivamente impiegato in applicazioni caratterizzate da moti rotazionali a velocità costante. Durante questo lavoro verrà descritto come tecniche simili siano applicabili più generalmente a processi stocastici ciclostazionari, dimostrandone l'efficacia nello studio del degrado di un componente.

Il potenziale del monitoraggio delle condizioni può essere impiegato anche nell'innovazione di prodotto, come è stato possibile dimostrare durante lo studio condotto al fine di confrontare un nuovo modello di componente con quello già previsto industrialmente.

Infine, anche lo sviluppo di nuove tecnologie è stato incluso tra gli ambiti applicativi del monitoraggio delle condizioni. Nello studio relativo a tale proposta verrà mostrato come questo approccio possa interfacciarsi con diversi tipi di dati, inclusi quelli provenienti dai sistemi di visione, entrando a far parte dei sistemi funzionali del processo ed integrandosi con il controllo qualità.

ACKNOWLEDGMENTS

Undertaking the Ph.D. was one of the most important opportunities I have ever received. The possibility to dedicate my time to what I am passionate about, with the possibility to continuously study and mature new knowledge is a privilege that not everyone can have. I am lucky to have had the opportunity to dedicate myself to research and at the same time to have had the opportunity to spend time in the industrial reality. From this experience I learned the importance of technological development and the need to continue to invest our resources in the research for new solutions, without limiting ourselves to what is already known. These years have been significant for me at training level, but they have been valued above all by the people involved.

The research presented in this thesis was conducted jointly at The Department of Management and Engineering (DTG) of the University of Padua (Italy) and at the company Ecor International S.p.A. (Schio, Italy), and partially, at the company Tetra Pak (Lund, Sweden). In each of these sites I had the pleasure of meeting people who offered their contribution to achieve the results reported in this thesis.
First of all, I want to thank my supervisor, Prof. Aldo Rossi, for guiding me during these three years and for always giving me valuable professional and personal advice. Furthermore, I am deeply grateful to Prof. Daria Battini, who coordinates the doctoral school in Mechatronics and Product Innovation Engineering.
This Ph.D. work would not have been possible without the scholarship funded by Ecor International S.p.A., and specifically without the contribution of the Eng. Nicola Pozzan. I want to thank all the employees of the company who have contributed in some way to the research work, and above all Giovanni Bao, 'master of automation' and example of practicality and determination.
I cannot fail to express my gratitude to Dr. Marco Montanari who made the experience at Tetra Pak possible. During that time I received excellent lessons both in terms of business dynamics and in terms of relationships. I met new cultures and people, including Eng. Anna Harder, who was not only the manager of the project I took part in but also a friend who welcomed me and made me feel at home.
I would like to thank all the Ph.D. candidates at the DTG department and in particular my colleagues Eng. Matteo Bottin and Eng. Nicola Comand with whom I had the honour of being part of the Mechatronics research group.

Finally, thanks to all the people who once again believed in me and never let me miss their support. Thanks to my friends who have always given me the opportunity to spend hours of fun with them. Thanks to my sister Valentina, Luca and the new family member we are all eager to meet. The biggest thanks goes to my Mum and my Dad, my biggest fans, those who taught me to be the person I am, the ones who gave me the strength to take this journey, those who have always advised me in important decisions and which allowed me to be free to choose. This thesis is also yours.

CONTENTS

1 INTRODUCTION

Maintenance costs are a major part of the total operating costs of all manufacturing or production plants. Depending on the specific industry, maintenance costs can represent between 15% and 60% of the cost of goods produced. [1]
This awareness and the introduction of new technology in Industry 4.0 paradigm represent the starting point for the implementation of new maintenance method such as condition monitoring.

The main features of Industry 4.0 and the main maintenance techniques are presented in the following paragraphs.

1.1 INDUSTRY 4.0

In the current competitive economic context, the concept of Industry 4.0 has acquired a primary role in industrial progress.
The 'Industrial 4.0' concept appeared first in an article published by German government in 2011 as a proposal for the development of a new economic policy based on high-tech strategies for 2020. In April 2013, the term 'Industry 4.0' appeared again during the Hannover Messe, and in recent years it has become a hotspot for global industry.
The German government strategy points to help industrial manufacturing maintain competitiveness against the labor-cost advantages of developing countries, encouraging industries to upgrade with high-tech solutions. [2]

After the help of water and steam power during the First Industrial Revolution, the electrical energy in the Second Industrial Revolution and the electronic and information technologies used to automate production during the Third Industrial Revolution, today manufacturing is driven by service innovation. [3]
The concept that combine cyber-physical systems (CPS), the Internet of things (IoT) and the Internet of services (IoS), has launched the factories into a new era: the Fourth Industrial Revolution.
Industry 4.0 implies profound changes to the industrial ecosystems with new architectures and new business processes that conditions also the enterprise organisation. Three necessary integration features are required [4]:

- *Horizontal integration*: integration of the network of different factories and between the IT systems implemented to manage logistics, production and marketing within the company.
- *Vertical integration*: integration of the various IT systems at the different hierarchical levels (e.g. actuator and sensor level, manufacturing and execution level, production management level, corporate planning levels) to deliver an end-to-end solution.
- *End-to-end digital integration*: integration throughout the engineering process across the products value chain and across different companies.

In order to achieve these goals, eight planning objectives must be developed [5]:

- *Standardisation and reference architecture*: a set of common standards to allow the connection and the integration of the network between different factories.
- *Managing complex systems*: appropriate plans and explanatory models need to be developed to optimise the management of smart factories.
- *Delivering a comprehensive broadband infrastructure*: development of a reliable, comprehensive and high-quality communication network on a massive scale.
- *Safety and security*: it should be ensured that production facilities and products themselves do not pose a danger either to people or to the environment, while preventing products misuse or unauthorised access.
- *Work organisation and design*: with content, processes, and changes in the environment, making higher demands on production management, to achieve humane, automation, green production and management.
- *Training and continuing professional development*: companies have the responsibility and obligation to train their employees to enable lifelong learning and help workers cope with new demands from the jobs and skills.
- *Regulatory framework*: mutual adaptation of new innovations with existing legislation to protect enterprise data, handle personal data and manage liability and trade restrictions.
- *Resource productivity and efficiency*: new materials, new process and new technologies can improve resource efficiency and reduce the environmental impact caused by pollution and destruction.

Due to the importance of these subjects and the innovation required, there has been a growing demand for research related to Industry 4.0 in order to provide insights into the issues, challenges, and solutions related to the design, implementation and management of this paradigm.[6]

In manufacturing companies Industry 4.0 applies data science and analytical models to analyse real-time data from multiple machines and processes; this allows to automate the production accordingly with the acquired information. So far, various industries have applied IoT and industrial IoT (IIoT) to advance production, maintenance, distribution and service. [7]

Following the trend of Industry 4.0, the automation of the different production processes has triggered the use of intelligent condition monitoring systems. Automatic data exchange and analysis offers the opportunity to further optimise production processes, improving their productivity, reliability and system availability.[8]
Thanks to the use of CPS, in fact, it is possible to obtain information that indicates the conditions and the stability or instability of processes and components, allowing the implementation of advanced monitoring methods.[9]
The integration of these approaches in manufacturing companies with large amounts of data from production processes can be further used in predictive maintenance or fault prediction.[10]

1.2 MAINTENANCE TECHNIQUES

In EN 13306:2017 'maintenance' is defined as the *combination of all technical, administrative and managerial actions during the life cycle of an item intended to retain it in, or restore it to, a state in which it can perform the required function*. [11]
Companies perceive maintenance differently, according to the driven-core of the maintenance management program:

- *Total productive maintenance (TPM)*: it is not properly a maintenance management program. TPM seeks to engage all levels and functions in an organisation to maximise the overall equipment effectiveness (*OEE*). [12]

- *Reliability-centred maintenance (RCM)*: it is based on the concept that every item on a piece of complex equipment has a right age at which complete overhaul is necessary to ensure safety and operating reliability. The reliability is a function of system design, and the goal of maintenance is to achieve and preserve that inherent level of reliability over the operational life of the system. [13, 14]

- *Time-based maintenance (TBM)*: maintenance decisions are determined based on the expected lifetime of the equipment estimated from failure time data or used-based data. [15]
- *Condition-based maintenance (CBM)*: it is a maintenance program driven by the equipment information collected through condition monitoring.[16]

Maintenance strategies can be classified into three basic types:

- Corrective maintenance;
- Preventive maintenance;
- Predictive maintenance.

1.2.1 *Corrective maintenance*

Corrective maintenance, also known as reactive maintenance, is the least advanced technique and it's performed to restore equipment to proper operational condition after a breakdown. The idea is to identify, isolate and rectify the fault with emergency corrections.
This maintenance could fall under two categories: planned or unplanned. In the first case, the maintenance is the result of a run-to-failure plan, so the equipment will be serviced when it breaks down. The second case is usually the effect of an unexpected breakdown and can cause high cost due to sudden downtime, backlog and the possible request for replacement material in a short time.
Despite its limitations, corrective maintenance is the most widespread in manufacturing.

1.2.2 *Preventive maintenance*

Emergency corrections related to corrective maintenance can be reduced with a preventive maintenance approach. This maintenance strategy is designed to maintain a certain level of reliability and availability by providing for scheduled inspection or recurring tasks. For these reasons preventive maintenance could be considered both a TBM program and a RCM program. The time-driven aspect of this maintenance program is based on the so-called bathtub curve (Figure 1) that represents the failure rate during the equipment lifetime.
Preventive maintenance contributes to prevent unscheduled downtime and premature equipment damage that require corrective maintenance.
In terms of complexity, this maintenance program falls between corrective maintenance and predictive maintenance.

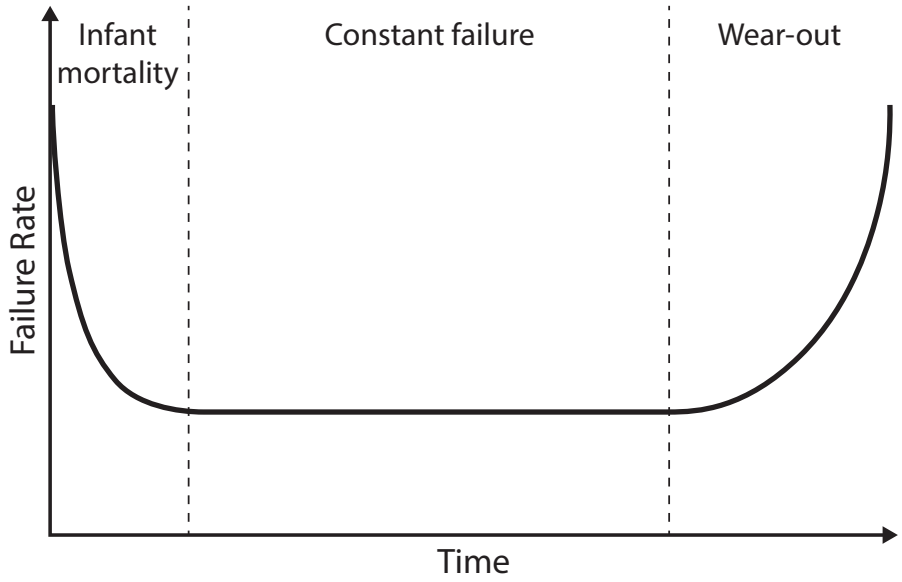

Figure 1: The bathtub curve represents the failure rate along the life time of the equipment. Three main parts can be identified: the *infant mortality* indicates that a component or a machine has a high probability of failure in the initial period of operation (i.e. due to installation problems), the *constant failure* zone (the useful life period) is characterised by a low failure rate due to random failures and after this the *wear-out* period shows an increasing failure rate due to the age and the wear of the product.

1.2.3 *Predictive maintenance*

Predictive maintenance overcome the paradigm of preventive maintenance, using the actual operating condition of plant equipment and system to predict when a failure might occur, allowing to plan maintenance operations. It is a clear example of a CBM program. Ideally, predictive maintenance allows to optimise machine availability, minimising the maintenance frequency and preventing unplanned corrective maintenance, without the costs due to the implementation of too severe preventive maintenance.

In preventive or corrective programs, repair or rebuild tasks must be scheduled based on the personal experience of the maintenance team. Instead, predictive maintenance is a condition-driven maintenance program that does not rely on equipment average-life statistics to schedule maintenance activities, preferring direct monitoring of the mechanical condition, system efficiency, and other indicators to determine the actual mean-time-to-failure or loss of efficiency. [1]
It is easy to understand how, in the context of Industry 4.0, preventive maintenance shows a growing relevance and a significant evolution over the last decade. The increasing digitalisation of all manufacturing processes is resulting in the recording of an increasing amount

of data by sensors used for control functions. With proper analysis, this information permits to define the status of the machines in order to identify the changes that warn of the development of a fault. Therefore, condition monitoring results in a natural integration in manufacturing processes with the aim to increase the reliability and the efficiency in production operation, acting on:

- Decrement of unplanned downtimes;
- Decrement of maintenance labour costs;
- Increment of machine availability and process reliability;
- Improvement of work safety.

The preventive maintenance could be applied not only on a single component or machine but could be extended to an entire manufacturing system, up to the whole production chain.
To apply this approach the status of each machine has a relevant role. This knowledge allows to optimise the working condition of the mechanical systems, their tasks and the maintenance operations. The introduction of CPS will facilitate the spread of these approaches, making the machines able to communicate with each other, decentralising the control systems and optimising the production. [17]

For these reasons condition monitoring is proposed as a fundamental integration of Industry 4.0.

1.3 BIG DATA

The implementation of the Industry 4.0 paradigm and the preventive maintenance program necessarily require to deal with a large amount of data. As the installed CPS increase, the amount of recorded data grows very quickly, resulting in new problems related to storage space and the extrapolation of information. The so-called *Big Data* is the result of the amalgamation of all the data collected from different sources such as PLC and DAQs systems. [18]
Not all acquired data contain significant information, or their relevance can be significant only in relation to other parameters: data mining and the correlation between the information are necessarily delegated to appropriate algorithms able to manage the massive collections to simplify their interpretation.
In modern industries, one of the most significant fields in which Big Data is involved is condition monitoring. Multiple sensors acquired real-time data for long-time operation of the machines, but they are generally not analysed as quickly as they are collected. The study of new methods to extract the characteristics from Big Data and the correlation with the corresponding health conditions has become a felt

topic in recent years. [19]
Condition monitoring, being related to the maintenance field and therefore to industrial processes and machines with a hopefully very long operating life, is closely linked to the continuous acquisition of information for long periods, requiring to extract specific features from large data collections.

Big data management is considered one of the most complex activities in the context of condition monitoring. As the structure and behaviour of production systems are getting more and more complex, the volume of machine operating data increases significantly, making it difficult even for highly experienced operators to respond to a fault timely and accurately.[8]
For these reasons, the proper management, storage and analysis of data appears to be a fundamental point in the implementation of condition monitoring systems. The centralisation of data in specific platforms, in fact, allows at any time to find information of interest, keeping track of the events that have occurred. It is clear that the possibility of analysing historical data is a significant incentive for industrial innovation, allowing continuous improvement in monitoring techniques and maintenance scheduling.

1.4 RESEARCH FIELD

In recent years the fervent industrial interest in condition monitoring has considerably influenced the research, which has proposed some frameworks for the standardisation of this paradigm and new methods of monitoring and data mining for different applications. In all these areas the condition monitoring has been exclusively evaluated as a predictive maintenance strategy, strictly following the common definition of this approach.
The research reported in this dissertation, instead, aims to expand the concept of condition monitoring, demonstrating how the implementation of these monitoring systems allows to increase the know-how on processes and components, to guide product design and innovation and to extract useful information for multiple business areas.
During this study, it was also possible to expand the scope of applicability of the typical techniques of condition monitoring, which in most cases found in the literature refer to applications characterised by rotational motions at constant speed.

In order to demonstrate the effectiveness of the proposed solutions, this Ph.D. research covered various applications typical of the food and packaging industry, thanks above all to the collaboration with the company that funded the project, Ecor International S.p.A., which designs and produces components and test rigs for the most important

companies in the sector, often carrying out internally commissioned test campaigns.
To provide a greater offer to customers and, at the same time, increase company know-how, Ecor International S.p.A. has invested in solutions for Industry 4.0 and in particular in the implementation of systems for the reliability of filling machines.

The economic development of many countries has also influenced global food and packaging business reaching multi-trillion dollars. This justifies the recent advancement in food processing and packaging, which is not just about satisfying production demand, but also the adoption of sophisticated automation and control and monitoring methods and technologies. [20]
In today's world of global markets and stiff competition, end-users of filling machines demand ever-higher process efficiencies, reducing costs and shortening times. [21]
In conjunction with the growing interest in technologies related to Industry 4.0 [22, 23], this business appeared appropriate for the development of condition monitoring solutions that allow to minimise maintenance costs and downtime.

1.5 OVERVIEW OF THE DISSERTATION

This dissertation aims to expand the concept of condition monitoring, often limited to mere use in the area of reliability and maintenance. In fact, in industrial realities, the study that precedes and follows the implementation of a monitoring system can lead to several collateral advantages:

- Increased knowledge of processes and components;
- Improvement of the design and development of processes and products;
- Comparison between competing solutions;
- Active correction of monitored processes;
- Quality control.

In order to demonstrate the potential offered by condition monitoring, the research was structured to satisfy requests of industrial interest, thus offering practical solutions.
The collaboration with the company Ecor International S.p.A. led to the implementation of the condition monitoring program on some test rigs and equipment typically used in the packaging and food industry.

New monitoring models have been proposed, developing theoretical and practical concepts partly already reported in the literature but never applied in the context of the food and packaging industry and/or never used for the type of study considered. A higher level of generalisation will allow the same approaches to be adapted in contexts that are very different from those studied.

In the following pages are reported some of the case studies considered. For each of these are highlighted some aspects of particular interest, such as:

- Acquisition system;
- Data analysis;
- Conclusions and deliverables.

In the first condition monitoring implementation, the object of study is a test rig designed to assess the degradation of some knives used in the packaging industry. This project is divided in two main parts:

1. *Chapter 2*: study of the cutting process and implementation of an acquisition system to monitor the process and the components conditions;
2. *Chapter 3*: to overcome the limits of the previous approach, an alternative study with a vibrational approach is proposed to assess the degradation level of the knife.

Chapter 4 presents the study conducted to compare a new rolling bearing model, which did not require periodic greasing operations, with that already used in the industrial applications. Also in this case, the vibrational behaviour was particularly relevant for the purposes of the study. Finally, in *Chapter 5*, it is shown how condition monitoring can be used in the development of a new product, becoming part of the process control functionality. This study conducted at the company Tetra Pak (Sweden), extrapolated the information from the acquisitions of a vision system, with the aim of obtaining a correct alignment of the graphic elements during the digital printing process. It will also be reported how the frames contained interesting information also for the quality control of the incoming packaging material. Conclusions and future developments are presented in *Chapter 6*.

Concurrently with the implementation of the condition monitoring systems, some platforms for data management and visualisation were tested: this investigation is summarised in *Appendix A*.

The research was developed with reference to the different phases of industrial design, starting from the monitoring of the events of

a typical industrial process, passing through the study of the critical components and the parameters related to their functionality and degradation, finally proposing a method of investigation of the performance and error correction in the development phase of a new production process. The study was initially aimed at investigating the most classic aspects of condition monitoring as a diagnostic tool, to highlight later its contribution to the design and functional field of industrial plants.

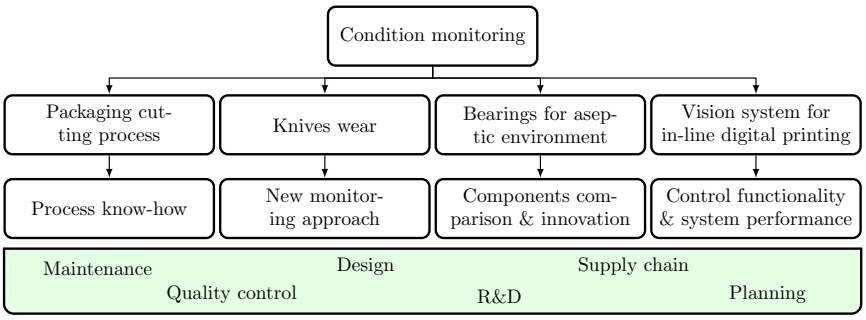

Figure 2: The condition monitoring systems implemented during this research provided information to several business areas.

2

CONDITION MONITORING FOR PACKAGING CUTTING PROCESS

This chapter presents a first approach to the condition monitoring paradigm related to a typical process of the packaging industry. In the following paragraphs, the industrial process under study is described, therefore the activities related to its emulation in the test rig, the modelling of the phenomenon, the acquisition system and the collected information are presented. At the end, the results and deliverables are reported.

2.1 PACKAGING CUTTING PROCESS

The packaging industry is characterised by the filling machines that allow to form the packaging material around the products. In many applications, the packaging material flows in a continuous stream and the packages are separated only downstream of the machine. A schematisation of the packaging process is shown in Figure 3.

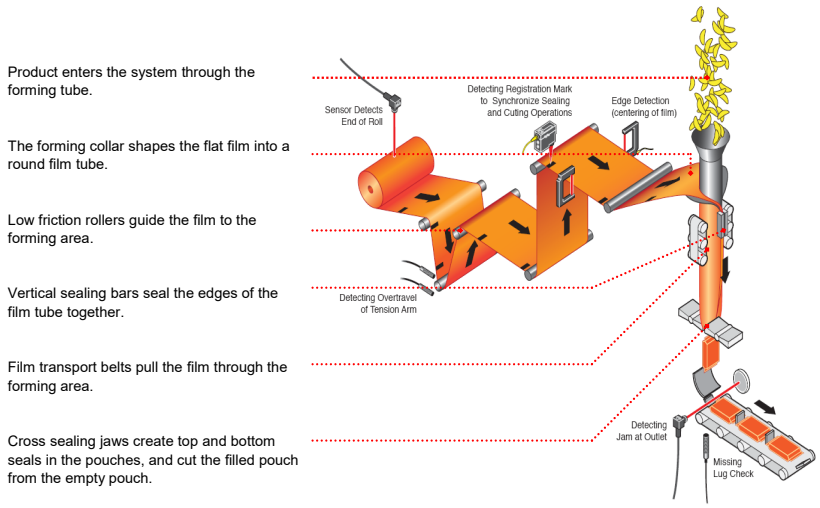

Figure 3: Schematisation of the typical packaging process in the filling machine. [24]

The most sensitive part of the process is the making of the cross seals as the package is filled with the product, closed and cut.
The cutting process has a significant influence on the sealing of the packages, thus on the packaging material integrity. In fact, the degradation of the components involved is due mainly to the accumulation of product and packaging residues left by the cutting process and the mechanical interaction with the cutting tools.

Figure 4: Residues accumulation on sealing jaws. [25]

Also the environment in which these operations are performed plays an important role. For example, in the food industry, the packaging material and all the mechanical components that interact with it and with the product must guarantee a high level of asepticity. To achieve this request, vaporised hydrogen peroxide (H_2O_2) is sprayed to sterilise the mechanical component. The chemical and thermal action cause an additional degradation effect on the mechanical components.
The humidity in the chamber where the described operations are performed, increases the adhesion to the components of the residual material of the cutting process, progressively reducing the quality of the sealing and cutting.
For perishable products, a package with a compromised seal can lead to a reduction in shelf-life, a decrease in product quality and an increased contamination risk.
It is easy to understand how the monitoring of the cutting process can play a primary role in ensuring the correct operation of the machine, reducing maintenance operations and preserving the quality of the packaging and the product.

2.1.1 *Sealing and cutting station*

The sealing and cutting station is located under the forming tube and has to perform 3 different tasks:

1. Clamping the packaging material;
2. Sealing the package;
3. Separate consecutive packages by performing the cut.

The first two tasks are usually demanded to the sealing jaws and the third to some cutting tools normally shaped as knives. The dual

functionality assigned to the jaws stems from the need to combine the separation of the packages with the sealing, in order to reduce the time required by these operations. For this reason the knife is integrated inside one of the sealing jaws as shown in Figure 5.

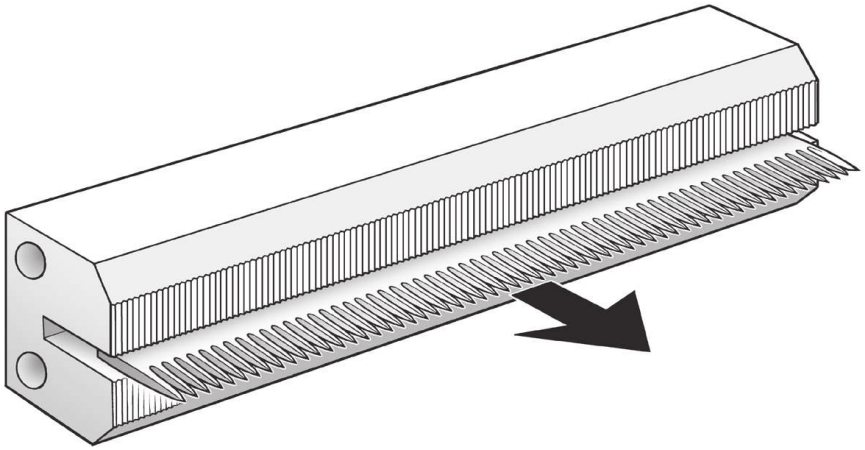

Figure 5: To perform the sealing and cutting operation, the knife moves inside the sealing jaws. [26]

The jaws and the knife are actuated by cams or by pneumatic or hydraulic cylinders. The first solution is typically applied to machines with greater production capacity, while the latter in machines with greater flexibility.

Sealing jaws

In each sealing unit, there are two pair of sealing jaws: one pair seals the top seam of the filled package, while the other pair seals the bottom of the following package.
Nowadays various technological solutions for sealing are proposed, which differ for the physical principle used. The choice is often dictated by the composition of the packaging material.
The most common solutions are:

- *Heat sealing*: used to melt the thermoplastic material that seals the package.
- *Induction sealing*: used for packaging material with aluminium foil coated with thermoplastic adhesive substance. The magnetic field induces eddy current, which generate a localised heat in the adhesive material that melts. [27]
- *Ultrasonic sealing*: mechanical vibration is converted to thermal energy due to molecular friction. When enough heat is generated the thermoplastic material melts and the package is sealed. [28]

- *Pressure sealing*: it is a cold sealing technique used in applications with heat-sensitive products such as in the chocolate industry. [29]

Knives

The knives used in the filling machines differ in geometry and material. Depending on the packaging material, these components have a different design. Sometimes the blade is flat, but is usually machined to obtain teeth with specific angles and pitch to easily penetrate the material.
Knife longevity is an important aspect to keep in mind when choosing it. For this reason the selection of the correct material is essential. The most commonly used are:

- *AISI 440 B and C*: it has good corrosion resistance and for this reason this steel is mainly used in the food industry and in wet applications.
- *AISI 420*: it is a martensitic stainless steel that can be hardened by heat treatment.
- *D-2*: it is not a stainless steel, but the high content of chromium gives it greater corrosion resistance. It has a high wear resistance that increments the life expectancy of the blade.
- *M-2*: it is more wear-resistant than D-2, but this steel oxidises easily.
- *Solid carbide*: this group of steels has a high level of wear resistance that allows a long working life for the tools.

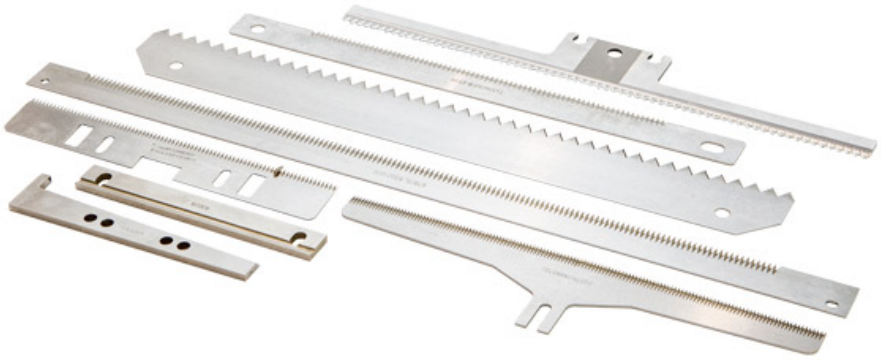

Figure 6: Some models of knives used in filling machines. [30]

Aseptic packaging

In the food industry, the packaging process has to guarantee the asepticity of the packaging material and the preservation of the operational conditions to prevent microbial contamination of the product.

Aseptic packaging involves the filling and sealing of microbiologically stable product into sterilised containers. In the filling machines the packaging material is sterilised and each component in contact with the product and/or the containers is subjected to periodic washing cycles.
The use of the sterilants in the food industry is regulated by the Food and Drug Administration (FDA) and the European Food Safety Authority (EFSA) in the USA and Europe respectively.
In the filling machines various methods for the sterilisation of packaging materials are used. Table 1 reports a comparison between the most common.

2.2 TEST RIG

The focus of this research was mainly related to the cutting process of the packaging material. Thanks to a test rig commissioned by an important supplier of filling machines to Ecor International S.p.A., it was possible to collect information on the cutting process. This test rig, designed to emulate the blade degradation of the knives used in the final phase of the packaging process, had most of the features of a filling machine for the food industry. The main phases were:

- Unwinding of packaging material;
- Sealing and forming of the tube;
- Cutting of the packaging material;
- Rewinding of the packaging material.

The only differences with real machines were the filling of the product and the management of the outgoing material due to logistical reasons of the test campaigns.
The reference machine was designed to fill and form packages for the food industry with specific formats and materials and with well-defined cycle times.
During their working life, the knives perform millions of cutting cycles that would have involved very long and expensive test campaigns to replicate their degradation. To overcome this problem, accelerated tests were required leading to some influences on the test rig design. To collect a greater amount of data 7 parallel cutting stations were mounted in a single chamber with a controlled environment.

2.2.1 *Packaging material*

The packaging material used for the test was the same as that used by the customers on their machines. As shown in Figure 7, it is a material with six layers with the following order from outside to inside:

Table 1: Methods for sterilising aseptic packages. [31]

Methods	Application	Advantages/Disadvantages
Superheated steam	Metal containers	High temperature at atmospheric pressure. Microorganisms are more resistant than in saturated steam.
Dry hot air	Metal or composite juice and beverage containers	High temperature at atmospheric pressure. Microorganisms are more resistant than in saturated steam.
Hot hydrogen peroxide	Plastic containers, laminated foil	Fast and efficient method.
Hydrogen peroxide/UV light combination	Plastic containers (pre-formed cartons)	UV increases effectiveness of hydrogen peroxide.
Ethylene oxide	Glass and plastic containers	Cannot be used where chlorides are present or where residuals would remain.
Heat from co-extrusion process	Plastic containers	No chemicals used.
Radiation	Heat-sensitive plastic containers	Can be used to sterilise heat-sensitive packaging materials. Expensive. Problems with location of radiation source.

1. *Polyethylene*: protection against outside moisture.
2. *Paperboard*: stability and strength.
3. *Polyethylene*: adhesion layers.
4. *Aluminium foil*: barrier for oxygen, light and flavour.
5. *Polyethylene*: adhesion layers.
6. *Polyethylene*: sealing for the contents.

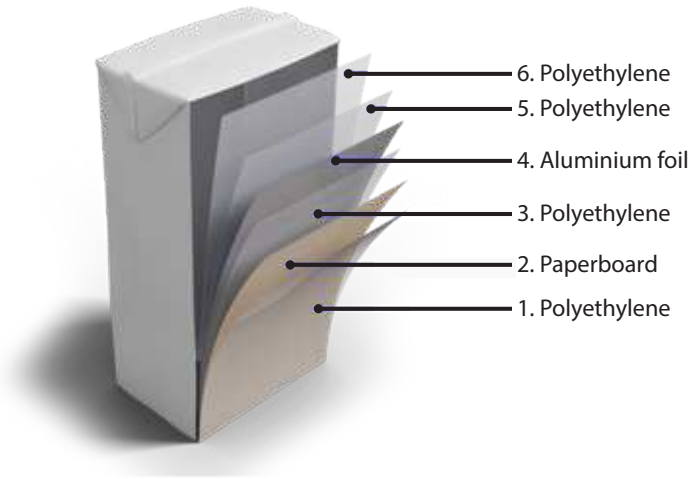

Figure 7: An exploded view of the layers that compose the packaging material.

2.2.2 *Cutting station*

The actuation of the jaws and the knife in the reference machine was performed by a cam profile which guarantees the synchronism between all the mechanical elements. In that case, in fact, the sealing and the cutting processes were integrated in a module that also allows the folding of the edges for outgoing packages.
The test rig was focused on the cutting process, therefore the folding operations were neglected, and the mechanism was synthesised as shown in Figure 8.

For the actuation of the jaws, two hydraulic cylinders were provided, and another one is designed for the knife. A hydraulic control units allowed to regulate the pressure in the actuator chambers.
The proposed design allowed a great flexibility of the test as different models of knife and working parameters could be set.

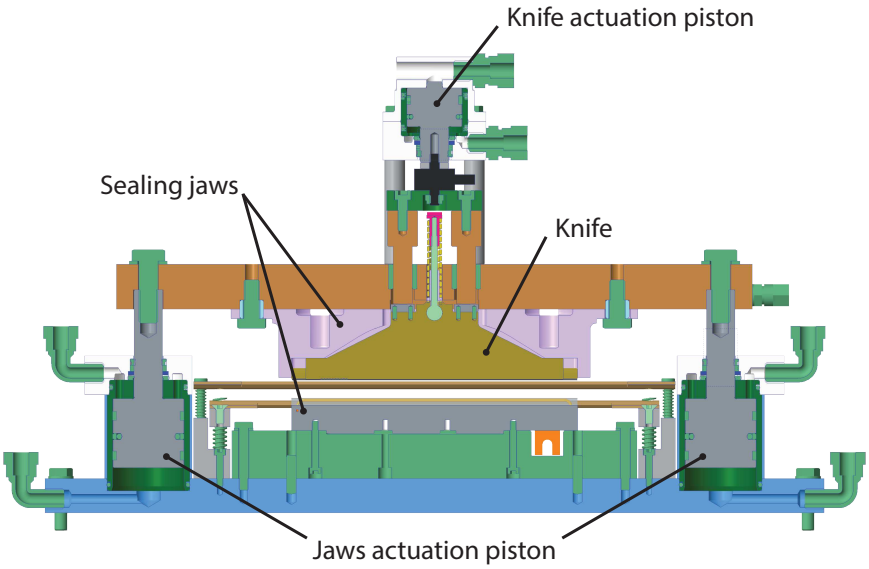

Figure 8: A section view of the cutting station designed for the test rig.

2.2.3 *Sealing jaws*

For the test rig the provided sealing jaws were based on the induction sealing. This solution was feasible thanks to the aluminium foil in the packaging material.
In Figure 9 the jaws appear different in shape and size due to their characteristic functionality. The upper jaw shows a recess to allow the housing of the knife in its resting position. Instead, the lower jaw presents the inductor to seal the packages.
The actuation of the two jaws allowed to clamp the packaging material during the cut. The clamping force was defined around 18 kN in order to accomplish the correct pressure distribution over the transversal seal so as to get a good quality seal.

2.2.4 *Knives*

The test rig was designed to test the models of knives that had a specific fastening system and with very similar dimensions and geometry. The main differences were related to the material and the manufacturing process. Some knives were machined from a single piece of martensitic stainless steel, others had a coated steel body and the blade in a cobalt-chromium alloys designed for wear resistance.
The knife was assembled with a link that connected and preloaded the return spring. This solution allowed to keep the tool in its resting position during the clamping phase of the jaws, and its return after the cut was performed. In the test rig also the hydraulic pressure contributed to speed up the latter phase in order to carry out accelerated test campaigns.

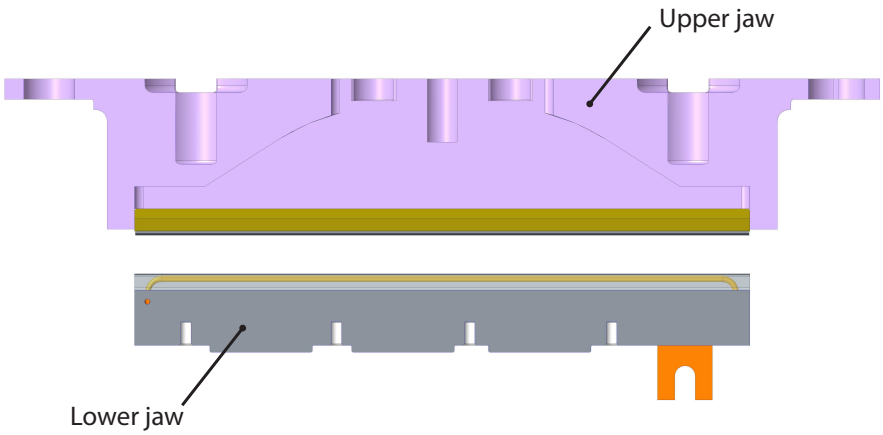

Figure 9: A section view of the jaws used for the test rig.

In order to allow a continuous stream of the packaging material and subsequent rewinding, the knives used in the test rig were machined to obtain two notches on the blade. With this solution the packages were not cut across their entire width, leaving two strips that gave enough stiffness to not tear the material when pulled.

2.2.5 *Environmental factors*

During the definition of the main characteristics of the test rig also the degradation due to the environmental factors was taken into consideration. In the filling machines of the customer, the web of packaging material was sterilised and the components were cleaned with automatic washing cycles during machine operation.
The main sterilising agent used in these machines was the hot hydrogen peroxide. The combination of the chemical vapours and heat had an additional degradation effect on the components under test. For this reason a kit to generate vaporised hydrogen peroxide was connected to the test rig in order to reproduce the environmental conditions that the real word machine presented.
Besides, to simulate the particularly aggressive chemical action of some food products, saline solutions were included in the sprayed flow.
The generated humidity led to a greater accumulation of residues produced by the cutting process of the packaging material. This progressively reduced the efficiency of sealing and package separation.

2.2.6 *Test rig parameters*

The test rig replicated the main operations performed by the reference machine with an accelerated cycle time.
After the longitudinal sealing of the packaging material the tube was stored in a magazine. Some motorised rollers pulled the packaging material through the chamber in which the cross sealing and the cutting processes were performed. When the buffer was empty the tube forming started to refill the magazine. A similar approach is used also in the real machines in order to compensate for any different speed between motors and processes.
For testing purposes, the packaging material was pulled with short indexing movements. This was to reduce the downtimes related to the movement of the tube compared to that of sealing and cutting. Furthermore this solution allowed a reduction in the consumption of packaging material during the test, performing numerous close cuts.
The proposed solution was closely related to the design choices. A schematisation is shown in Figure 10.

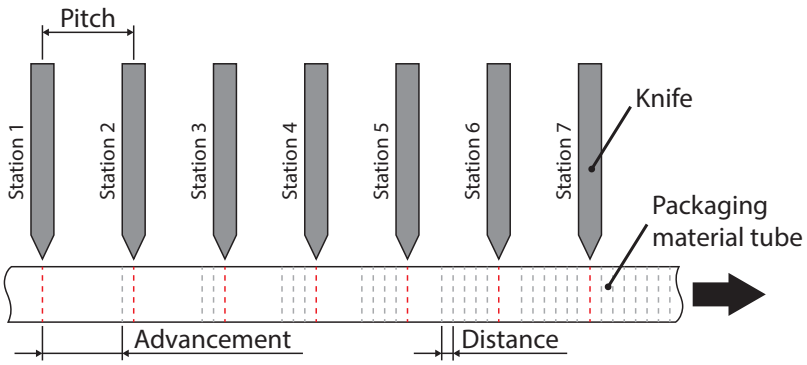

Figure 10: The pitch between the cutting stations determined the advancement length and the cuts distance.

The pitch p of the n cutting stations was the parameter that defined the advancement a of the packaging tube to obtain cuts at a regular distance d. These relationships are shown in the following equations:

$$\begin{aligned} a &= p \cdot \frac{n}{n+1} \\ d &= \frac{p}{n+1} \end{aligned} \tag{1}$$

To easily distinguish the cuts performed by the specific knife at the test rig output, an extra step in the advancement was taken in consideration in order to increase the gap g (otherwise equal to d) between consecutive series of a value equal to s as shown in Figure 11.

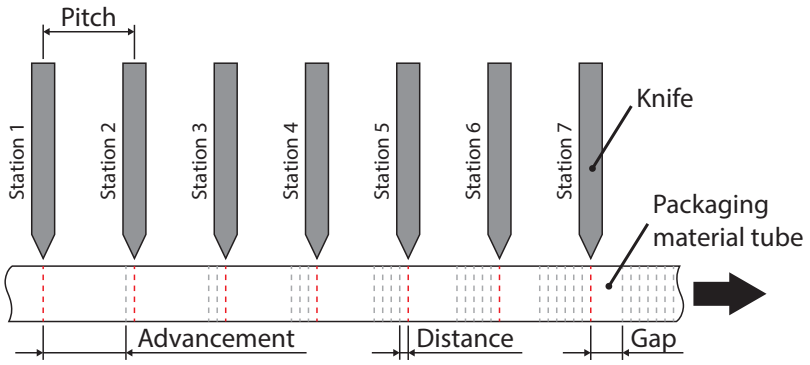

Figure 11: Among the series of cuts a gap was considered on the outgoing packaging material to easily relate the cut with the station.

Equations 1 became:

$$a = \frac{n \cdot p + s}{n + 1}$$
$$d = \frac{p - s}{n + 1} \tag{2}$$

and the gap was therefore calculable as:

$$g = d + s \tag{3}$$

For each station, the sealing jaws and the knife were actuated by some cylinders that shared the hydraulic circuits. The valves commands were common for each station, so the movements of the clamps were synchronous as were the cuts.
The minimum cycle time for the sealing and cutting stations on the reference machines with the highest productivity was around 900 ms. In the test rig these operations were performed every 800 ms. The sequence of the two signals is shown in Figure 12.

The actuation of the jaws remained high for 450 ms. The knife movement was triggered after 200 ms from the rising edge of the clamping signal and remained high for 250 ms to ensure the execution of the cut. Both signals had the falling edge at the same instant.
The signal activation durations were evaluated in order to ensure that the clamping and cutting conditions were reached as required by the technical specification.

All the parameters used for the test rig design and its operations are listed in Table 2.

It is important to compare the cutting frequency between the reference machine and the test rig. For the first, two knives alternated their movement, each performing a cycle every 900 ms at maximum productivity. In the test rig, 7 cuts were performed every 800 ms.

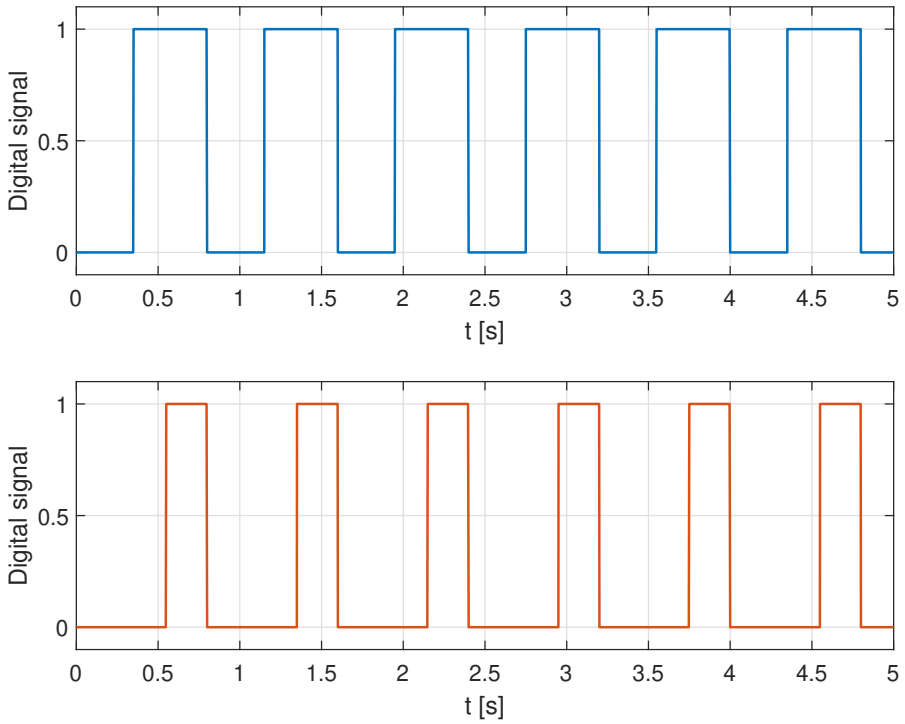

Figure 12: The digital signals that triggered the clamping of the jaws (blue) and the cut (orange).

For every hour of machine operation, 8000 cycles were performed, whereas in the test rig 31500 cycles: the test was therefore accelerated 4 times.
It is also important to underline the savings in packaging material obtained with the test rig. Under normal operating conditions, the real machine consumed about 1500 m/h of material, instead the test rig only 382.5 m/h. The material consumption reported to the number of cuts was 187.5 mm/cut for the machine and only 12.1 mm/cut for the test rig, with a saving of over 93%.

2.3 DATA ACQUISITION

To study the cutting process many parameters were acquired and monitored in order to apply the condition monitoring approach. The design of the data acquisition system was of primary importance for the project. In this phase specific choices were made for 3 main fields:

1. Signals;
2. Sensors;
3. Data acquisition system.

Table 2: Main parameters of the test rig.

Parameter	Value	Unit
No. of station	7	
Stations pitch	96	mm
Gap between sets of cuts	19	mm
Advancement	85	mm
Cuts distance	11	mm
Cycle time	800	ms
Clamping activation time	450	ms
Cut activation time	200	ms
Material consumption	382.5	m/h

2.3.1 *Signals*

The first step was the choice of the significant parameters to monitor. In reference to the operation of the rig already described pressure, force and temperature appeared as the most significant quantities to be measured.
Table 3 shows the complete list of the acquired parameters.
As a first attempt, a lot of data was acquired in order to collect all the possible information about the cutting system.

2.3.2 *Sensors*

For each of the previously listed parameters, an appropriate sensor was chosen, in reference to the accuracy and the measuring range required, as summarised in Table 4.

2.3.3 *Data acquisition system*

To be able to read with an appropriate resolution the signals of the test rig, the required data acquisition had to guarantee high performances. In fact, to obtain some features of the parameters such as maximum and minimum values, the signals had to be sampled at a sufficient high frequency. This requirement could not be met by the equipment normally used in the industrial field.
The most suitable solution was offered by the hardware produced by National Instruments (NI). This choice was related not only to the performance of the products but also to the possibility of integrating many different modules in order to manage all the signals type in a single system. Furthermore, NI offered the software environment to configure the acquisition and create algorithms suitable for data man-

Table 3: Parameters acquired on the test rig.

Parameter	Unit	Signal type	Description
Knife forces	N	Analog	For each station, between the knife and the relative cylinder a load cell was insert to measure the force applied to the tool during the cutting process.
Knife cylinders pressures	bar	Analog	For each cylinder used to actuate the relative knife, the oil pressure was monitored.
Knife cylinders counterpressure	bar	Analog	Each knife actuator was connected to a manifold that fed the counterpressure acting on the pistons to speed up the return phase.
Jaws cylinders pressure	bar	Analog	Each jaws actuator was connected to a manifold that fed the pressure acting on the pistons to clamp the packaging material.
Jaws cylinders counterpressure	bar	Analog	Each jaws actuator was connected to a manifold that fed the counterpressure acting on the pistons to push the jaws back.
Knives valve command	1/0	Digital	The command signal to control the valve that regulate the hydraulic actuation of the knives.
Jaws valve command	1/0	Digital	The command signal to control the valve that regulate the hydraulic actuation of the jaws.
Oil temperature	°C	Analog	The temperature of the oil in the hydraulic circuit.

Table 4: Sensors used in the test rig. [32, 33, 34]

Sensor name	Sensor type	Accuracy	Measuring range	Output signal	Parameter
Burster 8431-6005	Load cell	±0.2% FS	0...5 kN	2 mV/V	Knife forces
Trafag 8252.85.2517	Pressure transmitter	±0.5% FS	0...160 bar	0...10 VDC	Hydraulic pressures
Pentronic 6101000	Thermocouple Type K	±1.5 °C	−270...1200 °C	0...10 VDC	Oil temperature

agement.
Some of the proposed devices were also integrated in an architecture that NI realised for condition monitoring applications called NI InsightCM™(Appendix A).

The DAQ system consisted of a controller and some modules described in detail below.

Controller

The controller that was chosen was a NI cRIO-9068. This product is part of the CompactRIO systems that are characterised by a processor and a user-programmable FPGA. They are used as chassis in which several compatible modules can be connected.
The FPGA chip allows to execute truly parallel process, so different processing operations do not have to complete to access the same resources. As a result, the performance of one part of the application is not affected by the others. [35]
The architecture of this product allowed to develop an embedded system with high performance and flexibility in order to manage a big amount of data from different types of sensors. These features were necessary to meet the project specifications. In fact the 20 channels were sampled at high frequency up to 25 kHz and 5 s of all channels were periodically logged. Therefore, each file was a collection of about 2.5 million points in double precision. The optimisation of the code to manage the limited resources of the FPGA was fundamental to allow a continuous operation of the controller for the whole test campaign.
To give maximum flexibility to the acquisition system an 8-slot chassis was chosen so that further modules in addition to those already provided could be connected.
The main characteristics of the NI cRIO-9068 are listed in Table 5.

Table 5: Main characteristics of the controller NI cRIO-9068. [35]

No. of slots	8
Processor	ARM Cortex A9
	667 MHz Dual-Core
FPGA	Xilinx Zynq 7020
Memory	1 GB
RAM	512 MB

Modules

NI offers many modules, each of which can be connected to a specific type of sensor. For the considered test rig two models of modules were taken into consideration:

1. *NI-9237*: it contains all the signal conditioning required to power and measure up to four bridge-based sensors simultaneously, so it was used to read the strain gauge load cell signals.

2. *NI-9220*: it is an analog voltage input module that was used to read the pressure transmitter signals. For convenience, also the digital control signals of the valves were read in voltage after being generated by the PLC of the test rig.

Their characteristics are reported in Table 6.

Table 6: Main characteristics of the modules (a) NI-9237 and (b) NI-9220. [35]

Signal	Bridge analog input
No. of channels	4
Sample rate	50 kS/s/ch
Resolution	24 bits
Connectivity	RJ-50

(a)

Signal	±10 V Voltage analog input
No. of channels	16 differential
Sample rate	100 kS/s/ch
Resolution	16 bits
Connectivity	Spring terminal

(b)

Both modules had a sampling frequency not limited by the number of sampled channels, in fact the sampling frequency was correlated to the single channel. The use of no-multiplexed modules allowed, if necessary, to connect additional sensors, in order to acquire other information, without affecting the performance of the entire acquisition system.

To satisfy the chosen sensor configuration, the acquisition system was composed of a NI cRIO-9068, two NI-9237 and a NI-9220.

Before the test campaigns started, the possible curves of the parameters that would have been acquired were studied. To do this it was necessary to create a model that emulated the cutting process as described for the test rig. The results made it possible to investigate the real curves more easily, and the comparison also allowed to validate and optimise the model for subsequent studies and evolutions of the test rig.

The significant event to be simulated was the cutting process, so the movement of the jaws was neglected.
To simplify the proposed model, the effect of the packaging material was not taken into consideration in this first attempt.

The model was created using the graphical programming environment Simulink, whose block diagram is shown in Figure 13.

In the block diagram, it is possible to recognise the model of the hydraulic system with the digital command that actuates the valve. The cutting station was synthesised in a classic mass-spring-damper mechanical system. The force applied by the hydraulic cylinder caused a specific dynamics that was used to calculate the force generated.
To take account of the preload of the return spring, an additional force component was introduced in case the piston movement had begun.

The elastic constant k of the return spring was measured testing some samples. The results are reported in Table 7.

Table 7: Measurements of the elastic constant of the return springs.

Spring	k [kN/m]				Mean [kN/m]
1	29.76	32.79	33.90	33.33	32.45
2	37.45	32.57	33.33	32.36	33.93
3	36.23	32.05	34.72	34.01	34.25
Mean					33.54

The value that was chosen for the model was 33.5 [kN/m].
The obtained force curve is shown in Figure 14.

Some tests without the packaging material were performed before the start of the test campaign. These allowed to compare the proposed model with the real force curves acquired on the test rig, as shown in Figure 15.

The curves look similar in the shape, in particular for 3 main phases:

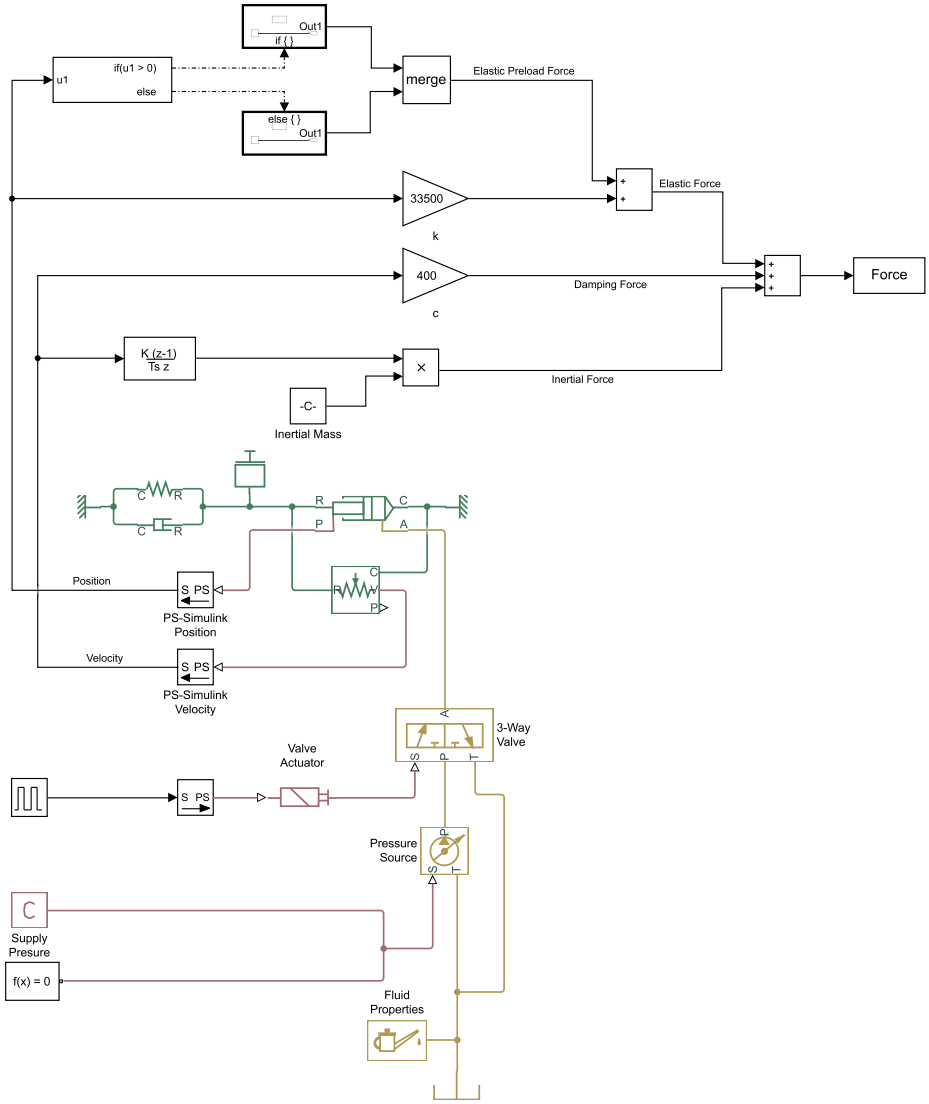

Figure 13: The block diagram of the simplified model made to simulate the cutting process.

1. Initial peak;
2. Force plateau;
3. Return phase.

The model allowed to investigate the contribution of each force component on the final curve. In fact, the initial peak can be attributed to the damping force mainly due to the hydraulic cylinder at the end of its stroke.
In the rising edge, a slight change in the slope of the force curve can be noticed, mainly in the acquired signal. This is related to the preload of the return spring, in fact before the dynamic system can be moved, the force generated by the hydraulic cylinder had to prevail

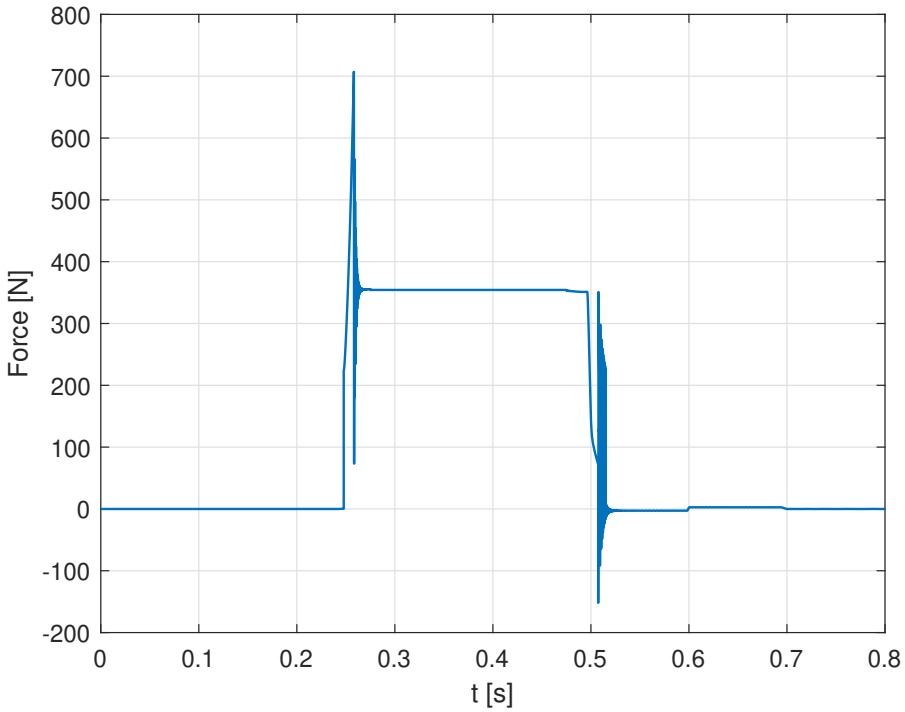

Figure 14: The force curve obtained from the simplified model of the cutting process.

on that resistance force (Figure 16). In the acquired curve this value appeared a bit higher, but this was related to the variability of the elastic constant and the manual preload of the return spring during the assembly operation.

The plateau represented the resting position of the piston at the maximum stroke, thus the force was completely related to the elastic component generated by the return spring.

The greatest difference could be noticed on the value of the plateau force and on the return phase. In both cases the differences were attributed to the mechanical behaviour of the system: the not ideal alignments between the components provoked some interferences and a higher resistance to movement. In the case of the plateau, this caused an early stop of the components downstream of the load cell, which measured a higher force than the ideal case due to the greater compression of the return spring.

The force fluctuations at the beginning of the forward and return movements were synchronised with what was obtained from the simulation with ideal conditions, so the piston did not appear to be influenced by significant friction effects.

On the other hand, the downstream components shown slowdowns that involved a different response on the force curve especially for the return phase.

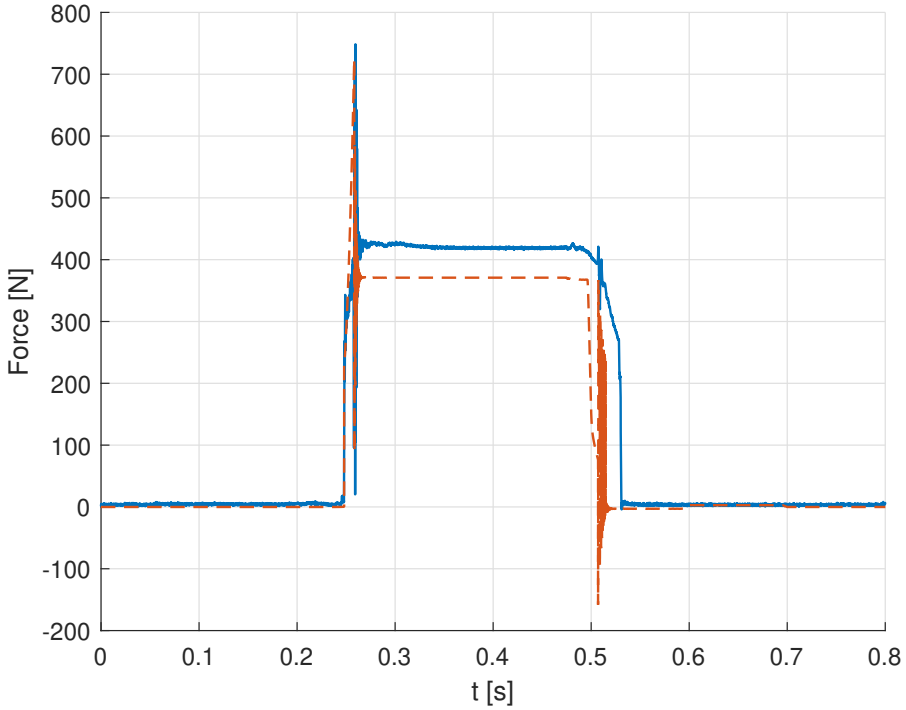

Figure 15: Comparison between the curve of the force acquired (solid) and that obtained by the simplified model of the cutting process (dashed).

2.5 ACQUISITIONS

A large amount of files and signals were acquired during the test campaign, and thanks to their investigation a lot of information about the cutting process was obtained.
In the following paragraphs, the curves of the most significant signals of the cutting process are reported.

2.5.1 *Force curve*

Undoubtedly the signal that contained more information was the force acquired by the load cell mounted between the piston and the shafts that pushed the knife.
Several tests were conducted in order to distinguish the different contributions that constituted the curve. To do that some tasks of the cutting process were suppressed during the acquisition.

1. Without packaging material
    a) Only jaws actuation;
    b) Only knife actuation;
    c) Jaws and knife actuation.
2. With packaging material

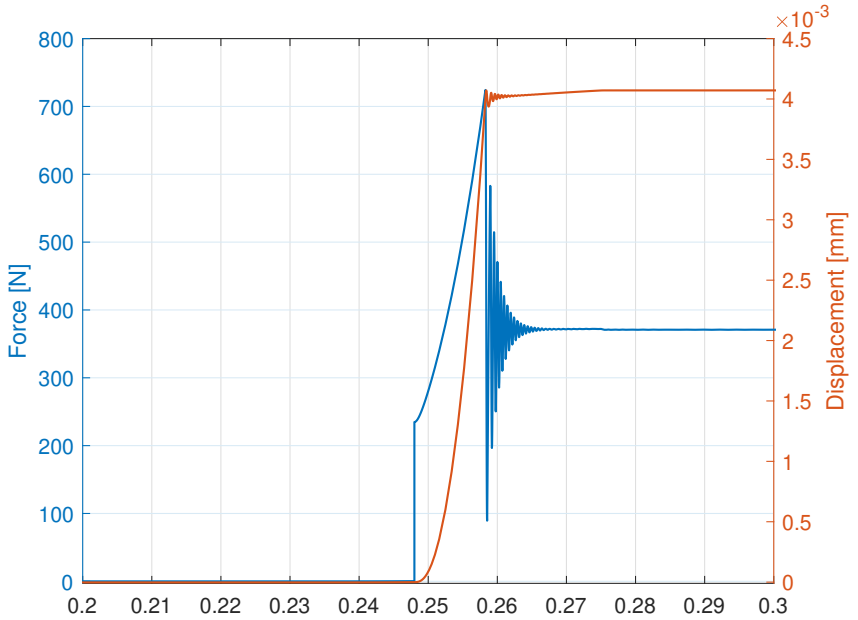

Figure 16: The movement of the dynamic system began only after the preload of the return spring was passed. In the force curve this point could be identify thank to the change of slope.

a) Only jaws actuation;

b) Jaws and knife actuation.

In the following paragraphs the curves of each test are reported, with a time interval in the abscissa axis of 800 ms to show a complete period of the test rig cycle, starting with the rising edge of the jaws actuation signal as in Figure 17.

Without packaging material

These first tests were conducted without the packaging material to focus attention on the other components of the system and to understand the influence of this material after comparison with the tests that included it.

ONLY JAWS ACTUATION This test was realised to understand how the movement of the jaws and the clamp action were perceived by the load cell. The curve is shown in Figure 18.

The signal acquired by the load cell presented some force fluctuations due to the inertial effects of the components connected with the sensor.
Some significant fluctuations were acquired after the jaws activation signal was turned off at 0.450 s. These were related to the beginning and the end of the return movement of the jaws.
The load cell perceived the contribution of force of the jaws through the movement of the components downstream of it. In fact, the sensor measured the impact of the floating part (knife and connection

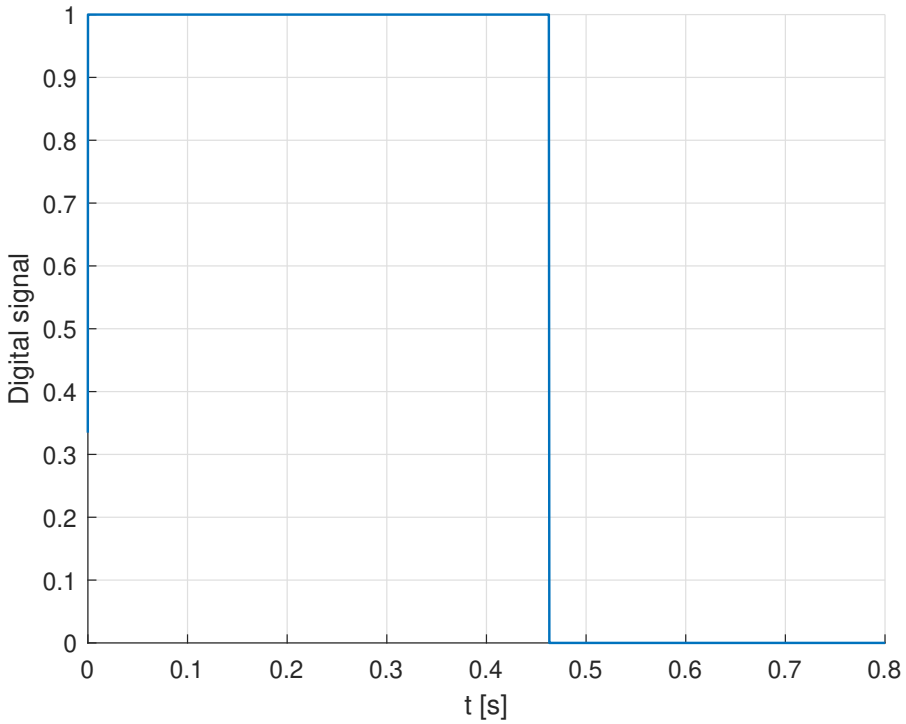

Figure 17: The jaws actuation signal for a single test rig cycle.

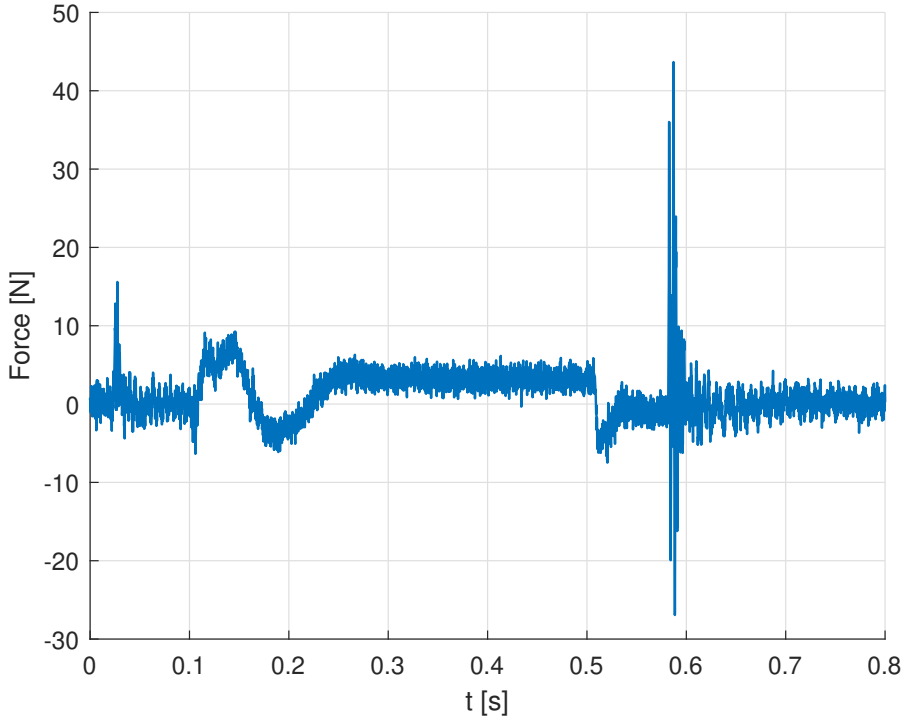

Figure 18: The force acquired by the load cell with the only actuation of the jaws and without packaging material.

components) with respect to the fixed part (knife actuation piston).

ONLY KNIFE ACTUATION The actuation of the knife without the action of the clamps, allowed to understand the effects of the inertial forces of the moving components and the elastic force generated by the compression of the return spring. This test was conducted with the jaws open so the knife was in contact with the only jaw that housed it and not with the other.
The acquisition is shown in Figure 19.

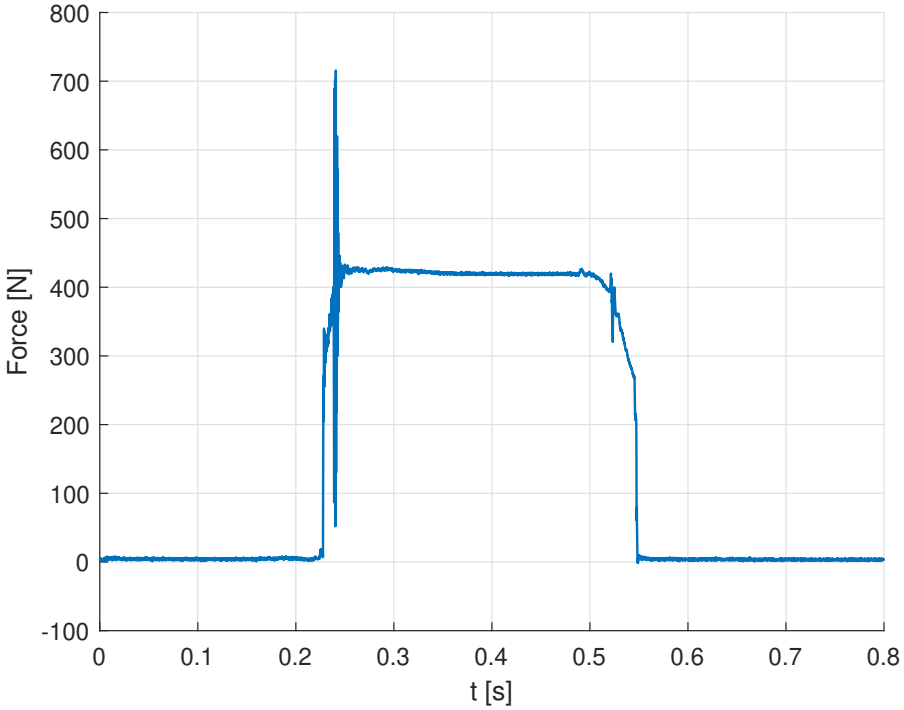

Figure 19: The force acquired by the load cell with the only actuation of the knife and without packaging material.

This test was also used to evaluate the reliability of the results obtained from the model discussed in the Section 2.4 which simulated only the movement of the cutting system without considering further effects such as the friction between the components and the resistance of the packaging material.
As previously discussed this curve showed the force of the return spring when it was compressed by the piston that actuated the knife. In correspondence of the preload value of the spring, it was possible to notice a change in the slope of the curve in the forward and backward movement phases.

JAWS AND KNIFE ACTUATION This test was useful for assessing whether the force perceived by the sensor was a linear combination of the contributions of the jaws actuation and the knife actuation. The result is shown in Figure 20.

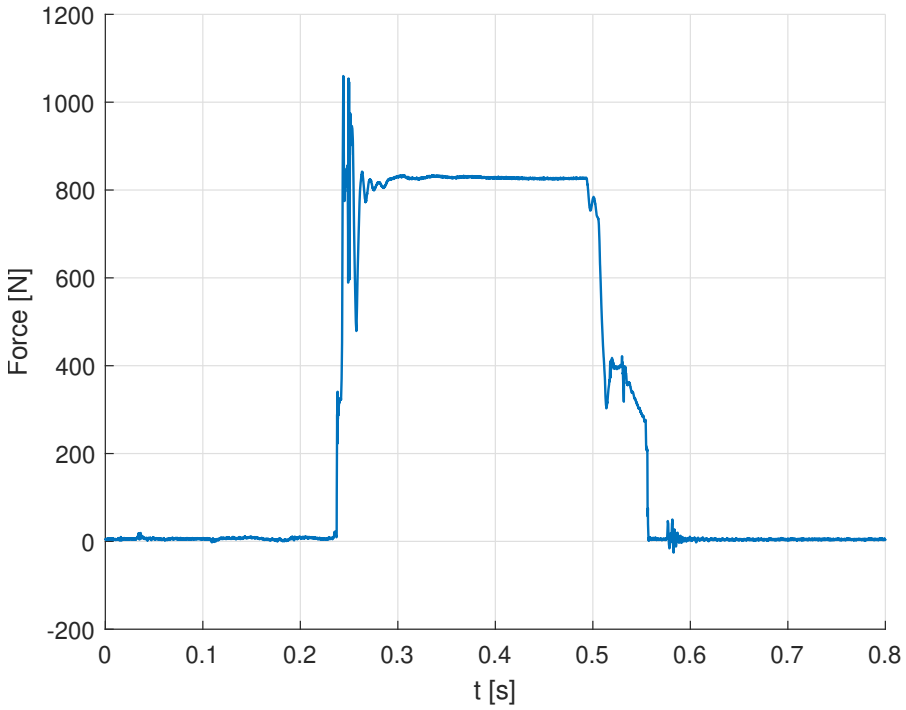

Figure 20: The force acquired by the load cell with the actuation of both the jaws and the knife, without packaging material.

The main peaks of the clamp action shown in Figure 18 can be found also in this curve.
The knife contribution, instead, appears quite similar in shape to that shown in Figure 19, but rather different in magnitude. This was a first evidence of the contact and the friction between the knife and the front jaw due to mechanical misalignment. In fact, in the return phase a rapid decrement of the force can be noticed, related to the exit of the knife from that jaw, and subsequently its adjustment to the curve found in the previous test. Although the actuation signals of the knife and jaws were simultaneously disabled, the exit phase was mainly influenced by the movement of the jaws that left the clamp position, in fact the knife had a greater delay in the return phase due to the response of the hydraulic system. This can be seen by comparing the force curves of previous tests with the current ones. In Figure 18 at about 0.5 s, some instant after the jaws signal was turned off, it was possible to notice a negative fluctuation of the force that represented the beginning of the movement of the jaws. The same feature can be seen also in the current test at the end of the rapid decrement of the force before the curve continues with the trend shown in the second test.
The same force fluctuation found in Figure 19 due to the return of the piston of the knife can be noticed in the second part of the backward phase of the current test. A few moments after the load cell was unloaded, another series of force fluctuations due to the contribution of

the jaws was found, consistently with what was found in the first test.

With packaging material

As already mentioned, the comparison between the tests already presented and the following ones allowed to evaluate the influence of the packaging material on the force curve.
The test with the only actuation of the knife was not considered since it would not have added any value to the investigation. In fact, the stroke of the piston was too short to allow the knife to come into contact with the packaging material in the case of non-actuated jaws.
The last test reported corresponds to the standard operating condition for the cutting stations.

ONLY JAWS ACTUATION The force curve obtained by the only actuation of the jaws is shown in Figure 21.

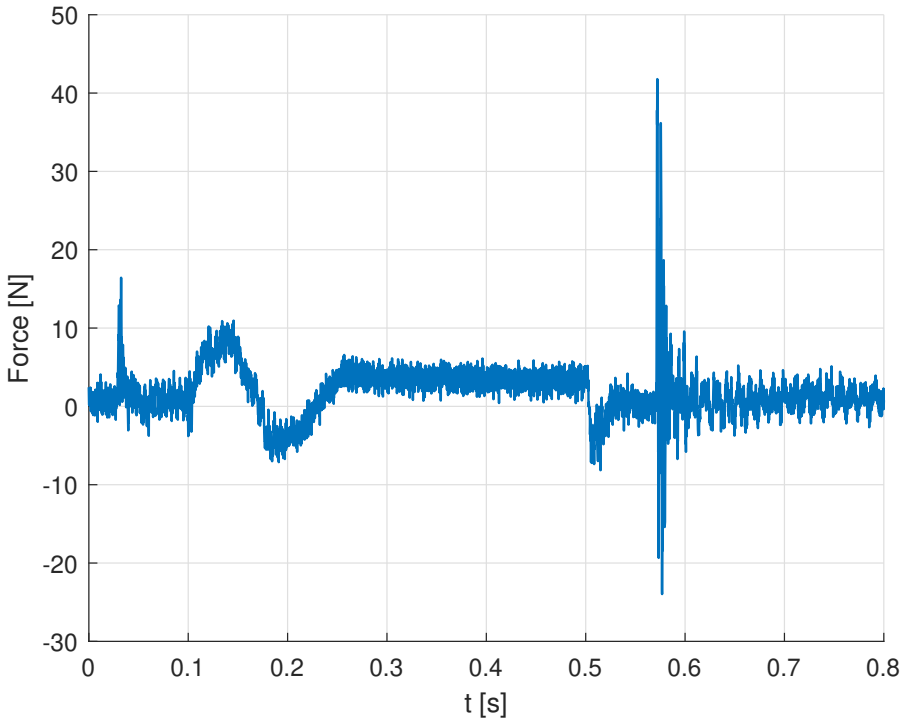

Figure 21: The force acquired by the load cell with the only actuation of the jaws and with the packaging material.

The curve appeared completely comparable with that obtained in the test without the packaging material. This means that the clamp was not significantly damped by the presence of the material between the jaws.

JAWS AND KNIFE ACTUATION Finally, the curve resulting from the standard configuration of the cutting station is shown in Figure 22.

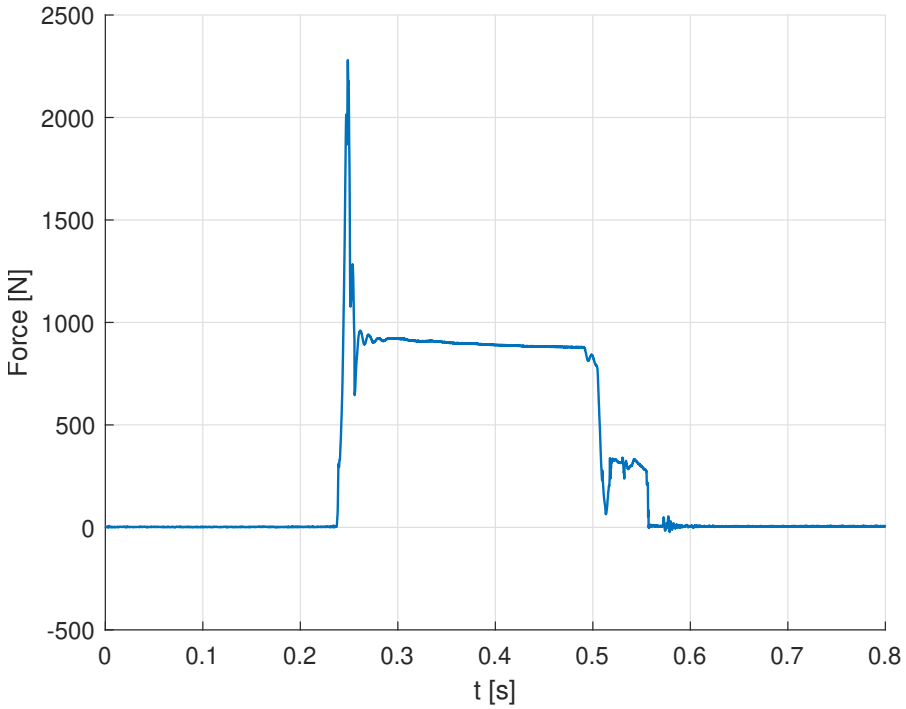

Figure 22: The force acquired by the load cell with the actuation of both the jaws and the knife, with the packaging material.

In this test, all the main features of the previous tests can be found, such as the force contribution of both the jaws and the knife.
The main characteristics of this curve can be highlighted by comparing them with those obtained for the test without the packaging material. It is easy to notice how the initial and the middle phase of the curve present higher values in reference to the other test.
With normal operating conditions the initial peak reached 2.3 kN due not only to the inertia of the components but mainly to the cutting of the packaging material. Focusing on this section (Figure 23) it is possible to notice distinctive peaks indicative of the cut of the first and second sheet of the packaging material.

The different magnitude of the two peaks was related to the stiffness of the sheets. In fact the first sheet required more force to be cut not only because it was supported by the stiffness of the rear one, but also because of the overlap at the longitudinal seam (Figure 24). After the cutting interface was created, it was easier to continue the operation. Thanks to this and to the lower resistance of the material, the successive sheet required less force to be cut. The difference between the two peaks was around 1000 N.
Comparing the peak values between the test with and the test without the packaging material it was evaluated that to perform the first

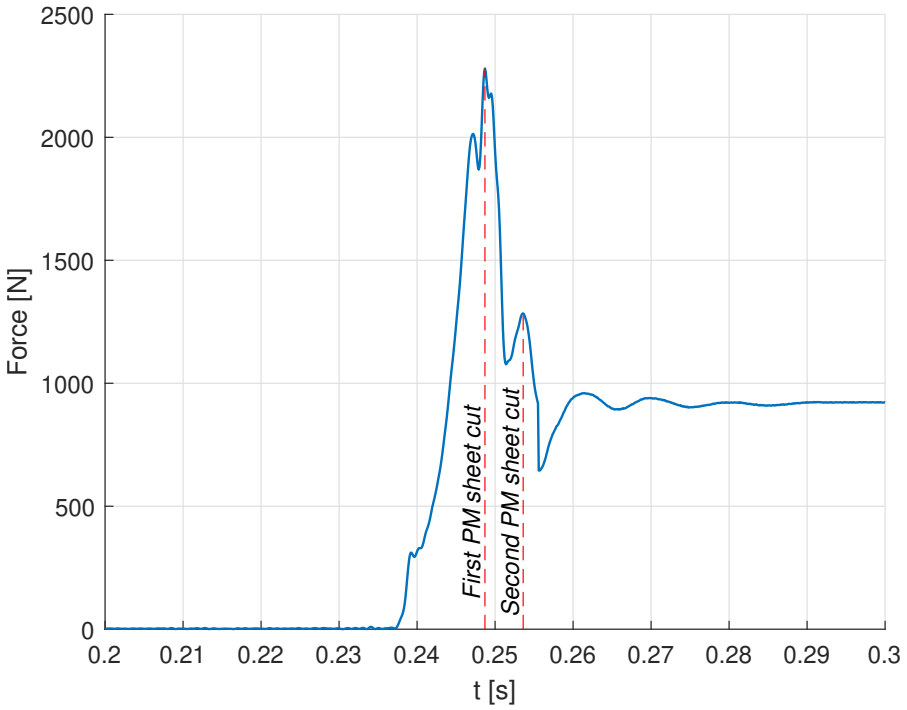

Figure 23: Detail of the peaks relative to the cuts of the first and second sheet of the packaging material.

cut a force of about 1.2 kN was required and for the second of about 350 N, considering also the frictional contributions due to the contact between the components.

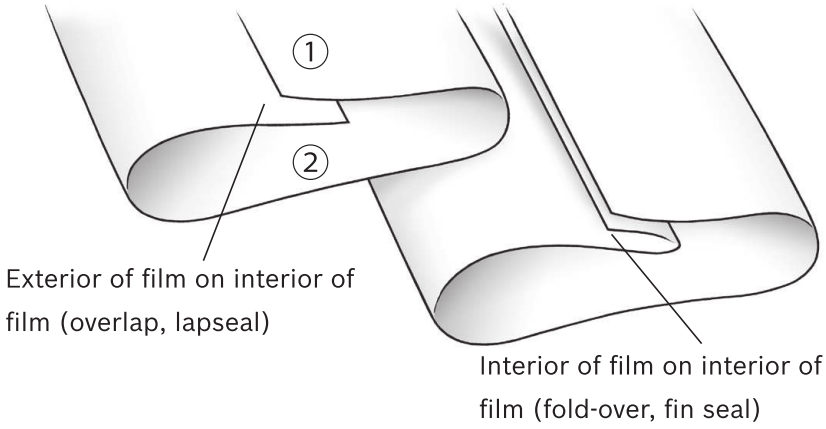

Figure 24: Different types of longitudinal seam. The configuration used in the reference machine is the left type with the overlap. The image also shows the references of the first and second sheet according to the order in which they were cut. [26]

Also the central part of the force curve was influenced by the presence of the packaging material and the movement of the knife inside

the second jaw. The mean value of the force was enhanced from 830 N of the third test to 900 N of the standard configuration.
All the factors already mentioned led to greater resistance to the movement of the knife and therefore to a lower stroke. On the other hand, the actuation piston reached its final stroke as in the previous cases, therefore the return spring was more compressed and the load cell perceived a higher force.

The remaining part of the curve was comparable to the previous results, with the characteristic fluctuation of force due to the movement of the knife and jaws.

Thanks to the tests carried out, it was possible to identify the different events that characterised the cutting process and correlate them with the related source. This information is summarised in Figure 25.

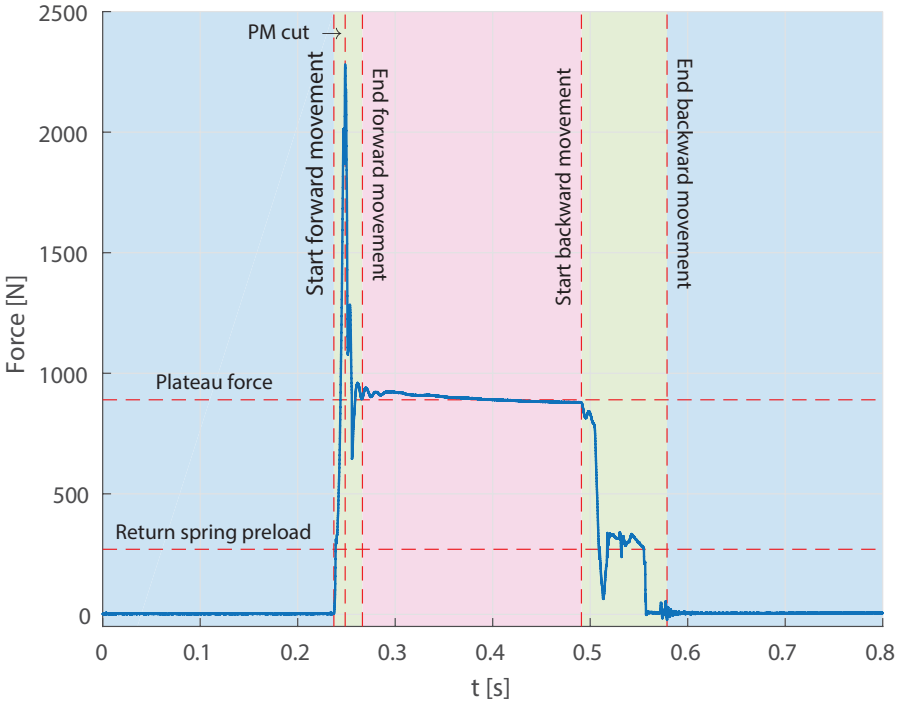

Figure 25: Summary of the events and the parameters of the cutting process identifiable in the force curve. The movements of the cutting system were included in the green area. During forward movement, the packaging material was cut. In the middle of it, the cut of the packaging material was performed. The blue areas show the part of the cycle with the piston in the resting position, instead the magenta areas when it was at the end-stroke. Also the preload of the return spring and the force of the central plateau were important for system monitoring.

Condition monitoring

During the test campaign, some interesting information was evaluated thanks to the monitoring of the force curve. From the knowledge obtained from the previous tests, a standard force curve was defined for the operational cycles of the test rig, which corresponds to that shown in Figure 22.
One of the problems encountered during the operation of the machine was related to the cleaning of the station. The residues produced by the cutting operation and the damp environment created a conglomerate that the movement of the knife pushed inside the second jaw. Over time this accumulation led to a limitation of the knife stroke and destructive effects on the jaw and the inductor housed in it.
The reduction of knife movement affected the compression of the return spring which was increased. The load cell, on the other hand, was subjected to a greater force, easily identifiable in the central phase of the acquired curve. In fact, a significant offset with respect to the standard conditions could be highlighted already in the early stages of the accumulation of residues.
An example of the progressive increase in the value of the central plateau of the force curve is shown in Figure 26.

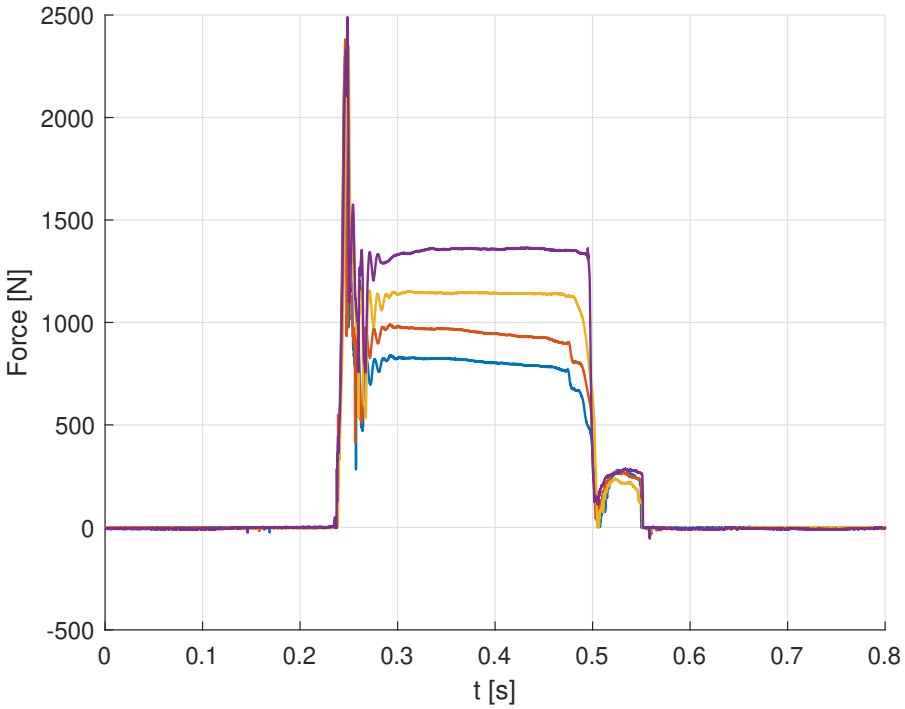

Figure 26: The accumulation of residues in the second jaw progressively led to an increase in the force value in the central phase of the curve. Each curve was acquired one hour after the previous one.

The curves shown are an example of a not too rapid accumulation of residues. In some cases, this progression occurred much more

quickly reaching higher force values, even above 2 kN.
The accumulation of material caused various negative effects on the cutting system, some immediately visible, others with degrading effects over time:

- Poor cutting interface for the packaging material;
- Increased pressure on the knife blade, which sometimes led to component failure;
- High pressures on the inner surface of the jaw, with possible breakout;
- Wear due to rubbing of components with residues;
- Greater compression of the return spring.

All these effects contributed to the reduction of the lifetime of the components, and therefore of the availability of the cutting system.
It is easy to understand the importance of detecting the accumulation of residues in the early stages to limit its effects, which became more harmful as the phenomenon progressed.
For the purposes of the test rig, developed mainly to evaluate the degradation of knives, the breakage of these components was not admissible in order not to waste the hours of test already performed.
It was at this point that the condition monitoring approach was applied to warn of the need for a cleaning operation. This precaution made it possible to minimise maintenance operations, increasing the availability of the test rig and therefore the possibility to perform more test hours in the same period.

It was not easy to determine how much was saved by implementing this monitoring since the events that affected the operation of the machine derived from multiple factors that were not always easily identifiable and that had different severity.
However, it was possible to make simplified assumptions based on what was reported in the log file by the operators assigned to the test rig.
Initially, the accumulation of residues was detected on average every 5 hours of operation, which corresponded to about 22500 cutting cycles. The cleaning operations on the jaws were performed only after malfunctions, noises or irregular cuts on the outgoing packaging material were reported, requiring more or less 25 minutes to complete. On such occasions, the accumulation was already at an advanced stage and on some occasions had already irreversibly compromised some of the components, with a consequent additional cost for downtime and the replacement of the parts.

To avoid this, scheduled maintenance was performed every 3 hours which included inspection of the jaws by an operator and, if necessary, the cleaning operation. This made it possible to cancel the breaking of the most critical components and all the problems inherent in the accumulation of residues. However, the hours of tests performed and the hourly cost of the test rig were heavily affected: the additional man-hours and the maintenance of the machine utilities were, in fact, an important cost for the company carrying out the test campaign.

With the condition monitoring an alert system was implemented to alert the operators of the need to clean the jaws already in the initial stages of the accumulation. This solution allowed to maintain the reliability of the preventive maintenance approach, reducing at the same time the number and the frequency of the cleaning operations.
Furthermore, the continued presence of the operator during machine operation was no longer necessary. In fact the previous solutions were bound to the work shifts of the operators, as the test rig required continuous monitoring to guarantee the functionalities necessary for carrying out the test. With the integration of the condition monitoring system, specific alarms were defined to stop the operation in the event that the detected conditions were potentially critical.

Different thresholds were set to warn the operator when residues started to accumulate in the jaw or to stop the machine in safe conditions before some components were damaged as this phenomenon progressed. To reduce the number of warnings, the cleaning request threshold was set to 1000 N. This value guaranteed a non-severe accumulation level for the components, and a cleaning operation request on average every 4 hours.
The alarm threshold that allowed to stop the test, instead, was set around 1500 N. The interactions generated between the components were considerable but without the risk of failures. This condition was significant mainly to progress the test without necessarily having continuous supervision, increasing the theoretical daily hours of operation for the test rig even outside the work shifts of the staff.

The reduction of the consumption of the packaging material and the implementation of the monitoring system to constantly evaluate the conditions of the cutting system allowed to perform even 24-hour tests, minimising maintenance operations, with an obvious profit for the company that sold test hours.

2.5.2 *Pressure curve*

During the test campaigns also the hydraulic circuit that actuated the jaws and the knives was monitored with pressure sensors. These in-

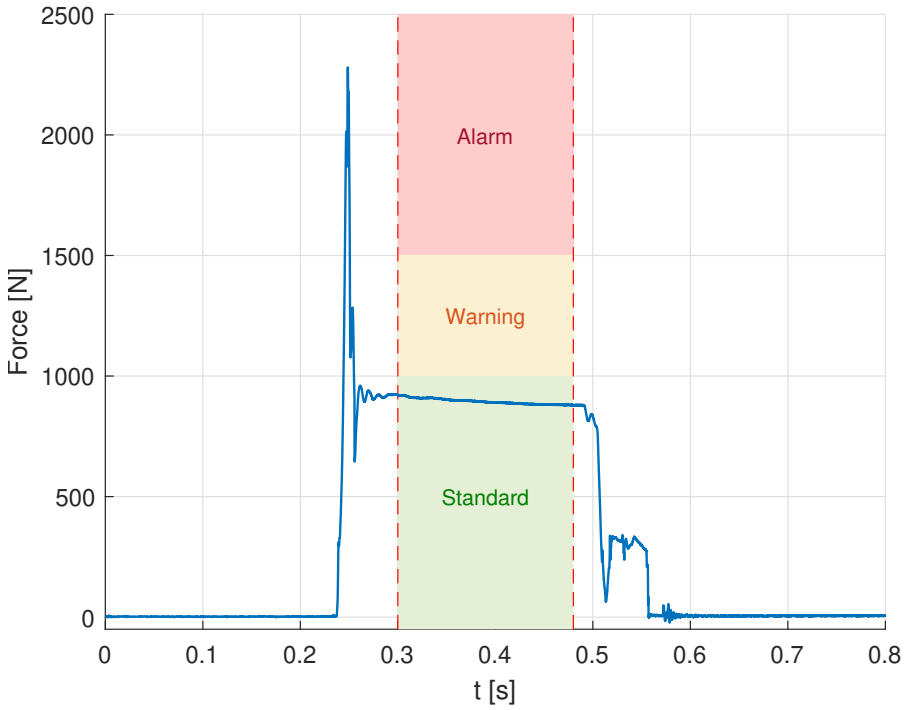

Figure 27: The different warning levels set to alert the operator of the need for a cleaning operation. If the central plateau of the curve reached the alarm area the test was interrupted.

tercepted the oil circuits on the ways that supplied the two chambers of the cylinders in order to evaluate the force generated.
The acquired parameters were:

1. Knife cylinders
    a) Pressure;
    b) Counterpressure.
2. Jaws cylinders
    a) Pressure;
    b) Counterpressure.

The term *pressure* is here used to indicate the hydraulic pressure measured in the chamber that was supplied when the actuation signal was high, whereas the term *counterpressure* is used to indicate the pressure that tended to restore the idle position of the actuated components.

For the interest of this dissertation, only the pressures for the cutting process will be reported since for the actuation of the jaws no useful features emerged for the implementation of the condition monitoring system.

Knife cylinder

The pressures measured in the circuits connected to the two chambers of the cylinder that actuated the knife were interesting to evaluate not only the force to cut the packaging material but also for adjusting the dynamics of this component. In the test rig the return of the knife was incentivised by the hydraulic counterpressure in addition to the action of the return spring.

PRESSURE The hydraulic pressure that actuated the piston that moved the knife was tuned around 80 bar to simulate the force produced in the real machine considering even the counterpressure.
The curve acquired is shown in Figure 28.

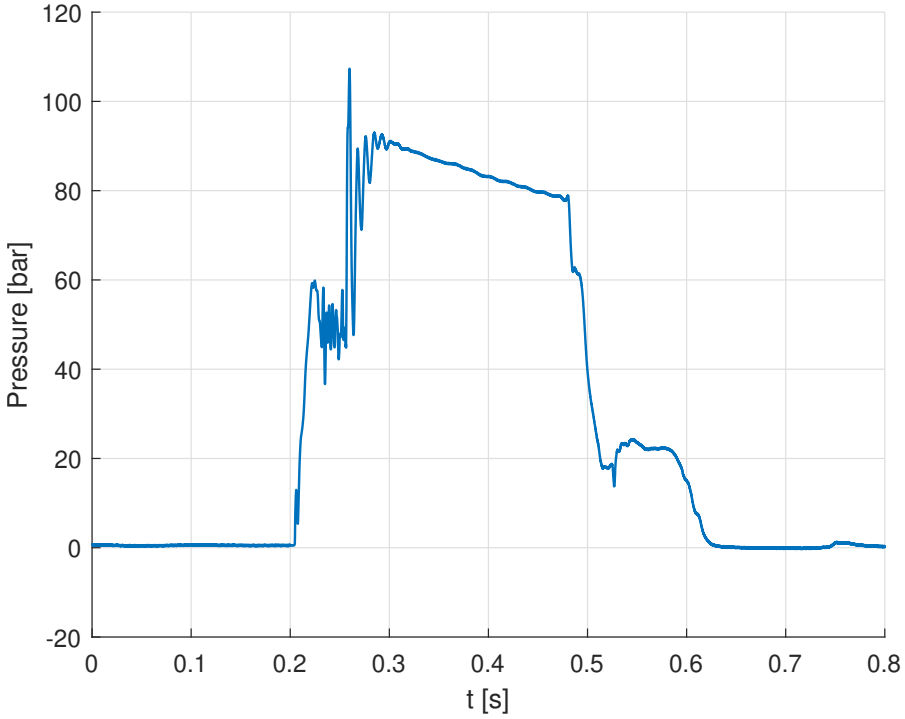

Figure 28: The acquired hydraulic pressure that actuates the knife to perform the cut.

In this curve the 3 main phases also found in the force curve can be recognised: an initial peak, a central phase and the return.
Some significant features of the pressure curve can be highlighted by comparing it with the force curve acquired by the load cell, as shown in Figure 29.

Unlike what was observed for the force curve, the central phase of the pressure curve showed a decreasing trend to reach the regulation pressure: this effect will be discussed later.
The peak that indicates the cut of the packaging material can be found in the pressure curve with a small delay in reference to the same event

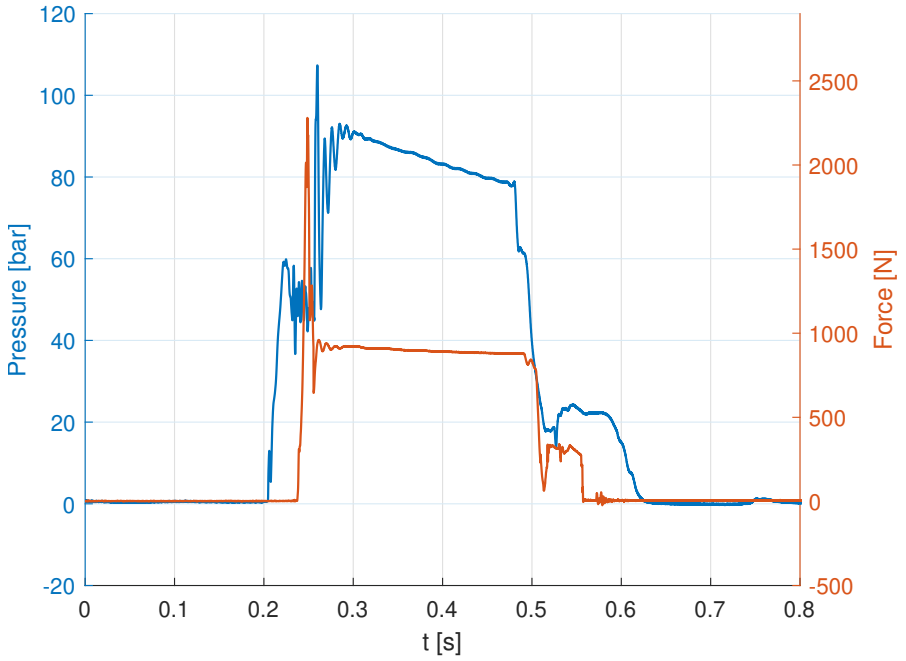

Figure 29: Comparison between the hydraulic pressure and the force curves for the actuation of the knife.

in the force curve. Also the return phase started in a different instant: in this case, the pressure curve had an early response with respect to the force curve.
These characteristics represented the correlation between the hydraulic pressure and the actuation of the mechanical components. In the first case, the force peak was reflected on the pressure curve, so the mechanical event influenced the hydraulic behaviour. On the other hand, the forward and backward movements of the knife were generated by the hydraulic system acting on the mechanical components.
In both cases the time difference was approximately 11 ms.

COUNTERPRESSURE As already mentioned the counterpressure was used to obtain a faster return phase for the knife. Its value was tuned in order to obtain the same force generated in the reference machine during the forward movement. In fact the opposite action of the counterpressure allowed to adjust the effect of the main pressure for the first phase of movement and, when the latter was lower, to add a return force in addition to that of the spring.
The curve acquired is shown in Figure 30.

The comparison with the force curve that is shown in Figure 31 confirms what has already been found analysing Figure 29. In particular, a valley in the pressure curve can be found with the same delay from the peak force already observed. Compared to the previous case there was a decrease in pressure due to the mechanical effect, in fact

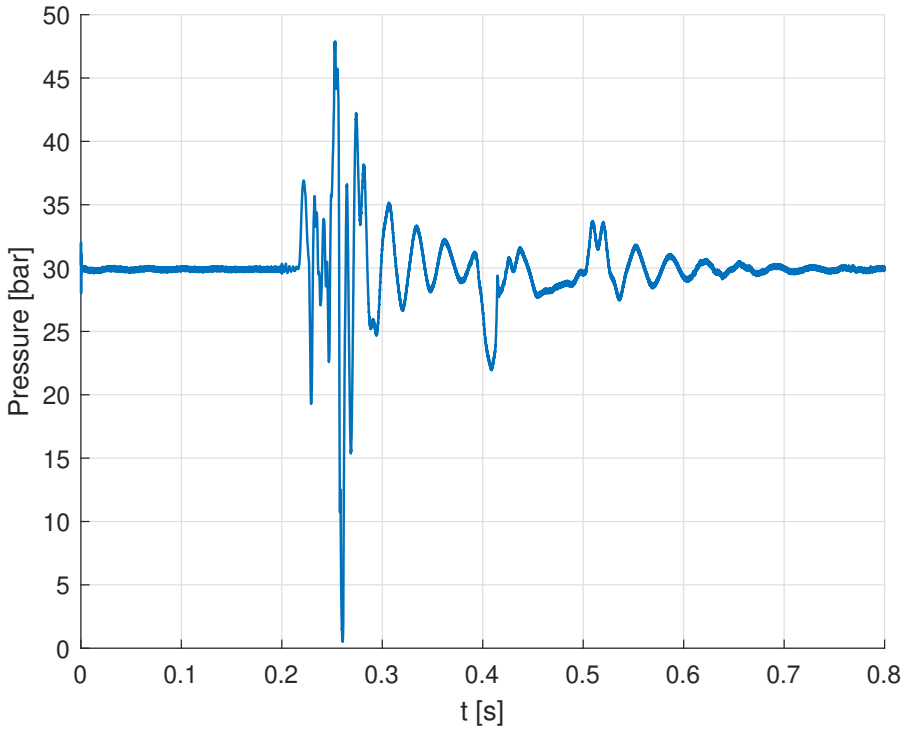

Figure 30: The acquired hydraulic counterpressure that speeds up the return phase of the knife.

the movement of the piston acted in the opposite way for the two chambers.

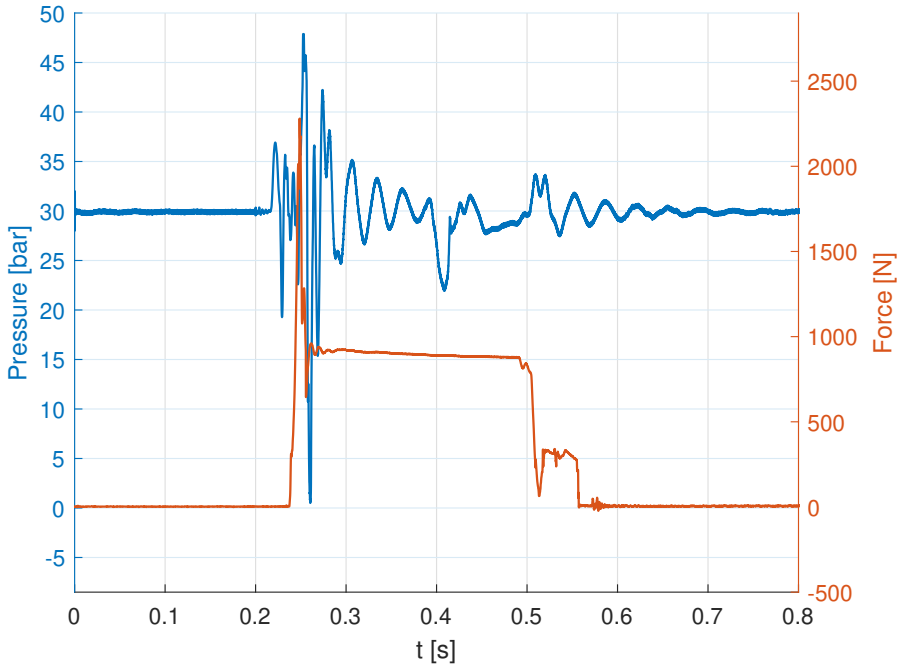

Figure 31: Comparison between the hydraulic counterpressure and the force curves for the actuation of the knife.

2.5.3 *Oil Temperature curve*

In addition to the acquisition of hydraulic forces and pressures, the oil temperature was also monitored during the test campaign in order to assess its influence on the process in question. Because of its physical nature, the acquisitions made on this quantity were performed at a lower sample rate than that of the parameters previously analysed: it was therefore more interesting to observe the trend as the operating hours increased rather than assessing the individual acquisitions.
An example of the thermal cycle of the oil is shown in Figure 32.

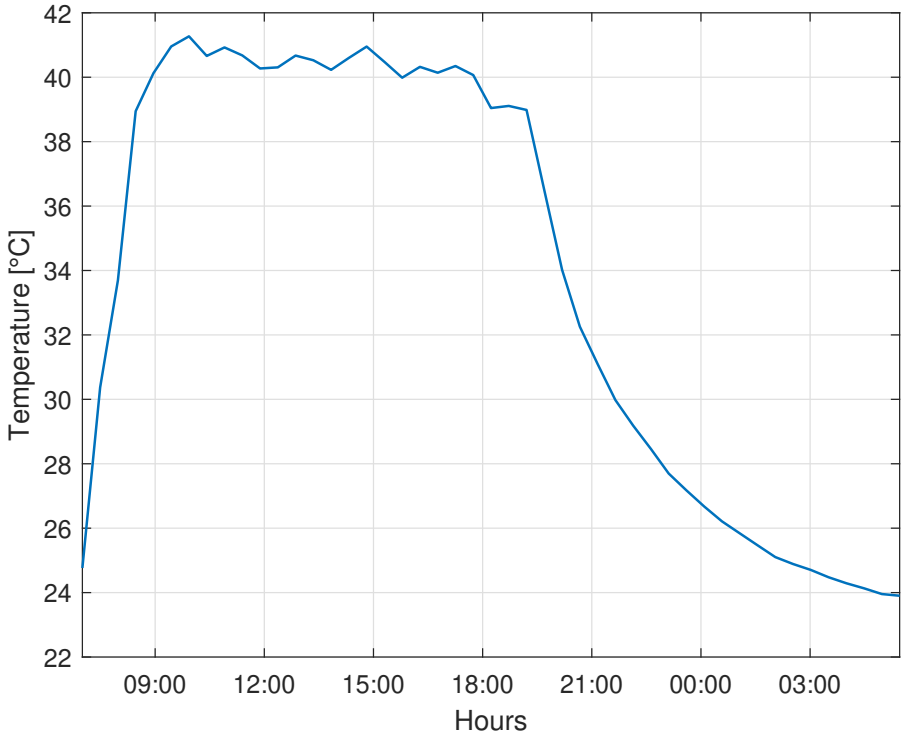

Figure 32: The oil temperature trend from a stopping phase to 12 hours of continuous operation, and subsequent stop.

Looking at the graph it is possible to notice how the oil temperature progressively grew with the hours of operation of the test rig. After 2 hours the equilibrium value around 40 °C was reached. The hydraulic system was designed to maintain this temperature value continuously, cooling the hydraulic fluid if this threshold were exceeded.
It is easy to notice that the temperature of the oil slowly decreased after 3 pm due to the influence of the ambient temperature. The oil temperature at time t due to convective cooling could be calculated with the well-known equation:

$$T(t) = T_a + \Delta T_0 \cdot e^{\frac{-t}{\tau}} \tag{4}$$

where T_a is the constant ambient temperature, ΔT_0 is the initial difference between the oil temperature T_0 and the ambient temperature and τ is the thermal time constant.
τ constant was found evaluating the time elapsed to reach the 63.2% of ΔT_0. For the case under analysis the ambient temperature was 23.5 °C, the initial temperature of the oil was 39 °C, then ΔT_0 was equal to 15.5 °C.
Figure 33 shows this process and the comparison between the acquired curve and the calculated one.

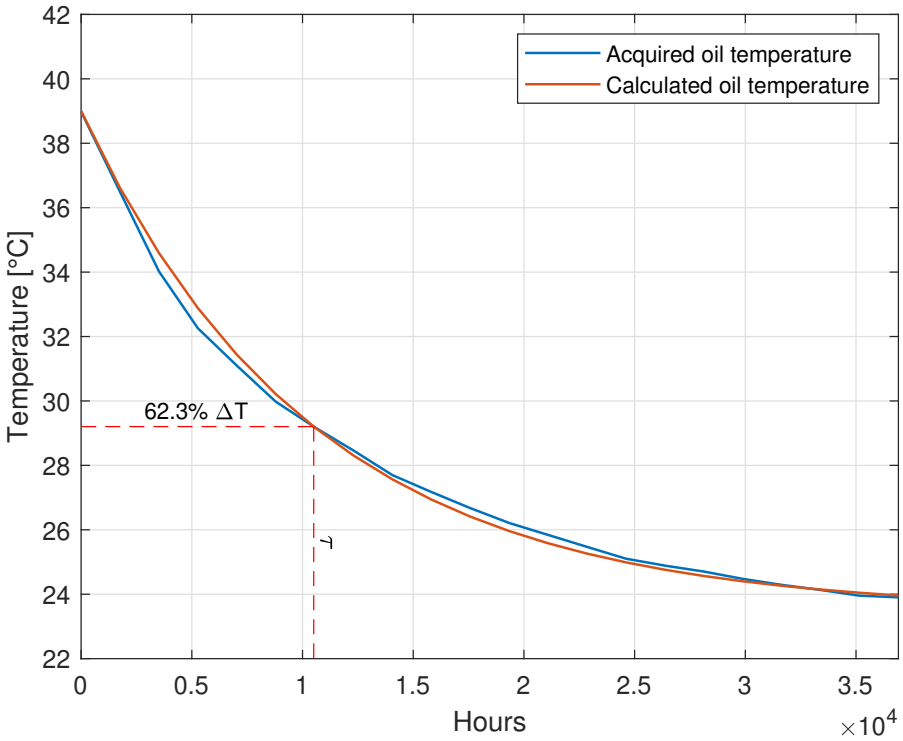

Figure 33: The thermal time constant τ can be found by evaluating the time required to reach 63.2% of the cooling. The calculated curve fits well the evolution of the acquired oil temperature.

Condition monitoring

Oil temperature acquisitions were not only useful for understanding the evolution of this parameter during machine operation but above all for evaluating the state of the process under study. In fact, an important relationship was found between the oil temperature and the mechanical operation of the test rig. To understand this relationship it was necessary to evaluate the hydraulic pressure curves discussed above.
Figure 34 shows the pressure curves obtained for the actuation of the knife cylinder at different oil temperature.

It is easy to notice how the temperature of the oil strongly influenced the peak and the central phase of the pressure curve: the higher

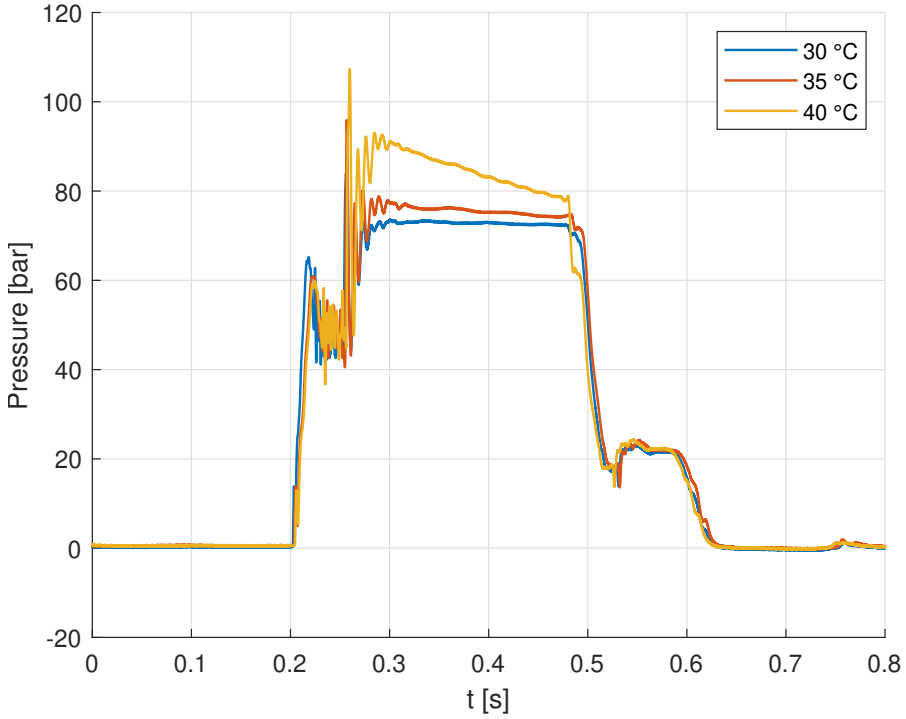

Figure 34: Pressure curves measured for the knife cylinder at different oil temperature.

the oil temperature, the greater the hydraulic pressure. The increase in pressure led to a descending trend in the central phase of the curve to adapt to the set pressure value.
This effect was caused by the reduction in the viscosity of the oil as its temperature increased, allowing an easier flow of the fluid. The dynamics of the hydraulic system was therefore improved, allowing a quicker response of the system.
To assess the responsiveness of knife actuation as the oil temperature changed, the delay between the rising edge of the knife actuation signal and the force peak was measured, thus obtaining a performance indicator. The result is shown in Figure 35.

As expected with the increase in oil temperature, the mechanical delay was reduced allowing a decrement between 15 ms and 25 ms. Fluctuations in the delay curve were mainly due to the force peak. In fact, the cutting time was variable due to multiple factors such as the position of the packaging material between the jaws, the thickness of the material, the influence of the hydraulic system and the frictions of the components.
Other mechanical references in the force curve could have been defined to reduce these influences, but the peak force was sufficiently explanatory and above all easy to implement on real machines.
The evolution of the oil temperature was comparable to that of the reference filler machines, allowing to extend the results obtained from the test rig also to the real application. These analyses allowed to

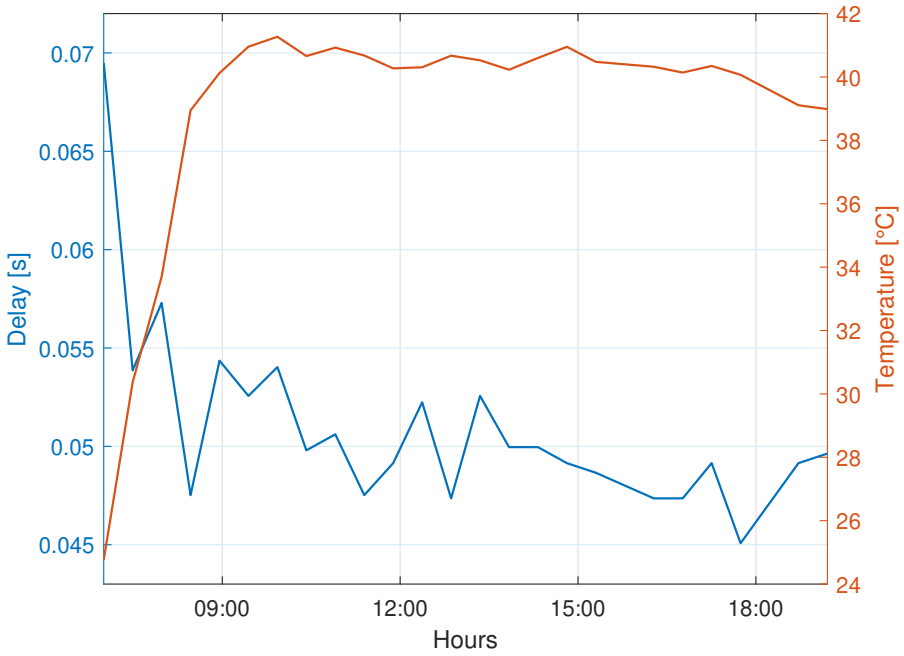

Figure 35: The oil temperature influenced the mechanical responsiveness of the system.

obtain new information never previously assessed on the actuation systems.

2.6 CONCLUSIONS AND DELIVERABLES

As a first implementation of the condition monitoring paradigm for the food and packaging industry, the package cutting process appeared interesting.
To study that process a test rig with seven stations was realised in order to acquired a significant amount of data, reducing the consumption of packaging material and the timing otherwise required on the reference machine to perform the same number of operations.
An embedded acquisition system was implemented to periodically acquired data that could describe the state of the components and the evolution of the process.
The force measurements allowed to distinguish the different phases of the cutting process and to evaluate the acceptable ranges for standard operations. Among the most important information obtained from the force curves, surely the value of the central plateau allowed the most interesting monitoring solution. Thanks to this evaluation, it was possible to establish a threshold to warn of the need to perform a cleaning operation. During operation, in fact, the residual material accumulated between the jaws, compromising the quality of the cut and resulting in more severe impact force that could seriously damage the state of the components involved.

The implemented monitoring system allowed to investigate some aspects of the operation of the cutting process never considered before, in particular the relationship between oil temperature, hydraulic pressure and the mechanical response of the system. The evolution of the oil temperature during normal operation and the influence on the pressure curve of the actuators were evaluated: a progressive increase in the pressure peak was highlighted as the temperature increased. This effect also influenced the mechanical response time, achieving greater system responsiveness with the increase in temperature.

The data collected during the test campaign not only led to the implementation of some important solutions to monitor the conditions of the process and the components, but they also made it possible to increase knowledge about them and their auxiliary systems, providing useful information both in the field of technological development and industrial design, in addition to the standard purpose related to maintenance.
This knowledge can be integrated with new studies on additional defects related to the cutting and sealing system, increasing the reliability of the filling machine.
The industrial implementation of these solutions will allow the evolution of the maintenance program in favour of condition-driven predictive maintenance, with the relative reduction of costs related to maintenance operations and the increase in machine availability.

3

VIBRATIONAL ENERGY FOR MONITORING KNIFE DEGRADATION

In this chapter, a new approach is proposed to monitor the degradation of the knife used for the separation of the packages in the last part of the filling machines. In the following paragraphs some of the ideas that led to the implementation of this new method to evaluate knife degradation are exposed. The test rig used, the acquisitions made and the results obtained from their analyses are also reported and described.

3.1 INTRODUCTION

The purpose for which the test rig described in Chapter 2 had been commissioned was the study of knife degradation as the number of cycles performed increased. Despite the large amount of data acquired in the cutting process and the numerous analyses carried out, it was not possible to detect any significant indicator of tool wear during the test campaign.
For the continuity with what was already achieved in the previous implementation, it was decided to improve the study on the knife with the aim of identifying a methodology that would allow to understand the level of degradation of the component during operation.
For this purpose, the second phase of the project focused on the correlation between knife degradation and the vibrational response.
Vibration-based damage detection is one of the most widely used tools in condition monitoring, not only in mechanical systems but also for civil infrastructure.[36, 37, 38]

Typically, vibration monitoring is based on certain rules defined to correlate the frequencies emitted by the machine to the physical fault condition. The analyses performed are based on unique fault characteristics, such as high amplitude peaks due to the excitation of characteristic frequencies. [39]
The implementation of these techniques on new systems necessarily requires initial training to be able to determine what the vibrational characteristics of the system are. In fact, to assess the conditions of a system it is necessary to define the difference between two states, one of which is assumed to be representative of the initial state, usually not damaged. [40]
Making reference to these guidelines, also for the evaluation of the degradation of the knives being studied, acquisitions and analyses were carried out to highlight significant characteristics between the worn and new components. Making reference to these guidelines,

also for the evaluation of the degradation of the knives under study acquisitions and analyses were carried out in order to highlight significant characteristics between the worn and new components.

The study was conducted not only to define a method for assessing the wear level of knives but also to compare two knife models with different geometric characteristics.

3.2 PROBLEM: DETERMINATION OF KNIFE DEGRADATION

In many applications the relevant physical quantities, and often the only observables, are of an energetic type.
This is even more true for studies related to the functionality of the system itself, as for the condition monitoring solutions, for which acquisitions and analyses must be performed during operation.
The interpretation of the energy distribution allows to derive information about the state of the system otherwise not assessable.
Starting from these assumptions, the idea of using energy analyses to implement condition monitoring solutions was proposed.
These methodologies were used to solve a practical case related to the study previously carried out on the cutting process: the determination of the knife wear level. In fact the parameters acquired in the first phase of the research did not show significant trends that could satisfy the need to monitor the deterioration of the tool, information of primary importance for the industrial application.

The impossibility to perform direct knife degradation measurements due to the functionality and layout of the cutting system led to search for alternative solutions. Several studies correlate tool wear to the vibrational energy generated during operation. Evaluating the limitations on feasible measurements and the energy relationship, it was decided to acquire the vibrations of the system by means of an accelerometer fixed to the link that connected the knife and the return spring.

3.3 ANALYTIC TOOLS FOR TIME-FREQUENCY DISTRIBUTION OF STOCHASTIC PROCESSES

In literature, it is possible to find several studies that correlate wear of mechanical components to their vibrational behaviour. [41, 42, 43, 44, 45]
Almost all the research focuses on vibrational monitoring of rotating mechanical systems, for which there are numerous analytical tools to detect defects and assess degradation.

However, automatic machines have mechanical parts with periodic movement laws but not strictly related to rotating parts. An example is the cutting process of the packaging material described in detail in Section 2.1.
The idea was to apply a similar approach to assess the degradation of the knife evaluating the cutting process as characterised by cyclo-stationary operations. This was the starting point for implementing a system capable of monitoring knife degradation based on vibrational energy. [46]
The energy of the signal $x(t)$ per unit time at the particular time t can be obtained as:

$$E(t) = |x(t)|^2 \tag{5}$$

as well as the energy density of the signal per unit frequency at the particular frequency f is given in the frequency domain by:

$$E(f) = |X(f)|^2 \tag{6}$$

where $X(f)$ is the Fourier transform of $x(t)$.
As already mentioned, condition monitoring is based on the evolution of specific features, but when the spectral content of the vibrational signal changes as the hours of operation increase, neither the time nor the frequency domain is sufficient to describe this progression. [47]
To overcome this limit, a frequency-time approach was proposed, which is intended to show how the energy of the signal is distributed over the two-dimensional (t, f) space.
It is therefore necessary to define an *energy distribution* $\rho(t, f)$ in the time-frequency domain such that:

$$E = E(t) = E(f) = \int_{-\infty}^{+\infty} \int_{-\infty}^{+\infty} \rho(t, f)\, dt\, df \tag{7}$$

Many authors have defined different time-frequency representations of signals [48], but one of the most common is the *short time Fourier transform* (STFT). It allows to analyse what happens at a particular time using a small portion of the signal thanks to a window function $w(\tau)$ centred around that moment. The energy spectrum is calculated and the procedure is repeated for each instant of time.
STFT at the time instant τ and at the frequency f for the signal $x(t)$ is defined as:

$$X_w(\tau, f) = \int_{-\infty}^{+\infty} x(t)\, w(t - \tau)\, e^{-j2\pi f t} dt \tag{8}$$

The signal energy distribution in the time-frequency plane, also known as *spectrogram*, can be evaluated by:

$$S_w(\tau, f) = |X_w(\tau, f)|^2 \tag{9}$$

The resolution of the STFT time frequency is inversely related to the width of the window: the more it increases, the higher the resolution of the frequency, while at the same time it reduces the temporal resolution of the distribution. [49]
This trade-off is due to the Heisenberg's uncertainty principle, which states that the window width in time and the window width in frequency are inversely proportional to each other. [50]

Starting from the STFT alternative time-frequency representations have been studied and one of the most powerful and fundamental is the *Wigner-Ville distribution* (WVD). The WVD has been applied in various studies as a fault diagnosis system [47, 51, 52] since its distribution can be used to describe the instantaneous energy density spectrum.
The Wigner distribution function (WDF) is a part of the more general set of bilinear representations covariant under a time-frequency domain called Cohen's class [53, 54] and it is defined as:

$$W_x(t,f) = \int_{-\infty}^{+\infty} x\left(t+\frac{\tau}{2}\right) x^*\left(t-\frac{\tau}{2}\right) e^{-j2\pi f\tau} d\tau \tag{10}$$

where $x^*(t)$ is the complex conjugate of the signal $x(t)$.
Equation 10 shows significant relations with the *autocorrelation function*, in fact the *power spectral density* $P(f)$ can be related to the Fourier transform (FT) of the signal autocorrelation function $R(\tau)$ with respect to the delay variable:

$$P_x(f) = \int_{-\infty}^{+\infty} R(\tau)\, e^{-j2\pi f\tau} d\tau \tag{11}$$

with

$$R(\tau) = \int_{-\infty}^{+\infty} x(t)\, x(t+\tau)\, dt \tag{12}$$

For the WDF a time-dependent autocorrelation function $R_t(\tau)$ is chosen as:

$$R_t(\tau) = x\left(t+\frac{\tau}{2}\right) x^*\left(t-\frac{\tau}{2}\right) \tag{13}$$

The power spectral density function can be rewritten as:

$$P_x(t,f) = \int_{-\infty}^{+\infty} R_t(\tau)\, e^{-j2\pi f\tau} d\tau = \int_{-\infty}^{+\infty} x\left(t+\frac{\tau}{2}\right) x^*\left(t-\frac{\tau}{2}\right) e^{-j2\pi f\tau} d\tau \tag{14}$$

which corresponds to Equation 10.

Sampling of real signals involves alias components in the WDF. To overcome this problem, Ville [55] proposed to use the analytic signal

in the time-frequency representation of a real signal. The analytic signal is defined as:

$$x_a(t) = x(t) + j\hat{x}(t) \tag{15}$$

where $\hat{x}(t)$ is the Hilbert transform of $x(t)$. A real signal $x(t)$ exhibits *Hermitian symmetry*

$$X(-f) = X^*(f) \tag{16}$$

where $X(f)$ is the FT of $x(t)$, so the negative-frequency components can be deduced from the positive-frequency. The spectrum of the analytic signal can be obtained as:

$$X_a(f) = X(f) + j\hat{X}(f) = X(f) + sgn(f)\,X(f) = \begin{cases} 0, & \text{if } f < 0, \\ X(f), & \text{if } f = 0, \\ 2X(f), & \text{if } f > 0 \end{cases} \tag{17}$$

that contains only the non-negative frequency components of $X(f)$. In practical applications, this property allows to avoid interference between positive and negative frequencies in WVD.

Despite its many desirable properties, the WVD has some other limitations. Some artefacts, also known as *cross-terms*, appear midway between true signal components in the case of multicomponent signals. These cross-terms can cause interferences and lead to negative values for the WDF. A method to suppress these spurious features is to smooth the WDF by inserting an averaging window function $h(t)$ that slides in the time-frequency plane:

$$W_w(t,f) = \int_{-\infty}^{+\infty} x_a\left(t + \frac{\tau}{2}\right) x_a^*\left(t - \frac{\tau}{2}\right) h(t)\, e^{-j2\pi f\tau} d\tau \tag{18}$$

The smoothed WVD is often called the *pseudo Wigner-Ville distribution* (PWVD).

The implementation of the proposed time-frequency analysis is typically used in physical processes with a strong periodicity. However, many practical applications, such as the cutting process, are characterised by non-deterministic operational cycles that can be evaluated as *cyclostationary*. By definition, cyclostationarity represents stochastic processes characterised by variable statistical properties with respect to some generic variable. [56]
The vibrations generated by these processes seem at first sight to be random, but from a careful inspection it is possible to identify modulations that continue to repeat themselves identically for each cycle.

From the condition monitoring point of view it is important to define the observed stochastic process $Y(t)$ as:

$$Y(t) = p(t) + X(t) + N(t) \tag{19}$$

for which the deterministic part of the signal $p(t)$, and its non-deterministic part $X(t)$ are distinguished, and the background noise added in the term $N(t)$.
From the discretised signals $y[n]$ it is possible to define a new stochastic process $Y[m]$ splitting the measurements in I cycles, each one with N samples. In this way, each point m of the stochastic process is defined by a set of I values.
It is clear that any function $g[m]$ applied to this stochastic process can be calculated by applying it to the values averaged over the I cycles. This can be formally defined as:

$$\langle g[m] \rangle_N^I = \frac{1}{I} \sum_{i=0}^{I-1} g(y[m + iN]), \quad m = 0, \ldots, N-1 \tag{20}$$

where $\langle \cdot \rangle_N^I$ is the average over I cycles of length N.

These analytical tools have been applied to study the vibratory signals of the knives during operation, allowing to extract interesting information for the study of the components and the implementation of the condition monitoring system.

3.4 TEST RIG

To acquired reliable vibrational signals that allowed to monitor the degradation of the knife during the cutting operation, the fastening of the accelerometer had to guarantee the perception of the knife's contribution, minimising the influence of the other mechanical components on the signal. Due to the layout of the cutting station, the most direct measurement could be performed by fixing the sensor to the nut used to preload the return spring, as shown in Figure 36. This component was in fact connected to the link of the knife, reducing the influence of the other components.

The acquisitions were performed on a test rig different from the one previously described because it was considered not suitable for the proposed vibrational study. Indeed, several factors would have compromised acquisitions, including:

1. The influence of multiple not perfectly synchronous cutting stations would have introduced vibrational components difficult to interpret;

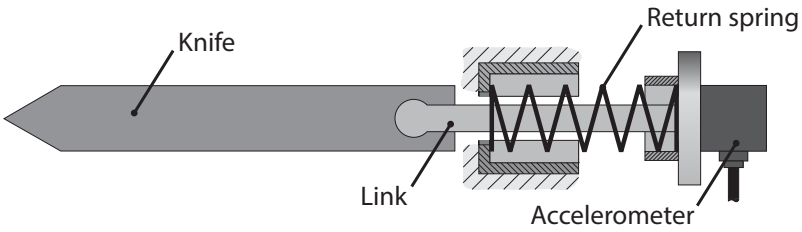

Figure 36: Scheme of the accelerometer mounted on the link that connected the knife and the return spring.

2. The accelerated cycles that would not have allowed to obtain from the vibrational measurements information consistent with those of the real machine;

3. The counterpressure used to speed up the return phase of the knife which would have led to a different vibrational behaviour of the cutting station compared to the real application;

4. The difference between the components and the methodology used to actuate the cutting station which did not guarantee the same vibrational response of the reference system.

The test rig was designed to emulate the operation of the cutting station as performed in the reference filling machines, and, to achieve maximum consistency, the actuation control system and the hydraulic system were the same as those used in the real machine, as were the components of the cutting station, so that even the performed acquisitions could refer to the actual application.
Although it did not directly concern the cutting operation, for the sake of consistency the same jaw actuation system was used as in the machine. Despite the solution based on hydraulic cylinders adopted in the previous test rig could replicate the dynamics and forces of the filling machines, the vibrations induced by the catch of the original mechanical components could not be emulated in the same way. In this case, in fact, the jaws were approached and forced against each other by means of a hydraulically operated hook system.
The cutting station as installed in the test rig is shown in Figure 37.

Test rig parameters

As already mentioned, the operation cycle for the test rig under study was the same set on the real filling machine. The cycle time was, therefore, 900 ms, with the signal used to actuate the jaws high for 450 ms and the signal to trigger the cut active for 66 ms, as shown in Figure 38. The temporal difference of the latter with respect to the signal used in the test rig described in Chapter 2 was due to the type of

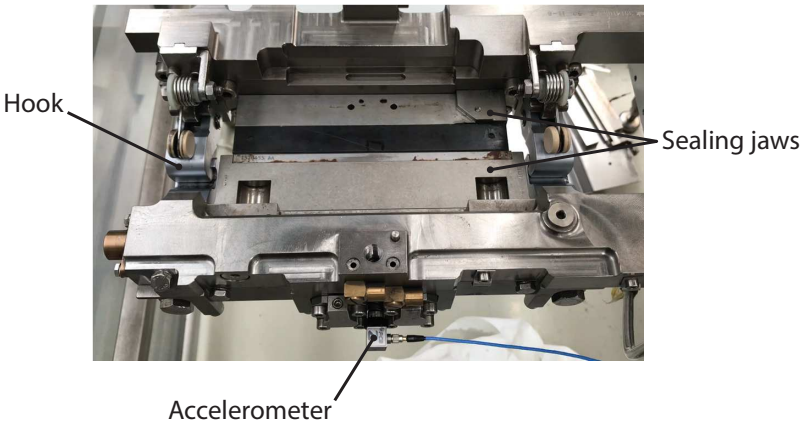

Figure 37: The cutting station installed in the test rig was the same used in the reference filling machine.

actuation used: in the previous case, in fact, a signal tuning was performed to obtain dynamics comparable with the real application but with an accelerated cycle. The use of the counterpressure to speed up the knife return phase, in fact, caused a delay in the forward phase, thus requiring an anticipation of the cutting signal and a coherent maintenance.

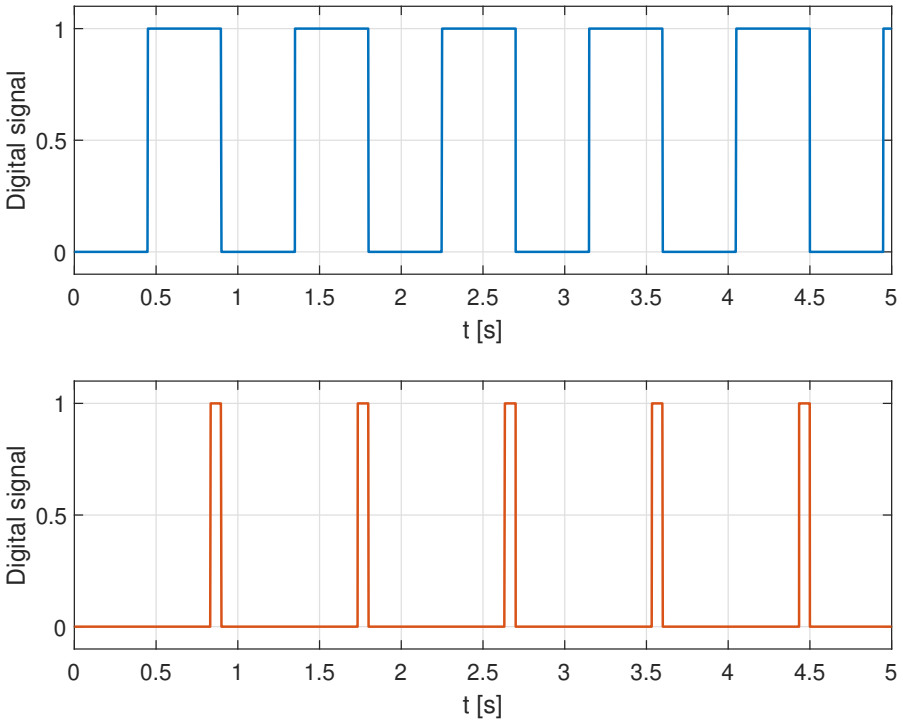

Figure 38: The digital signals that triggered the clamping of the jaws (blue) and the cut (orange).

3.4.1 *Knife samples*

The test conducted to study the vibrational behaviour of the knife in relation to its degradation was also focused on the comparison between two models of this component. As shown in Figure 39 they differed for the bevel angle of the teeth.

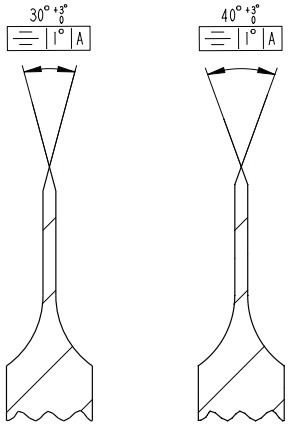

(a) (b)

Figure 39: The geometrical difference between the two tested knife models.

Hereafter the model with the 30° angle (Figure 39a) will be designated as *K1*, while the one with the 40° angle (Figure 39b) as *K2*.

To compare the vibrational behaviour of the knife in different stages of wear, two samples of *K1* were tested, each with a different number of cutting cycles performed in reference to the samples available from the test campaign of the previous study. Specifically, they performed 400000 cycles and 2.5 million cycles respectively.

3.5 DATA ACQUISITION

As is well known, a fundamental part of condition monitoring is the design of the acquisition system and the choice of parameters to monitor. The following paragraphs contain and justify the choices made in order to guarantee reliable acquisitions that allowed the collection of relevant information.

3.5.1 *Signals*

In addition to the vibrational signals, other parameters relating to the cutting station operation were acquired. Table 8 shows all the main

sampled signals.

3.5.2 *Sensors*

For the type of research proposed essential was the integration of an accelerometer in the monitoring system for vibrational measurements. The sensors used to acquire the pressures were the same as those used in the previous test rig. Instead, the digital signals were acquired directly from the PLC outputs that controlled the cutting process.
Table 9 is a summary of the sensor characteristics.

3.5.3 *Data acquisition system*

In order to collect the vibrational signals and those that characterised the test rig operation, a data acquisition system similar to the one used in the previous study was installed. The choice was not only guided by the need to acquire the channels with a reliable and high-performance hardware, but also by the possibility of integrating this system with the one previously proposed for monitoring the cutting process.
The controller used was an NI cRIO-9068, the same model chosen for the previous test, although the number of signals was much smaller. The modules used were:

1. *NI-9232*: it is a dynamic signal acquisition module used to performed measurements from integrated electronic piezoelectric (IEPE) and non-IEPE sensors such as accelerometer.

2. *NI-9205*: it is an analog voltage input module that was used to read the pressure transmitter signals and also the digital signals that controlled the actuations of the cutting station.

Their characteristics are reported in Table 10.

3.6 ACQUISITIONS

Among the acquired parameters, the only one that is worth mentioning in this section is the vibrational signal. In fact the other signals were used only to perform post-processing operations.

3.6.1 *Knife vibrations*

Although a triaxial accelerometer was used, the measurement axis containing the information of greatest interest was obviously the one

Table 8: Parameters acquired on the test rig.

Parameter	Unit	Signal type	Description
Knife vibration	m/s^2	Analog	The vibration of the cutting process was acquired by referring to the movement of the link that connected the knife and the return spring.
Knife cylinder pressure	bar	Analog	The cylinder oil pressure used to actuate the knife was monitored.
Catch pressures	bar	Analog	The oil pressure in the hydraulic line used to activate/deactivate the catch of the jaws was monitored.
Knife valve command	1/0	Digital	The command signal to control the valve that regulate the hydraulic actuation of the knife.
Catch valve command	1/0	Digital	The command signal to control the valve that regulate the hydraulic actuation of the jaws.

Table 9: Sensors used in the test rig. [57, 33]

Sensor name	Sensor type	Accuracy	Measuring range	Output signal	Parameter
PCB Piezotronics 356A32	Triaxial IEPE accelerometer	± 0.003 m/s^2 rms	± 491 m/s^2 pk	7...16 VDC	Knife vibration
Trafag 8252.85.2517	Pressure transmitter	$\pm 0.5\%$ FS	0...160 bar	0...10 VDC	Hydraulic pressures

Table 10: Main characteristics of the modules (a) NI-9232 and (b) NI-9205. [35]

Signal	±30 V Voltage analog input
No. of channels	3
Sample rate	102.4 kS/s/ch
Resolution	24 bits
Connectivity	BNC

(a)

Signal	±10 V Voltage analog input
No. of channels	16 differential
Sample rate	250 kS/s
Resolution	16 bits
Connectivity	DSUB

(b)

along the knife actuation direction.
Numerous tests were performed to analyse the influence of the different phases of the cutting process on the vibrational signal and to compare the knife models taken into consideration.

1. *K1*
    a) Without packaging material;
    b) With packaging material.
2. *K2*
    a) Without packaging material;
    b) With packaging material.

Further acquisitions were made to compare the samples at different levels of wear by performing tests with the packaging material.

Based on the type of information to be extracted from the acquisitions, different analysis algorithms were applied, but all had in common a vibrational energy approach analysed by means of the time-frequency distribution of the signals.

In order not to be redundant, a representative vibrational curve acquired for a single cutting cycle is shown in Figure 40. In fact, before the elaboration, the performed acquisitions did not allow to highlight significant differences by comparing the signals of the different tests.

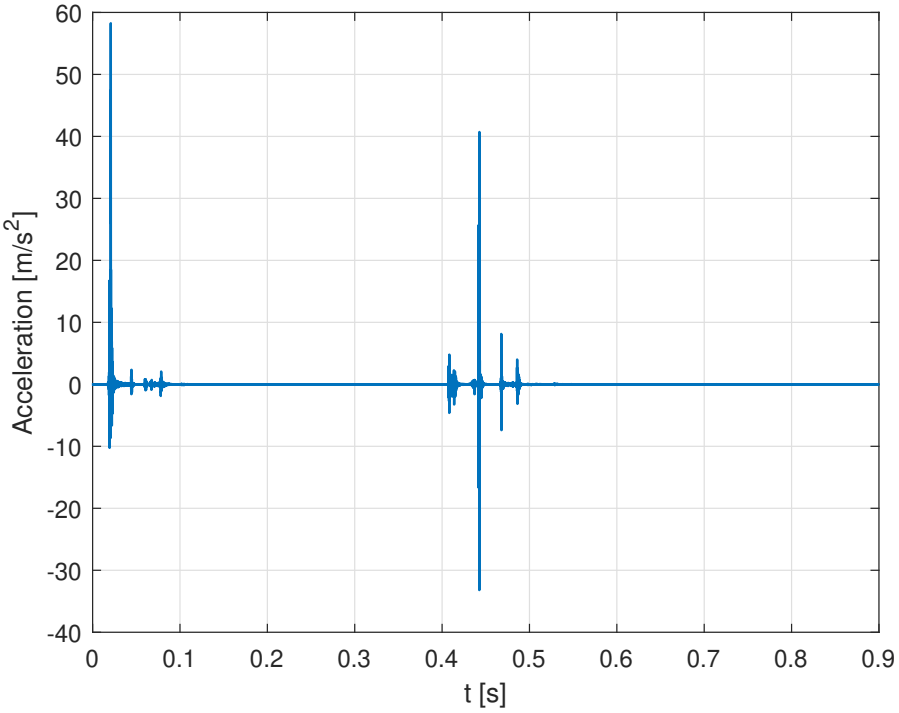

Figure 40: The vibratory signal acquired during a cutting cycle.

The curve is reported starting from the rising edge of the catch command signal and with a time interval of 900 ms, in order to show a complete period of the cutting cycle.
As will be reported later, it was possible to evaluate the different phases of the cutting process from the vibratory signals. The first and highest peak was due to the actuation of the jaws to which the accelerometer was sensitive because the knife and all the components connected to the jaws were moved together. The second set of vibrations was instead related to the actual cutting operation except for the last peak due to the return movement of the knife and the jaws to the initial position. The first three peaks of this set can be easily related to:

- Start of knife actuation;
- Cutting of packaging material;
- Start of backward movement.

For the purpose of this research, the second set of peaks was particularly interesting, while the effect of the jaws could be omitted.

3.7 ANALYSIS OF VIBRATIONAL DATA

As already mentioned by the raw vibrational signals it was not possible to obtain significant information that would allow to compare the

behaviour of the tested samples. To do this, adequate post-processing was necessary. Initially, it was decided to define the characteristics of the stochastic cyclostationary process, obtaining useful information for subsequent analyses.
To investigate the influence of the packaging material on the cutting cycle, tests were performed with and without it, keeping all the cutting station actuations active.
Then the two knife models were compared to see if the cutting process could be influenced by the different angle of the teeth.
Finally, the data obtained from the comparison tests between different levels of wear were analysed.
To reduce the amount of data to be processed, only the neighbourhood of the cutting instant was extrapolated, leaving out the parts of the signal that were not directly related to the investigation. This was only the first of the solutions implemented in order to reduce the computing resources required by the monitoring system.
All the proposed analyses aimed to study the cutting process, and specifically the knife, in order to develop a new approach for the condition monitoring of a non-rotary application, verifying its reliability and in parallel increasing the know-how on the process and the component.

3.7.1 *Cyclostationary stochastic process*

Based on the definition expressed by Equation 19 the signal of a cyclostationary stochastic process can be decomposed in:

- Deterministic part;
- Non-deterministic part;
- Background noise.

To determine the composition of the acquired vibrational signal several tests were performed and compared.
To separate the deterministic part from the other components, an average operation was performed on the numerous cutting cycles acquired applying Equation 20. Evaluating the fronts of digital signals it was possible to extrapolate a neighbourhood of the cutting instants, synchronising the points of each cycle with those of the others, as shown in Figure 41.

From the numerous acquisitions, a significant statistical population of the cutting cycles was obtained. The idea was that the average of the synchronous data extrapolated from the files could bring out the deterministic part of the signal, reducing the influence of the random components.

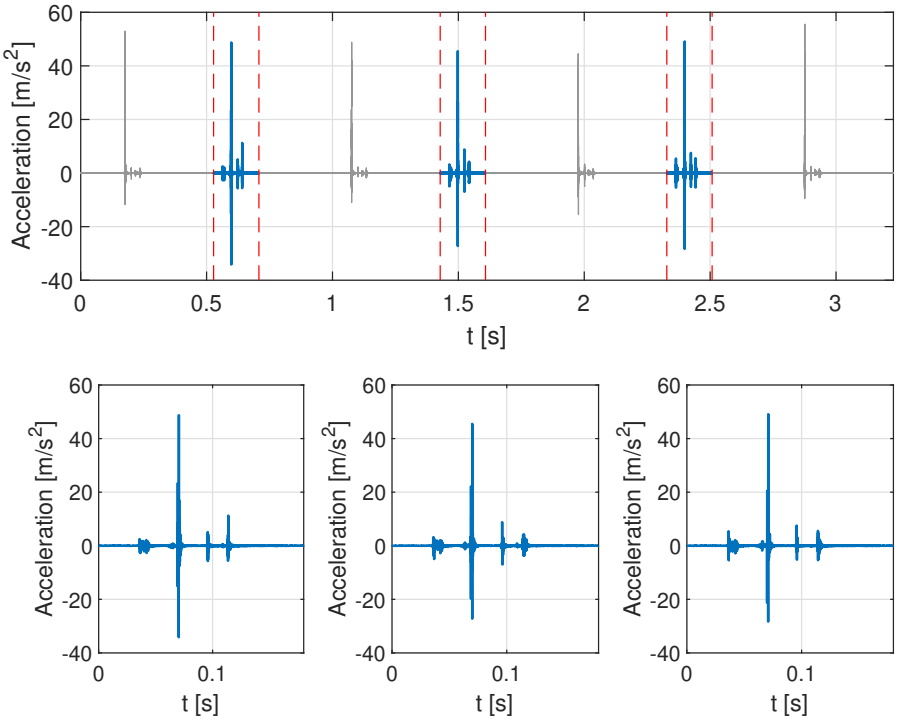

Figure 41: The intervals related to the cut operations were extrapolated from the acquired files and their points synchronised.

The background noise of the signal was negligible for the acquired data, also considering that the average of the cycles reduced its influence further. To obtain the perception of the noise magnitude, the accelerometer signal was evaluated in static conditions.
Figure 42 shows the estimation of the signal components.

3.7.2 *Test comparison with and without packaging material*

One of the first evaluations carried out on the acquired data concerned the interpretation of the vibrational peaks recorded in relation to the events of the cutting process. The determination of the cut of the packaging material was therefore essential, not only as a reference for the other events but also to assess whether it was possible to clearly distinguish it from the other components.
To this end, the acquisitions made during the tests without and with the packaging material were compared. The respective curves are shown in Figure 43 and Figure 44.

From the comparison of the obtained curves it was easy to detect clear differences in the central part of the time interval, highlighting:

1. A peak at the instant the packaging material was cut;
2. The increase of vibrations at the beginning of the backward movement of the knife.

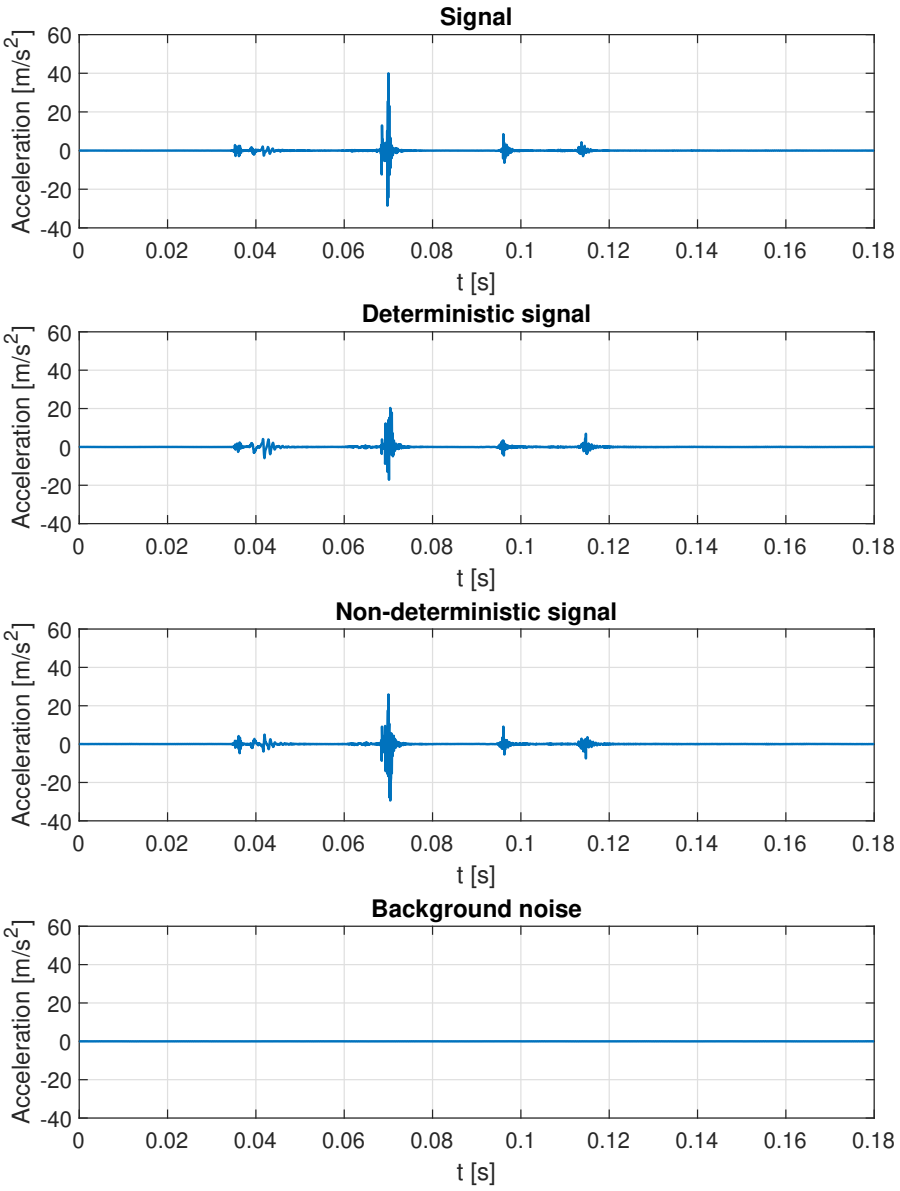

Figure 42: The signal was decomposed into its deterministic, non-deterministic and background noise components. The latter was negligible compared to the other components.

From the performed acquisitions, the cut was particularly evident compared to the other vibrational components, guaranteeing the possibility of evaluating its characteristics from vibrational measurements. The identification of the cut instant allowed the determination of the main events of the knife operation. As already mentioned, it was possible to distinguish respectively the beginning of the forward movement, the cutting of the packaging material, the beginning of the backward movement and finally the stop at the initial position.
The presence of the packaging material did not only affect the cut, but also the successive movement. In particular, the beginning of the return movement of the knife showed greater vibrations.

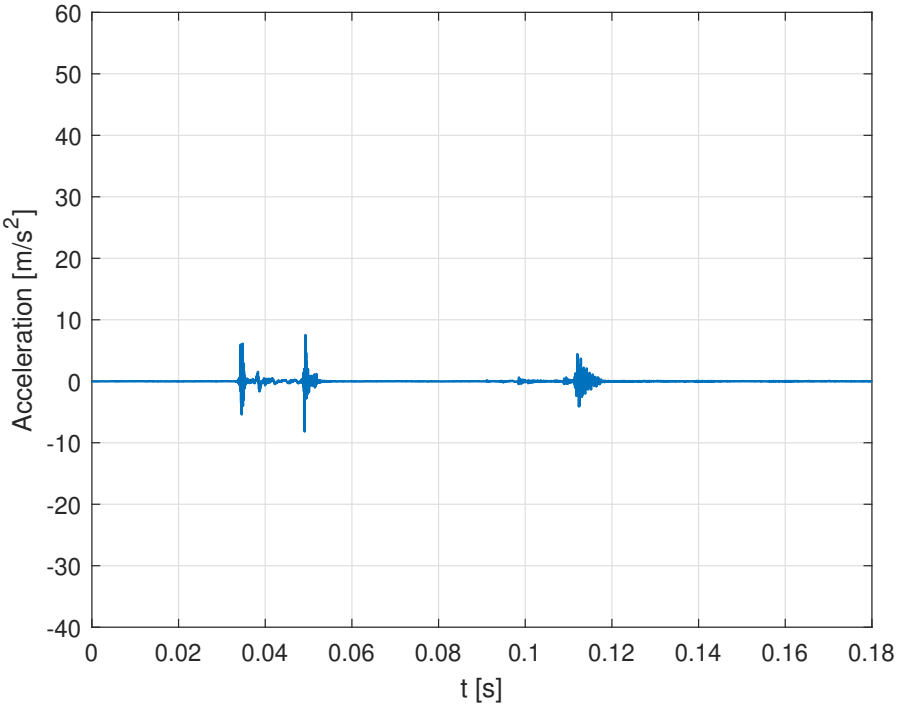

Figure 43: Vibration curve acquired for the test without packaging material.

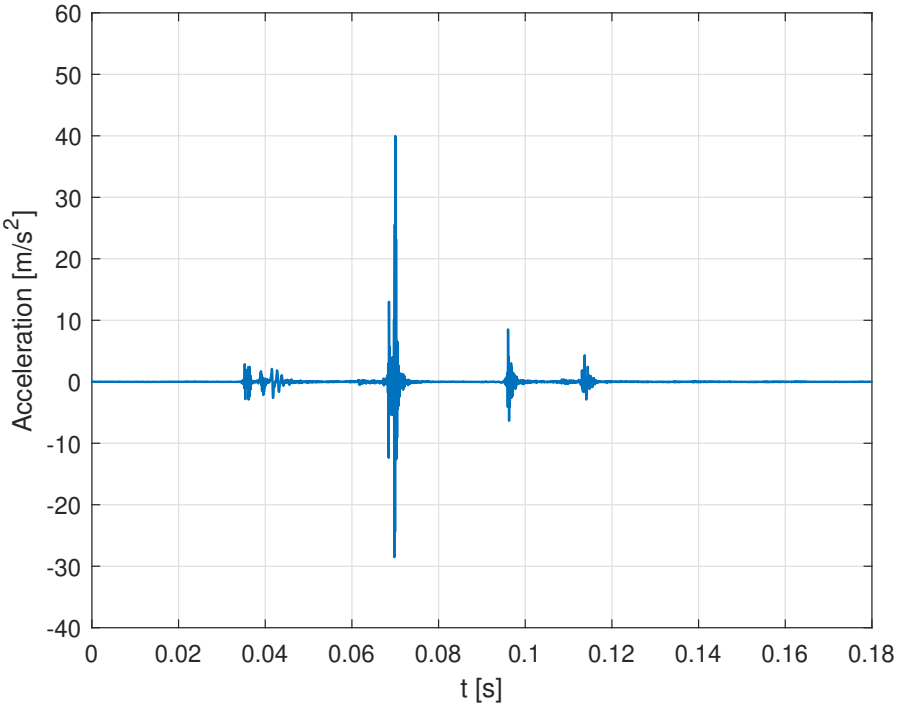

Figure 44: Vibration curve acquired for the test with packaging material.

Although the packaging material was already cut, this led to greater resistance in the return phase. The critical moment was the beginning of this phase, not only because of the evolution from the static to the dynamic condition but also due to the insertion of the material edges

in the slot of the jaw, as shown in Figure 45.

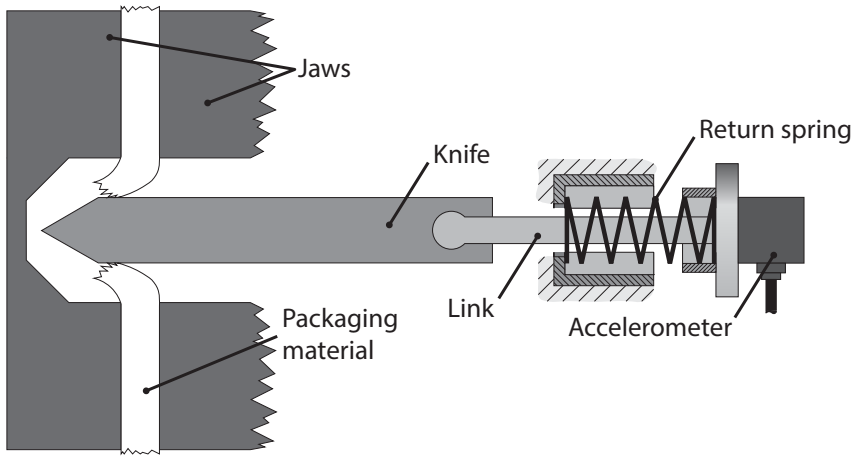

Figure 45: The edges of the cut packing material pushed into the slot of the second jaw generated resistance against the return movement of the knife.

Taking into account the influence of the packaging material on the movement of the knife, it was possible to consider the abrasive effect of the first on the second as the main source of the tool wear.

3.7.3 *Test K1 vs K2*

The evaluation of the vibrational behaviour through the implemented acquisition system allowed the comparison of two models of knives used in industrial filling machines.
These tests were initially performed to evaluate the ability of the analysis algorithm to highlight distinct vibrational characteristics for some samples of the same component with small variations of the geometric profile.
The two compared knife models differed in the bevel angle of the blade teeth. Although there were no other geometric differences between the two components, a change was expected at the cut instant, mainly due to the penetration of the blade into the packaging material. For this reason, the time-frequency distribution was essential to evaluate the behaviour of the samples.
The implemented algorithm was able to extrapolate the neighbourhood of the cutting instant from the acquisitions, in order to perform the PWVD. A Hanning window was used to smooth the signal.
The distributions obtained for the two knife models are shown below. For the sake of comparison, the axis limits have been set equal for all tests. Colour mapping was instead scaled based on the values of the single distribution.

In order to evaluate how the time-frequency distribution varied, also in this case, the tests were performed with and without the packaging material.

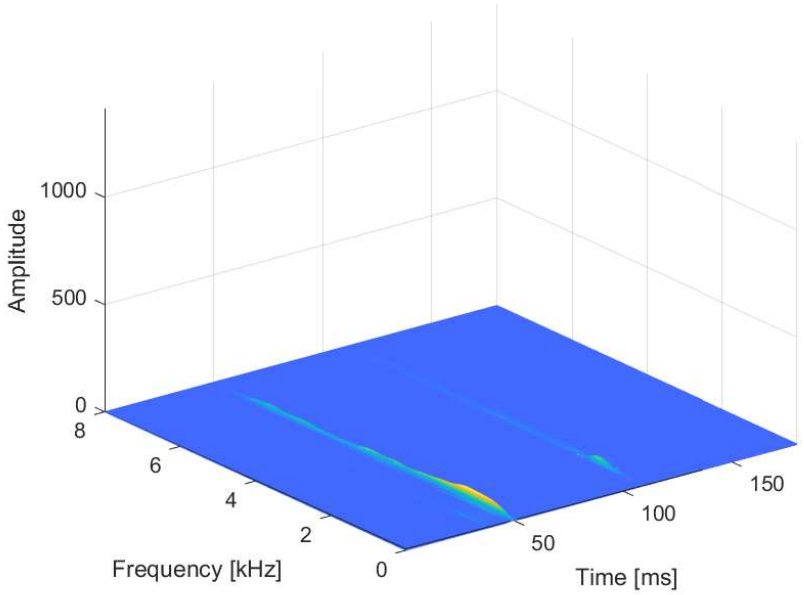

Figure 46: PWVD of the actuation of *K1* without packaging material.

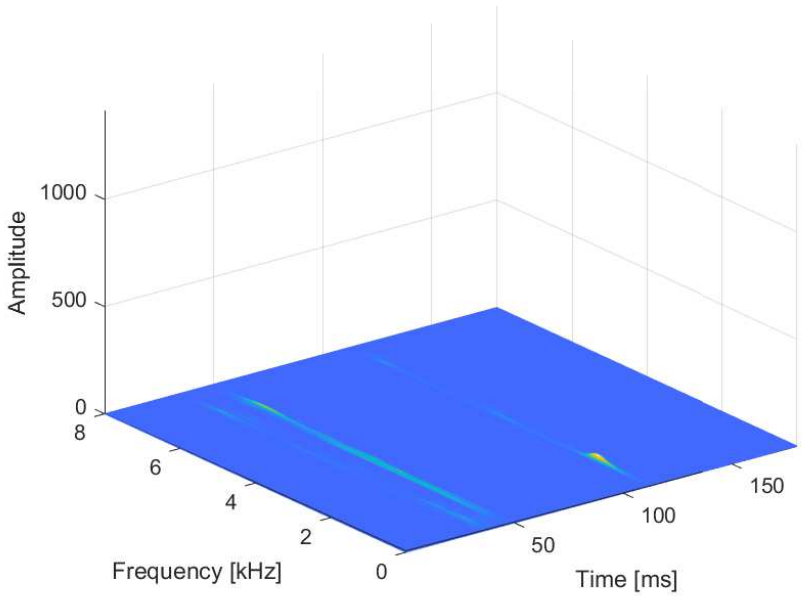

Figure 47: PWVD of the actuation of *K2* without packaging material.

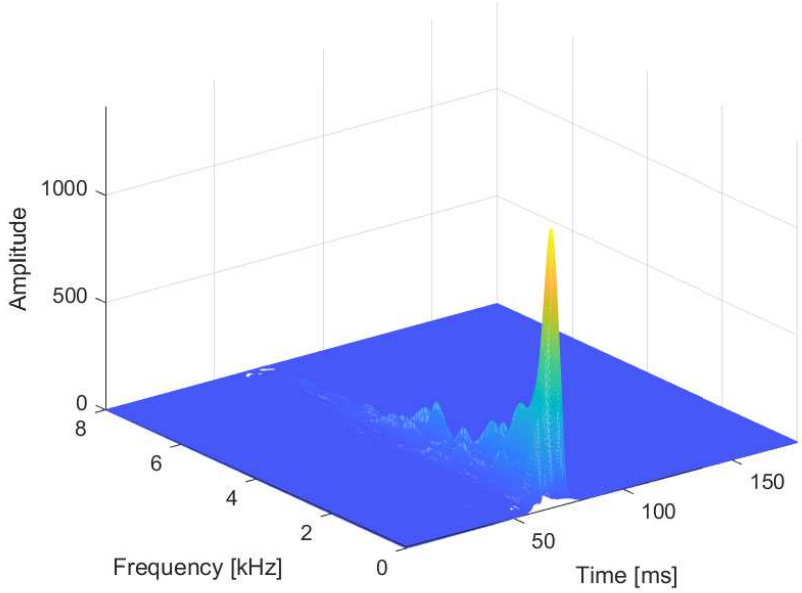

Figure 48: PWVD of the actuation of *K1* with packaging material.

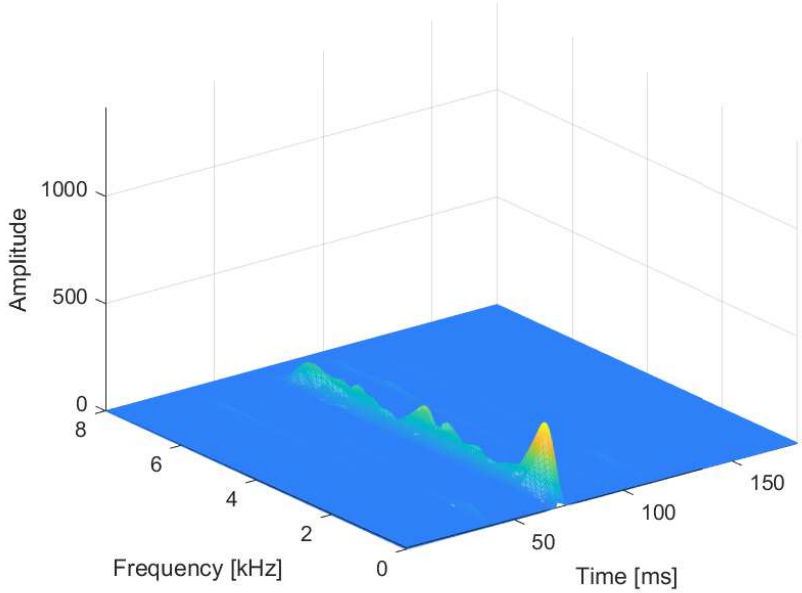

Figure 49: PWVD of the actuation of *K2* with packaging material.

The first observation concerned the effectiveness of this monitoring implementation, which clearly highlighted the cut compared to the other components. As expected, the greater energy contribution of the signal was related to the packaging material cut.

The distributions of the tests without packaging materials did not provide significant information to compare the considered knife models. In both cases, two main fronts were evident, due to the movements of the knife as already reported by the acquired vibrational signal. The forward movement of the knife seemed to give a greater vibrational contribution than the return one, exciting a wider range of frequencies.

From the comparison between the graphs obtained for the tests with the packaging material, instead, a substantial difference in the maximum peak value was evident: for *K2* the maximum value obtained was about 30% of that of *K1*.
It was interesting to note that for *K2* a wider spectral range was excited. This was a sign of a different distribution of the cutting energy for the two knife models, concentrated around a specific frequency for *K1*, more distributed for *K2*. This information was significant related to the results obtained from the comparison tests of knives with different levels of wear, as will be reported.

3.7.4 *Test degradation*

After the verification of the effectiveness of the acquisition system and the analysis of the time-frequency distribution to characterise the different models of knives and the respective behaviours in relation to the cut of the packaging material, an evolution of the previous algorithm was tested, in order to identify a method to monitor knife wear. For this purpose, samples of the same knife model with different wear levels were tested. These samples were used in the test described in Chapter 2, performing 400000 and 2.5 million cutting cycles respectively.
From the inspection carried out, the degradation of the first sample was not significant, resulting comparable to a new knife. For the second sample, however, the wear of the teeth of the knife was evident, so much so that it was no longer considered reliable to perform cutting operations.

Unlike previous tests, a different approach was preferred for evaluating the evolution of the degradation phenomenon. Similar to what was also done in [58], the PWVD was computed by calculating the average of the cycles obtained from the acquired files, after the extraction of the synchronous media.
This solution allowed to eliminate many interferences generated by the raw data, which would have led to a difficult interpretation of the PVWD. It was clear that the interferences theoretically cancel each other out if they were mutually statistically uncorrelated. To this end,

the deterministic part of the signal had to be subtracted. Figure 50 and Figure 51 show the results obtained.

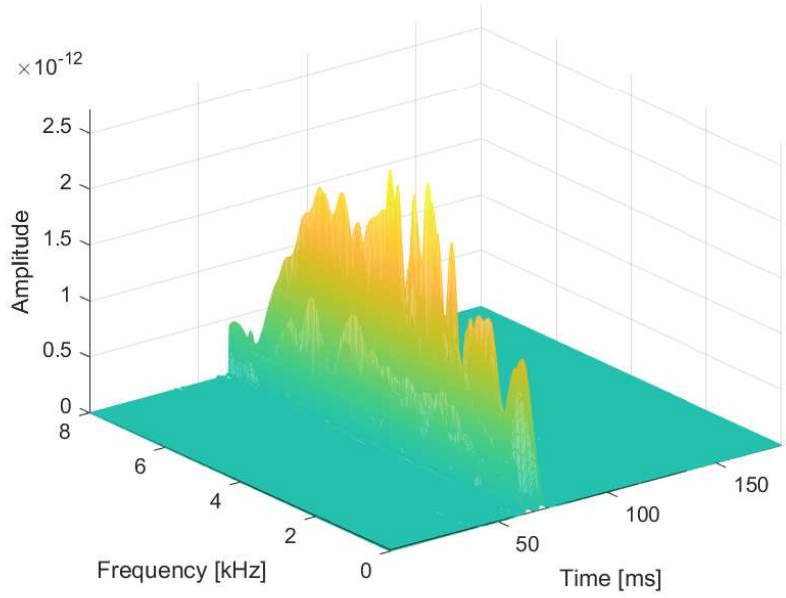

Figure 50: PWVD of the residual signal for the test carried out with the knife that had already performed 400000 cutting cycles.

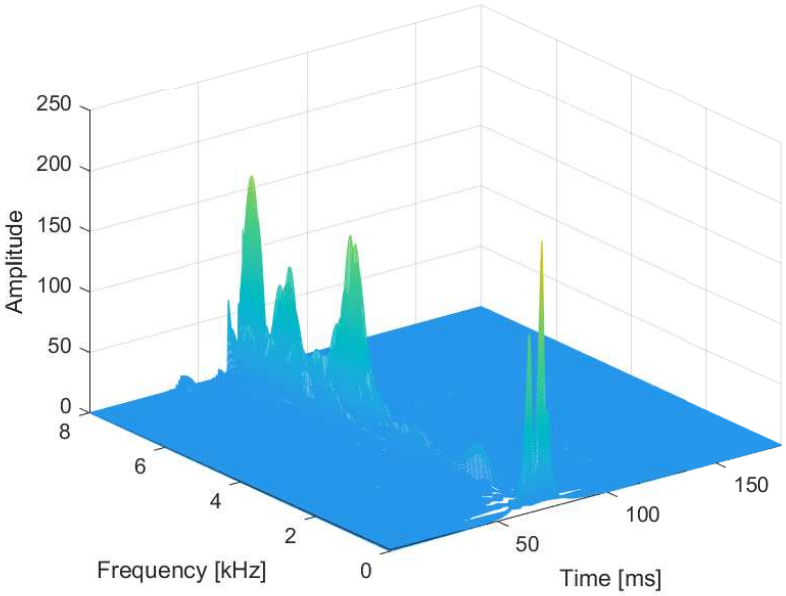

Figure 51: PWVD of the residual signal for the test carried out with the knife that had already performed 2.5 million cutting cycles.

From these tests, it was noted that the vibratory energy of the residual signal calculated for the knife which had already carried out 2.5 million cycles was much higher. The same value was almost irrelevant to the other knife, supported by the fact that this sample could be evaluated comparable to a new component. This effect was attributed to the wear of the knife, which involved an increase in the energy used to overcome the resistance of the packaging material. A part of this energy was dissipated in the mechanical vibrations measurable by the implemented acquisition system.

In addition to the amplitude also the spectral distribution was distinctive for the cutting instant. For the not degraded knife, the energy was well distributed along the considered spectral range, instead for the knife with evident wear specific frequencies were excited. In particular, it was estimated that the peak around 5 kHz was the most significant in relation to the blade degradation level.
The concentration of energy around a frequency led to an increment of the wear action: indeed the degradation of the knife was slight for the first million cuts, but it accelerated close to 2 million cycles.
This was also in accordance with the results obtained for the tests carried out to compare the two different knife models, in fact, according to the industrial application statistics, *K1* had a shorter useful life than *K2* which had a wider spectral distribution of the cutting energy compared to it.

3.7.5 *Spectral moment*

It was possible to demonstrate how the PWVD was able to highlight the characteristics of the knife, but a simpler solution would have been better for the industrial implementation of condition monitoring.
The WVD can be considered as a temporal sequence of spectral energy densities, and therefore it is reasonable to consider that the typical characteristics of the density functions can be evaluated valid also for this distribution. Starting from this idea, it was possible to search for features that could summarise the information already obtained from the time-frequency distribution.
From the probabilistic theory it is known that the distribution functions can be well described by their moments, which for the WVD can be defined as:

$$m_n(f) = \int_0^\infty W_w(t, f)\, f^n \, df \tag{21}$$

where $m_n(f)$ is the n-th spectral moment.
These parameters allowed to describe the characteristics related to

the shape of the curves. For the vibrational study, the most significant seemed to be the zero-order moment, which represented the area under the spectral energy density function, hence the mean instantaneous vibration power dissipated.
The spectral m_0 could be calculated as the average of the values in the interval of interest [59], which in the case of the considered analytical signal became:

$$m_0(m) = \langle |x_a[m]|^2 \rangle_N^I \tag{22}$$

In Figure 52 and Figure 53 the results obtained for the two knives with different wear levels are reported.

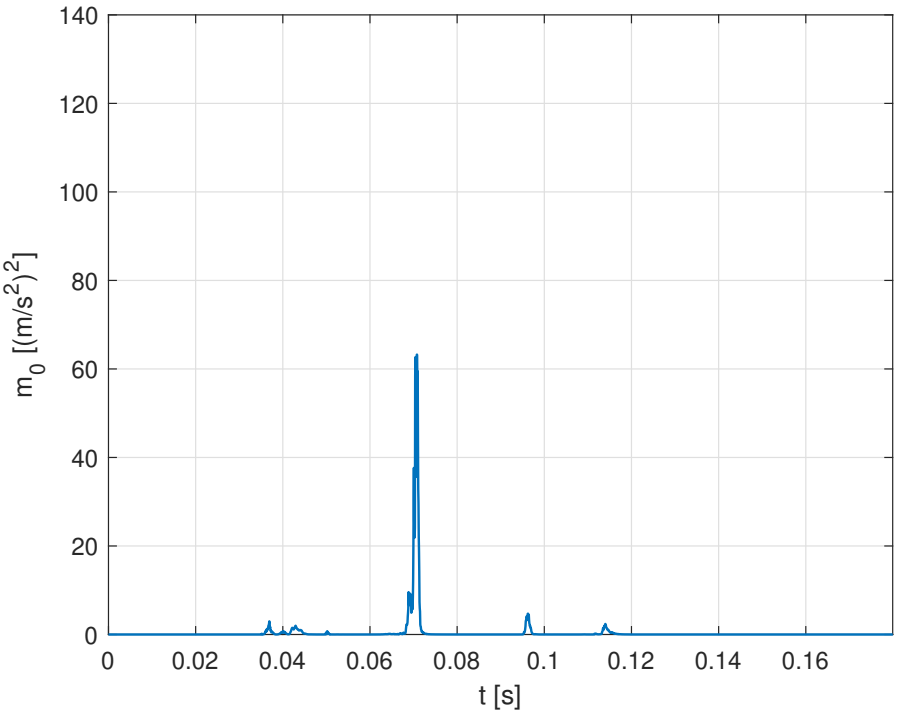

Figure 52: Zero-order spectral moment of the knife with 400000 cutting cycles already performed.

From these curves, it was easy to correlate the cut instant with the peak of dissipation of the vibratory power, as demonstrated also by the previous analyses.
Specifically, it was noted that this value was much higher with the progress of knife wear. For the knife that had already performed 2.5 million cutting cycles, in fact, the vibrational power dissipated was particularly high compared to that of the other sample with negligible wear.
The effect of wear affected two parameters of the tooth profile:

1. Rounding of the cutting edge;
2. Irregularity of the profile and depth of the teeth.

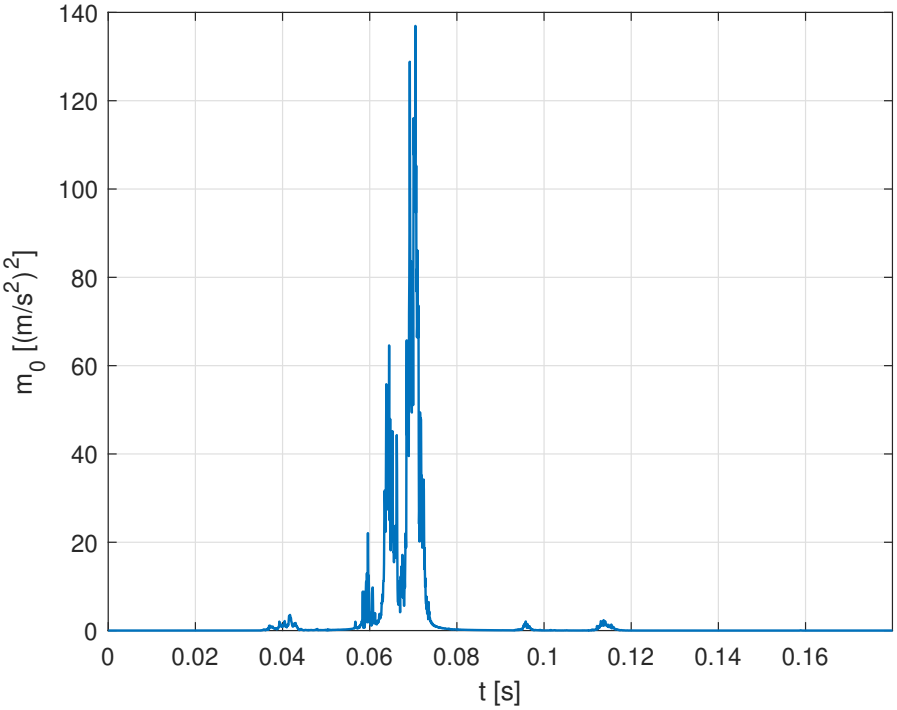

Figure 53: Zero-order spectral moment of the knife with 2.5 million cutting cycles already performed.

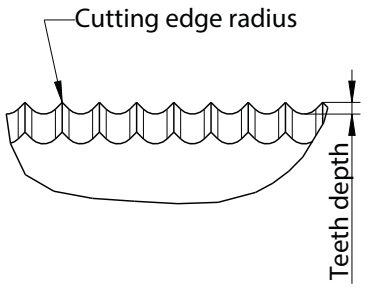

Figure 54: The main geometric parameters of the teeth of the knife influenced by wear.

A smoothed cutting edge led to an increase in the rubbing of the packing material on the sides of the blade, and therefore of the energy needed to perform the cut. In fact, a sharp knife facilitated the creation of the cutting surface and therefore the penetration of the material, reducing its contact.
At the same time, the irregularity of the profile of the teeth led to high temporal dispersion of the triggering of the cutting surfaces along the length of the blade. This affected the succession of the cutting process by increasing the dissipated vibratory energy.
These effects were also identifiable in the curves of the zero-order moment, not only from the increase of the peak value but also from the amplitude and the presence of further significant peaks in the neighbourhood of the cut instant.

To confirm this interpretation it was possible to visually evaluate the cutting profile obtained using knives with different levels of wear. As already known from the industrial application, degraded knives caused irregularities in the edges of the packaging material, sometimes leading to rips due to deformation of the material rather than a clean cut.

This information was found to be sufficient for the industrial implementation of a knife degradation monitoring solution.
Wear information had to be easily transmitted to technicians and maintenance operators, without the request for curve interpretation. To improve the notification on the status of the knife, a warning system based on thresholds was implemented.
Based on the results obtained, it was possible to define ranges indicative of the progress of knife degradation in reference to three levels. A graphical representation of this is shown below in Figure 55.

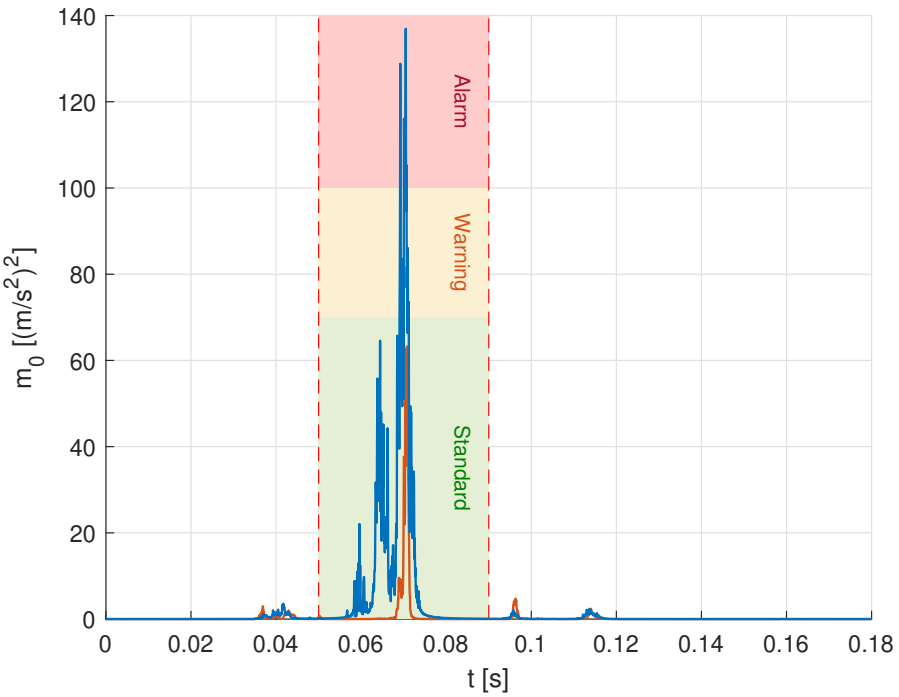

Figure 55: The knife wear level was defined with reference to the m_0 value. The zero-order spectral moment for the worn knife (blue line) reached the alarm area, instead it remained in the standard range for the sharp knife (orange line).

3.8 CONDITION MONITORING

From the vibrational data, it was possible to obtain information on the cutting process and in particular on the level of wear of the knives

used in the cutting stations of the filling machines.
The acquisition system proposed for measuring vibrations during the cutting process was implemented with the aim of proposing it also for industrial applications. The processing of the acquired signals involved two approaches depending on its purpose:

1. The PWVD for the study of the characteristics and events that occurred during the cutting process;

2. The evaluation of the zero-order spectral moment for the definition of the knife wear level.

Thanks to the time-frequency distribution of the first solution, it was possible to study in detail the energy contribution of each event of the cutting process, resulting adequate in a context of investigation of the process. This allowed to identify different distributions and characteristics depending on the model and/or the wear level of the knife.
The second approach, instead, made it possible to reduce the required computational resources, extrapolating useful information to define the level of knife wear. The evaluation of the zero-order moment in relation to the definition of some acceptability thresholds, therefore, constituted an adequate solution for industrial implementation.
The condition monitoring model turned out to be well defined by the procedures described above.

The proposed condition monitoring system was implemented on an industrial application in order to evaluate its effectiveness. With a greater level of generalisation, it is however possible to apply the same procedures to investigate and monitor the conditions of different industrial processes and components. This model allows to overcome the concept of condition monitoring strictly related to rotary machines, extending their applicability to the more general cyclostationary stochastic processes.
A generalisation of the proposed condition monitoring model for process and tool wear investigation is shown in Figure 56.

3.9 CONCLUSIONS AND DELIVERABLES

The need to monitor knife wear led to the study of vibrational signals of the cutting operation. Nevertheless, the vibrational approach is typically used to monitor rotary systems.
Starting from these premises, an alternative method of investigation was proposed based on the evaluation of the cutting operation as a cyclostationary stochastic process. The vibrational signals were then analysed according to the PVWD which allowed to highlight characteristics related to the vibrational energy dissipated as a function of

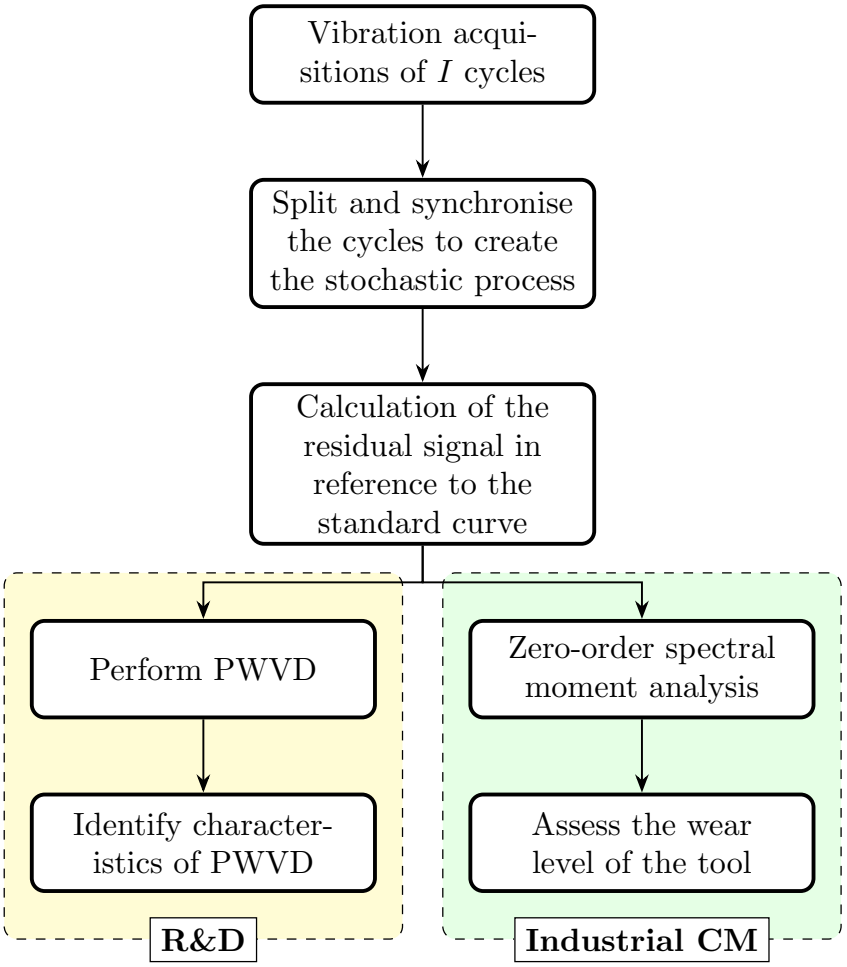

Figure 56: Proposed condition monitoring model to study cyclostationary stochastic processes and to assess the wear level of the tool based on vibrational measurements.

time and frequency.
It was thus possible to create an investigation system useful for studying the vibrational behaviour of the process and of the component which in the specific case of packaging material cutting led to important considerations including:

1. Concentration of vibrational energy at the instant the cut was performed;
2. By comparing two knife models it was noted that a greater bevel angle excited a wider spectral range, better distributing the dissipated vibrational energy.;
3. The comparison of knife distributions at different wear levels showed an increase in vibrational energy specifically around 5 kHz.

The study of the proposed time-frequency distributions seems to be applicable for the study of processes and components, resulting particularly useful in an R&D context.
However, the industrial request was focused on monitoring the wear of the tool used for cutting the packaging material. In this context, it is also essential to evaluate the computational resources required by the data acquisition and analysis system.
For these reasons, an alternative method was proposed in order to extrapolate the essential information to assess the level of tool wear based on the evaluation of the zero-order spectral moment that was related to the mean instantaneous vibration power dissipated. From the comparison of samples with different wear levels it was possible to define important characteristics that correlated m_0 to the degradation of the knife:

1. A worn knife caused a higher peak value at the cut instant due to the increasing difficulty in triggering and propagating the cutting surface;

2. The irregularity of the profile of the degraded blade teeth implied a worsening of the edges of the packaging material, which could also be detected by the greater width of the curve correlated to the cut and by the presence of numerous other peaks.

Since the design phase of the acquisition system, the industrial application was taken into consideration, in fact the hardware was chosen compatible with the one already proposed in the previous study. In this way, it was possible to integrate the two solutions into a single system to monitor the cutting process and the degradation of the knife.

The approach based on the vibrational energy released by the mechanical system can also be considered valid for other similar industrial applications, for example metal cutting processes. But its scope of applicability can be extended more generally to the study of mechanical systems that present periodic operations and the need to monitor the degradation of components and/or the occurrence of failures during their working life.
In this context, it is also possible to foresee an evolution of the proposed system through the implementation of artificial intelligence techniques such as machine learning or deep learning.[60, 61, 62]
In this case a study based on the image obtained from the 2D representation of the PWVD that links the graphical representation to the state of the system would be conceivable.
The investigation could also be improved by testing components with specific defects, in order to map their energy characteristics.

4

VIBRATIONAL MONITORING OF BEARINGS FOR ASEPTIC ENVIRONMENTS

The following paragraphs report the vibrational study conducted to monitor the conditions of some models of rolling bearings installed in filling machines used in the food industry. The study developed the aspect of the investigation of bearing conditions as a method of product innovation on the one hand and as an industrial condition monitoring approach on the other.
The test rig used to compare the characteristics of the considered samples, the acquisition system of vibrational signals and the results obtained are described.
It is important to consider that the research was carried out always keeping in mind the industrial application, but proposing a general approach to innovation and monitoring of rolling bearings.

4.1 INTRODUCTION

Following the study focused on the implementation of a system for monitoring the conditions of the cutting process and the level of wear of the knife, a new aspect of condition monitoring related to the industrial field was studied. As already underlined in the previous chapters, the design of a condition monitoring system allows to increase the know-how on the processes and the behaviour of the components. Starting from these characteristics, an evolution in the field of industrial component innovation was proposed in order to improve its reliability, also influencing design choices and machine maintenance specifications.

As in the previous cases, the study was conducted taking into account the real industrial cases related to the food and packaging industry, allowing to practically apply the proposed approaches. In particular, the study conducted to innovate a rolling bearing model was considered.
This component was installed in the mechanical system that allowed to form, seal and separate the packaging material in the final part of the filling machine. Since it was a food application, it was essential to guarantee that the process was aseptic, a feature also influenced by the interaction of mechanical components with the product and the packaging material.
Among the possible contaminants, one of the most frequent was the grease used to preserve the functionality of rolling bearings.
In order to reduce its influence, a new bearing model was designed

that did not require periodic greasing operations. To assess whether its functionality was comparable to that of the model already installed in the filling machine, durability tests were performed.
Precisely in this context, condition monitoring was integrated, proposing a methodology to compare the two different models.

The use of vibrational measurements to monitor the occurrence of component damage is well known for monitoring rolling element bearings.[63, 64, 65, 66]
Also for the research proposed here, a similar approach was adopted, but its purpose was extended to a different investigation than the simple use for monitoring. The main purpose of the tests carried out was in fact to compare the reliability of bearings that were periodically greased with that of non-greased bearings as the number of operating hours increased. Thanks to the data acquired from this study it was later possible to define also a monitoring model that could be implemented in industrial applications.

4.2 TEST RIG

Also for this study, it was necessary to design and implement a test rig that would allow simulating the operating conditions of the bearings. To test more samples at the same time, 12 stations were provided, each actuated by a pneumatic piston. In order to best replicate the operating behaviour of the system, the same supporting and fastening components of the bearings installed in the reference machine were used. In the upper end of the shaft that fixed the inner ring of the bearing, the grease fitting also used in the industrial application to perform the periodic greasing operation was installed. Figure 57 shows the assembled system.

The bearings under study were part of a chain system composed of several stations connected by some links. Each of these stations ran along a profile thanks to the bearings that were thus subjected to periodic loading cycles.
To simulate the real dynamics the bearings were pushed by pneumatic pistons against a cam, making them spin. This solution also made it possible to load the samples under test with a force comparable to that to which they were subjected in the industrial application, controlling it through the adjustment of the compressed air pressure of the actuators.

The environmental operating conditions were also replicated. The considered bearings, in fact, worked in an environment at a temperature of 55 °C and were subjected to periodic washing cycles used

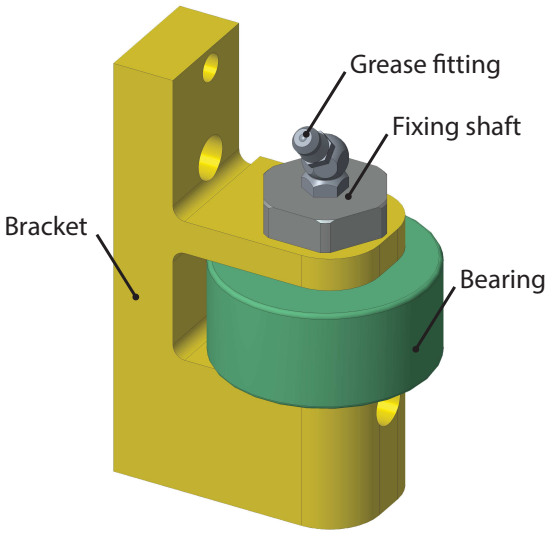

Figure 57: The same supporting and fastening components of the bearings installed in the reference machine were used for each station of the test rig.

to guarantee the cleaning of the mechanical system that formed and separated the packages in the final part of the filling machine. The thermal cycles to which the bearings were subjected, the environmental humidity and the chemical action of the detergents, in fact, had an important effect on the durability of the bearings and grease.
The 12 stations were therefore installed inside a chamber in which the temperature was controlled and modulated to maintain the set-point and water was sprayed to keep the environment humid. The diluted industrial detergent was periodically sprayed into the chamber to simulate cleaning operations.
The test rig then appeared as shown in Figure 58.

4.2.1 *Test rig parameters*

The bearing load cycle was characterised by a period of contact with the cam followed by one of inactivity in which the bearings were not subjected to any force. This idle interval, compared to the real cycle, was reduced in the test rig guaranteeing in any case the stop of the bearing before the next contact with the cam. Attention was paid to this detail because if the bearing was not completely stopped, the difference between its tangential speed and that of the cam would have been lower at the moment of contact, reducing the inertial effects to which the samples were subjected.
The characteristics of the test are summarised in Table 11.

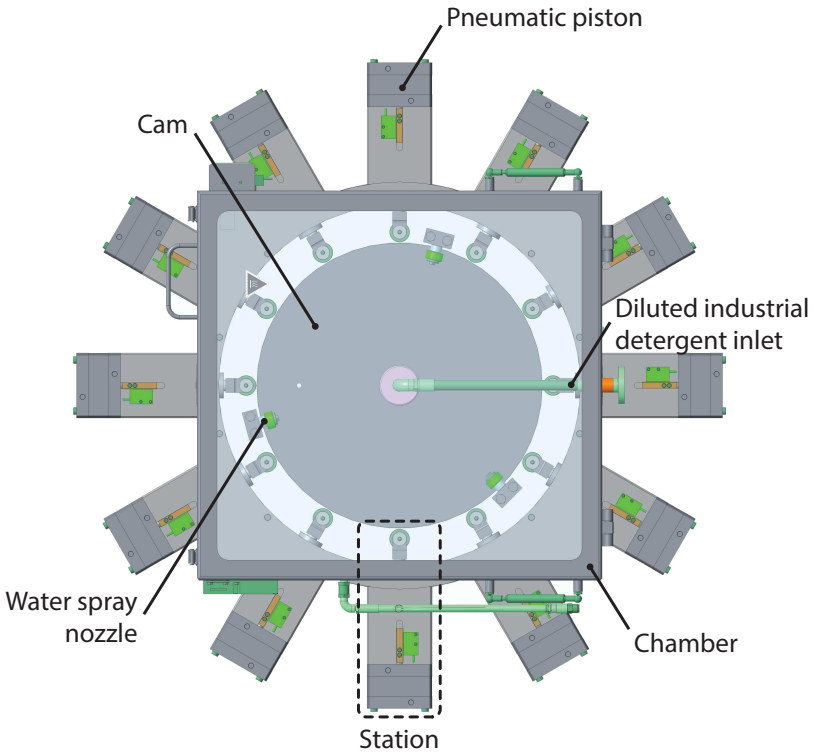

Figure 58: The test rig used to emulate the load cycles and environmental conditions to which the bearings were subjected in the reference machine.

4.2.2 *Bearings samples*

The tests were conducted on two models of rolling bearings:

1. *B1*: the standard bearing model that was used on the reference machine.
2. *B2*: the new proposed model compared with the standard one.

The two bearing models had identical geometric characteristics, but for *B2* there was no need for periodic greasing operations, unlike *B1*. The geometrical characteristics of the two bearing models are shown in Table 12.

Since the test was mainly aimed at the study of the new bearing model compared to the one adopted as standard, 10 bearings *B2* and 2 bearings *B1* were installed in the test stations.
During the test campaign, the samples of the reference model required that periodic greasing operations be performed to maintain the same operating conditions that they would have had in the real machine. For the purposes of the study on the influence of bearing greasing, it was decided to perform this operation also for 2 of the

Table 11: Main parameters of the test rig.

Parameter	Value	Unit
No. of station	12	
Cam speed	230	°/s
Tangential speed	930	mm/s
Contact period	0.8	s
Release period	1.6	s
Cycle time	2.4	s
Contact force	3200 ± 50	N
Release force	0	N
Water spray	1 s every minute	
Washing cycle	Once a day	
Greasing operation	Once a week	

Table 12: Main geometrical characteristics of the bearings.

Parameter	Value	Unit
Inner ring diameter	20	mm
Outer ring diameter	52	mm
Width	25	mm
Balls diameter	7.938	mm
Contact angle	30	°
Pitch diameter	34.50	mm
No. balls	8	

10 *B2* bearings, in addition to that already scheduled for the other model.
The distribution of the bearings was therefore like that shown in Table 13.

Table 13: Bearing arrangement in the test rig stations.

Model	Position	Greasing
B1	1, 7	•
B2	2, 8	•
	3–6, 9–12	

4.3 DATA ACQUISITION

As already mentioned, the monitoring of bearing conditions during the test campaign was based on vibrational signals. To do this, a data acquisition system similar to the one implemented to monitor the vibrations in the study described in Chapter 3 was used.
Vibrational measurements generally involve the use of an accelerometer with the measuring axis along the radial direction of the bearing, therefore mounted on the outer side of its housing. For the considered application, this configuration was not possible because the outer ring was the rotating one and the layout of the station and its functionality did not allow to fix the sensor as in the standard solutions.
The idea was to fix the accelerometer in the thread used for the grease fitting, in the upper end of the fixing shaft, in order to propose a suitable solution also for a subsequent implementation on the industrial machine. As can be guessed, the evaluated measurement axis was the one with the same direction as the bearing radial axis, as shown in Figure 59.

Acquisitions were carried out weekly, when the greasing operations of the bearings were scheduled. On this occasion the bearings were forced against the central cam individually to make them spin, so as to acquire the vibratory signals for a duration of about 30 s. This timing was chosen in order to obtain a sufficiently high-frequency resolution for the considered study phase. For the industrial implementation of the proposed condition monitoring system, this timing could be decreased, in order to reduce the amount of data to be managed and therefore also the storage and calculation resources.

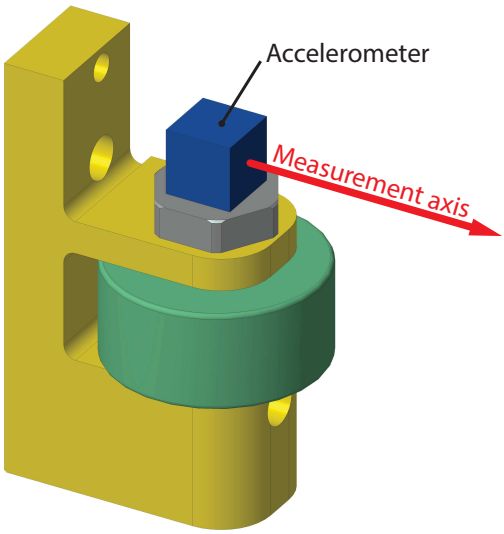

Figure 59: Accelerometer mounted on the bearing fixing shaft. The selected measurement axis was the one with radial direction.

4.3.1 *Data acquisition system*

The implemented data acquisition system was almost identical to that used for the vibrational acquisitions in the previously described study. The characteristics of the accelerometer can be found in Table 9, whereas those of the NI-9232 module in Table 10a.
However the controller used was a NI cRIO-9063 with characteristics similar to those of the NI cRIO-9068 installed in the previous case studies. Its characteristics are shown in Table 14.

Table 14: Main characteristics of the controller NI cRIO-9063. [35]

No. of slots	4
Processor	ARM Cortex A9
	667 MHz Dual-Core
FPGA	Xilinx Zynq 7020
Memory	512 MB
RAM	256 MB

4.4 ACQUISITIONS

The only signals acquired for monitoring purposes were the vibrational signals, from which it was possible to obtain interesting information only after the conversion from the time domain to the frequency domain. For the sake of completeness, the acquisitions per-

formed to calibrate the actuation force of the pneumatic pistons that pushed the bearings against the central cam are also reported.

4.4.1 *Bearing vibrations*

Although the macroscopic defects of the bearings could have a considerable influence on the raw signal acquired by the accelerometer, little information could be extrapolated for the purposes of predictive maintenance. In fact, observing the accelerometer signal curves, of which an example is shown in Figure 60, it was not possible to notice any significant characteristic that could define the state of the bearing.

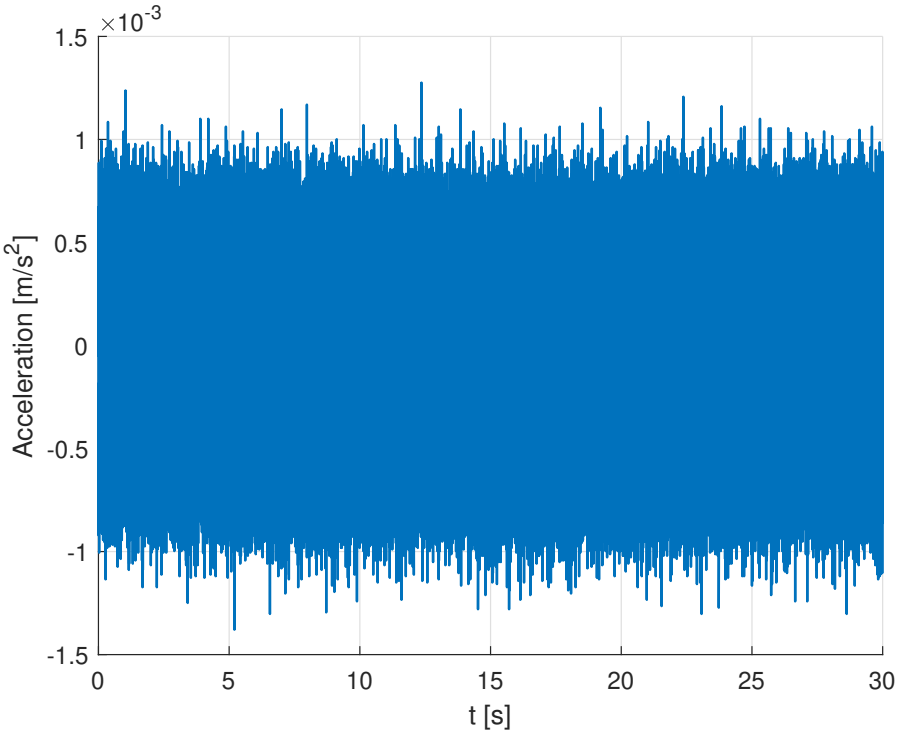

Figure 60: An example of the raw signal acquired by the accelerometer with the bearing pushed against the rotating central cam.

4.4.2 *Pushing force*

Before starting the test campaign, it was necessary to adjust the compressed air pressures so that the pneumatic pistons generated a pushing force equal to that to which the bearings were subjected in the industrial application. An example of these measurements is shown in Figure 61.

To ensure a good emulation of the working conditions, the force to which the bearings were subjected had to remain around 3200 N. The

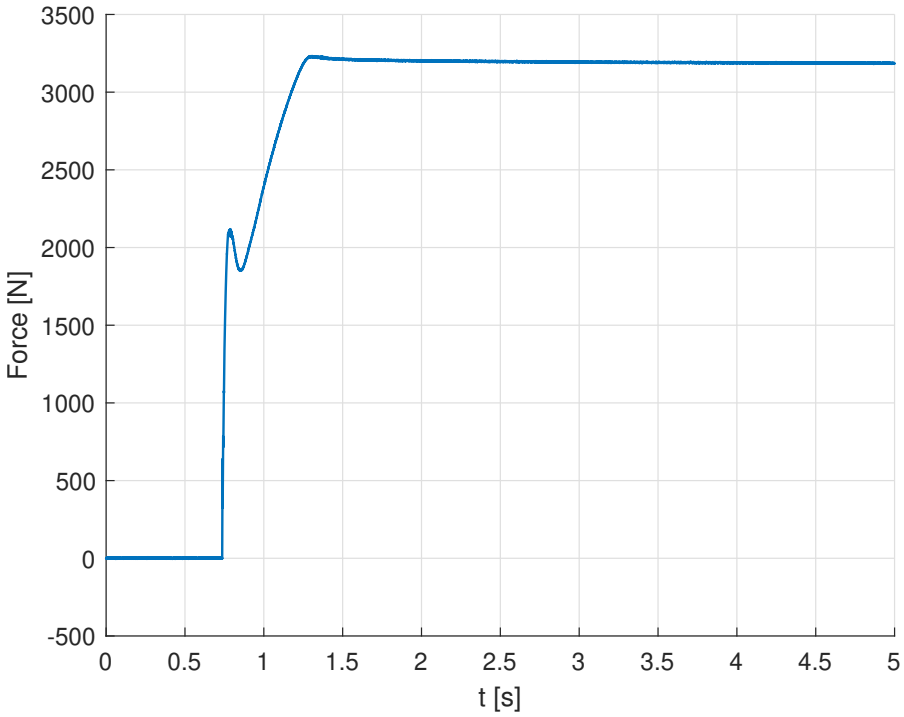

Figure 61: The force generated by the pneumatic pistons to push the bearings against the central cam.

resulting curve did not present any particular overshoot that would have compromised the durability of the samples.

4.5 ANALYSIS OF VIBRATIONAL DATA

In the practice of bearing condition monitoring, the envelope of the vibrational signal is performed before using the FT for the conversion from the time domain to the frequency domain. [67, 68]
The envelope analysis allowed to demodulate the signal in order to obtain a representation of the pulse train, so as to highlight the frequencies related to specific faults, providing more diagnostic information than the raw signal analysis. [69, 70]

Starting from this approach, further considerations were developed to monitor the condition of the bearings during the test campaign.
In order to compare the behaviours of the tested components and monitor the evolution of their conditions as the hours of operation increased, the spectral curves were reported in waterfall plots.
The following paragraphs compare the 3 different test configurations summarised in Table 13, referring to the curves obtained during the test campaign. Explanatory examples of the results are shown in Figure 62, Figure 63 and Figure 64.

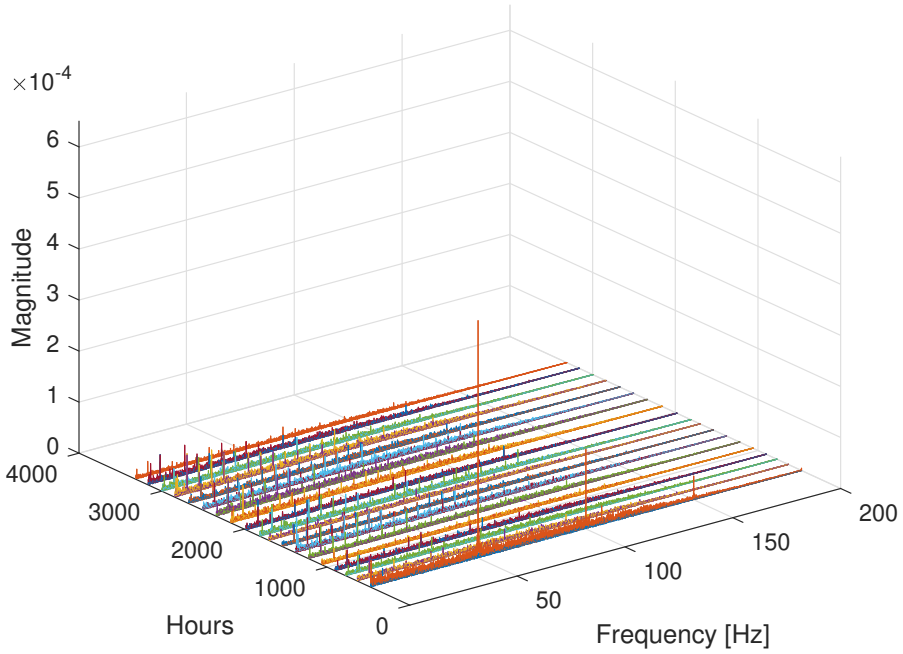

Figure 62: Waterfall plot of spectral signals for a *B1* bearing with periodic greasing operations.

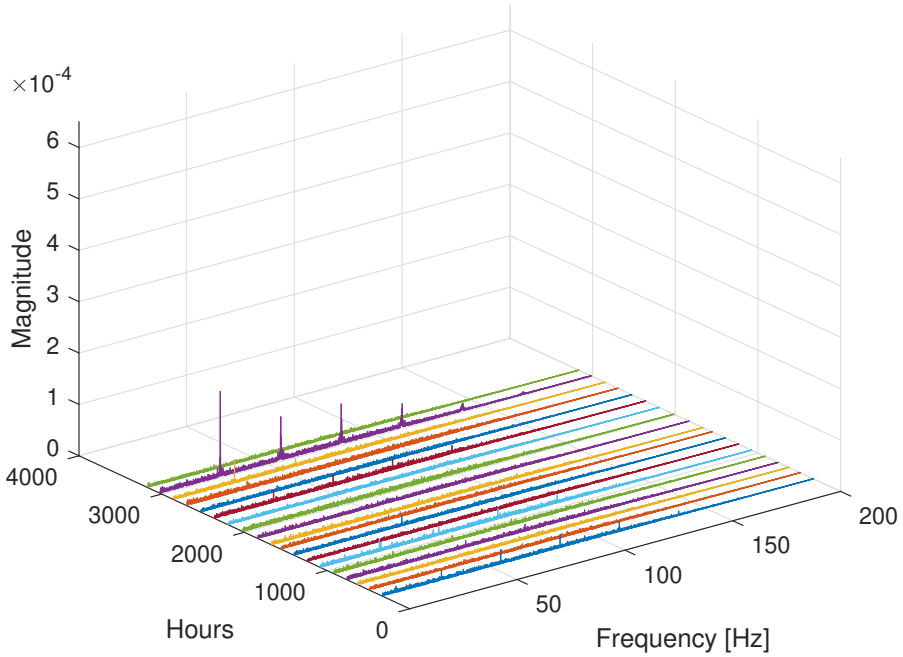

Figure 63: Waterfall plot of spectral signals for a *B2* bearing without periodic greasing operations.

4.5.1 *B1 vs B2*

The purpose of the test campaign was to compare the new proposed model of bearing with the standard model. In order to evaluate the behaviour of the two components in their standard operation condi-

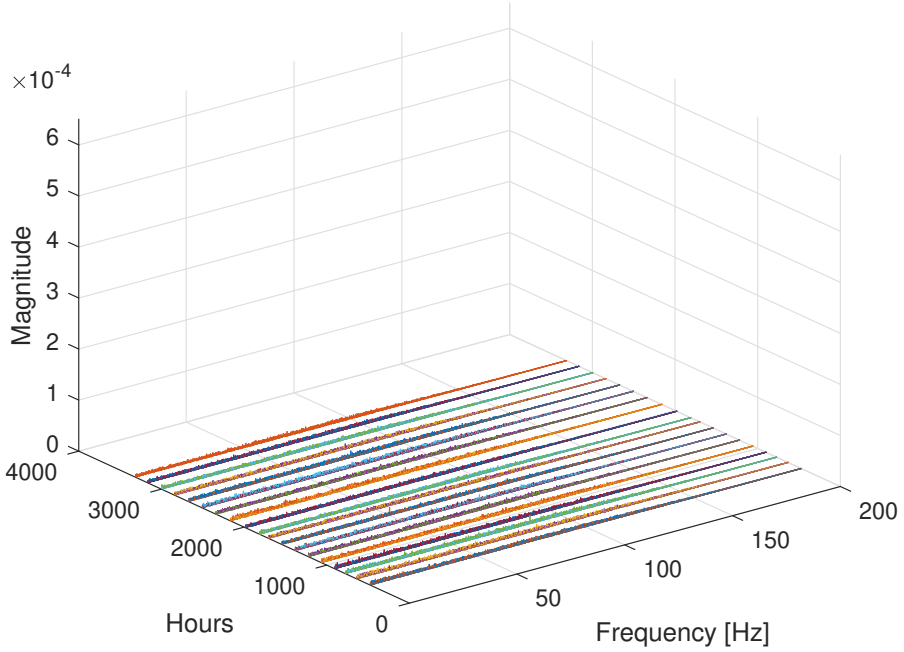

Figure 64: Waterfall plot of spectral signals for a *B2* bearing with periodic greasing operations.

tions, the waterfall plots in Figure 62 and Figure 63 were examined. It was easy to see how *B2* had a vibrational amplitude generally lower than the previous model. In fact, the waterfall plot of *B1* showed that some frequencies were already excited in the initial phase of the test. This observation allowed to evaluate how the proposed new model had less vibrational dissipation, indicating a better stability of the rotation and a lower energy demand to spin the bearing.
However, in the last hours of testing of bearing *B2*, some peaks in the spectrum related to the effect of component wear emerged. From this point of view, *B1* seemed to be less sensitive to the degradation inevitably generated by the repetition of the load cycles.

4.5.2 *Greased vs non-greased*

In addition to the performance comparison of the two tested bearing models, the influence of periodic greasing operations on component degradation was investigated. For this purpose, periodic greasing was also carried out on two samples of bearing *B2* for which no maintenance operation was foreseen during normal operating life.
Comparing Figure 63 with Figure 64 it was possible to detect a clear improvement in terms of wear resistance for the station with periodic greasing.
Therefore, periodic greasing also seemed to affect the operating life of the proposed new model, significantly reducing the effects of the

degradation as the hours of operation increased.

Thanks to the acquisitions performed before and after the greasing of the stations concerned, also for the *B1* model it was possible to notice how this operation influenced the vibrational behaviour of the bearings. In particular, it was found that during the test campaign this model occasionally reported significant peaks in the vibrational spectrum, which were attenuated after the greasing operation.
From this result, it was possible to further highlight the need for the *B1* model to be subjected to periodic greasing operations in order to maintain its functionality. A worsening of the vibrational behaviour due to the degradation of the grease would have in fact led to a greater dissipation of energy generated by the friction of the rolling elements on the bearing rings, and the consequent premature wear of the component.

4.5.3 *Faults*

In order to preserve the test rig and evaluate possible failures to the bearings under test, the piston stroke was monitored at each load cycle using a linear encoder. In the event that a bearing broke, this measurement would exceed the limit set for normal operation, generating an alarm that would disable the station.
Thanks to this warning system, two faults were reported during the test campaign, both on non-lubricated *B2* bearings. The final state of the bearings is documented in Figure 65.

In the case of the break of the bearing shown in Figure 65a a crack in the inner ring was the cause of the fault whose warning was reported by the monitoring system of the test rig after only 1300 hours of operation. Instead, the bearing defect shown in Figure 65b was less severe and was reported after more than 2500 hours of operation.

The evaluation of the waterfall plots of the vibrational spectrum for these two stations, also shown in Figure 66, was particularly interesting.

In both cases, it was possible to notice how the vibrational content increased in the last acquisitions made before reaching the fault.
In the case of the broken inner ring, the signal was very high compared to that measured during normal bearing operation. The first symptom of the triggering of the crack could be perceived already from the acquisition carried out after 800 hours of operation. The progressive increase of the signal was an indication of the evolution of the crack through the inner ring.
Even in the case of damage to the lateral seal of the bearing, signifi-

(a)

(b)

Figure 65: The defects occurred during the test campaign concerned two *B2* non-lubricated bearings: for (a) a crack on the inner ring of the bearing was detected, while for (b) the lateral seal was broken.

cant variations could be detected despite the damage was less significant than the previous one. For this bearing the damage caused a progressive leakage of the grease which was not restored since no greasing operation was scheduled during operation. This caused greater friction, thus accentuating the wear and the dissipation of vibrational energy.
These evaluations would have allowed the definition of a basic condition monitoring system based on the threshold values of the vibrational spectrum, but an alternative solution was proposed in order to obtain more information on the status of the components.

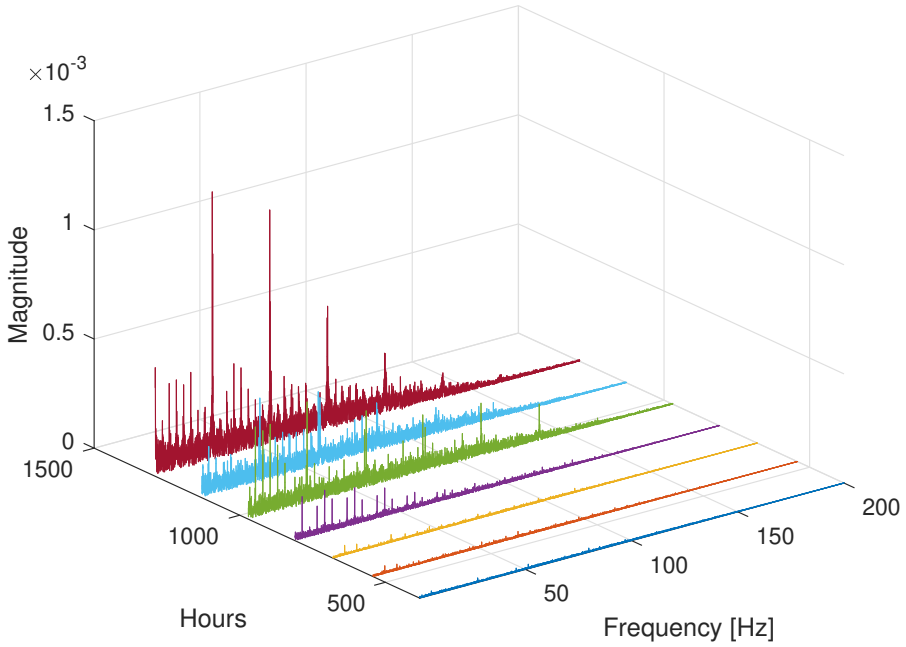

(a)

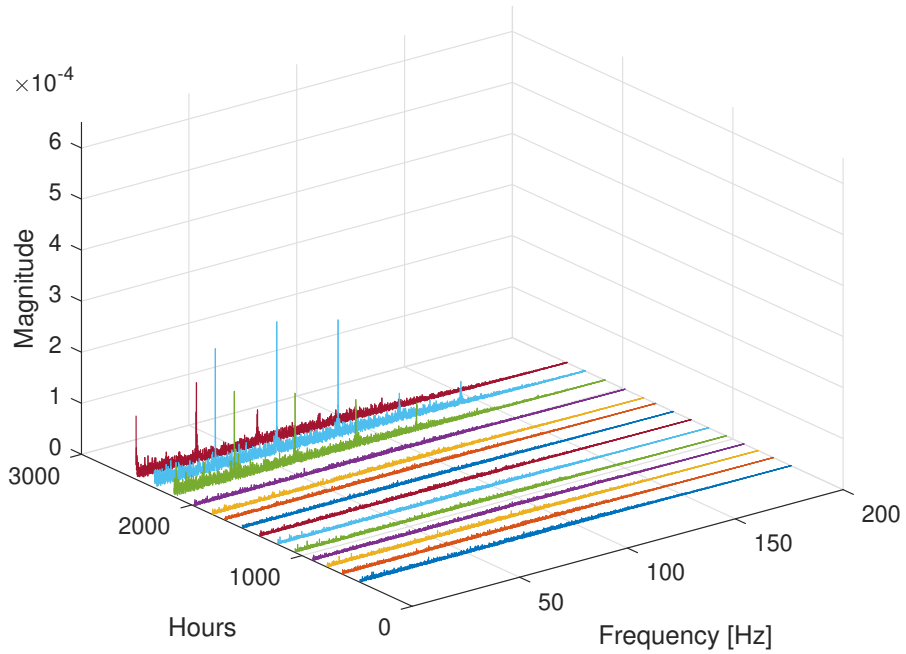

(b)

Figure 66: Waterfall plots of spectral signals for the bearing on which (a) the inner ring failure or (b) lateral seal failure occurred.

4.5.4 *Condition monitoring*

To diagnose the type of faults typical of rolling bearings, specific frequencies of the components are often evaluated, also influenced by

their geometric characteristics.
For a general case the equations used are:

$$BPFI = \frac{N\,|f_o - f_i|}{2}\left(1 + \frac{D_b}{P}\cos\theta\right) \tag{23}$$

$$BPFO = \frac{N\,|f_o - f_i|}{2}\left(1 - \frac{D_b}{P}\cos\theta\right) \tag{24}$$

$$FTF = \frac{f_o + f_i}{2} + \frac{f_o - f_i}{2}\frac{D_b}{P}\cos\theta \tag{25}$$

$$BSF = \frac{|f_o - f_i|}{2}\frac{P}{D_b}\left[1 - \left(\frac{D_b}{P}\cos\theta\right)^2\right] \tag{26}$$

where:

- *BPFI*: is the ball pass frequency of the inner ring.
- *BPFO*: is the ball pass frequency of the outer ring.
- *FTF*: is the fundamental train frequency.
- *BSF*: is the ball spin frequency.

and f_o and f_i are the rotation frequencies of the outer and inner ring respectively, N is the number of rolling elements, D_b is the diameter of the rolling elements, P is the pitch between opposite rolling elements and θ the contact angle. Some of these parameters are shown in Figure 67.

In the case of the bearings considered, the equations were simplified by evaluating $f_i = 0$.
These frequencies were therefore calculated by referring to the geometrical characteristics reported in Table 12, in order to examine specific ranges of the vibrational spectrum.
Especially in the presence of defects, the loads for the individual rolling elements vary according to their position in the bearing, causing different rolling speeds. On the other hand, the cage forces these elements to remain at a uniform distance, causing them to slip. In such cases, the signals are not strictly periodic, as assessed in the theoretical formulas that are closely related to pure rolling. [71]
Bearing in mind the influence of this phenomenon, some neighbourhoods centred on the calculated frequencies were taken into consideration in order to identify the peaks corresponding to the specific fault.
Thanks to these assessments, it was possible to identify damaged bearings during the test campaign and to define a condition monitoring approach.

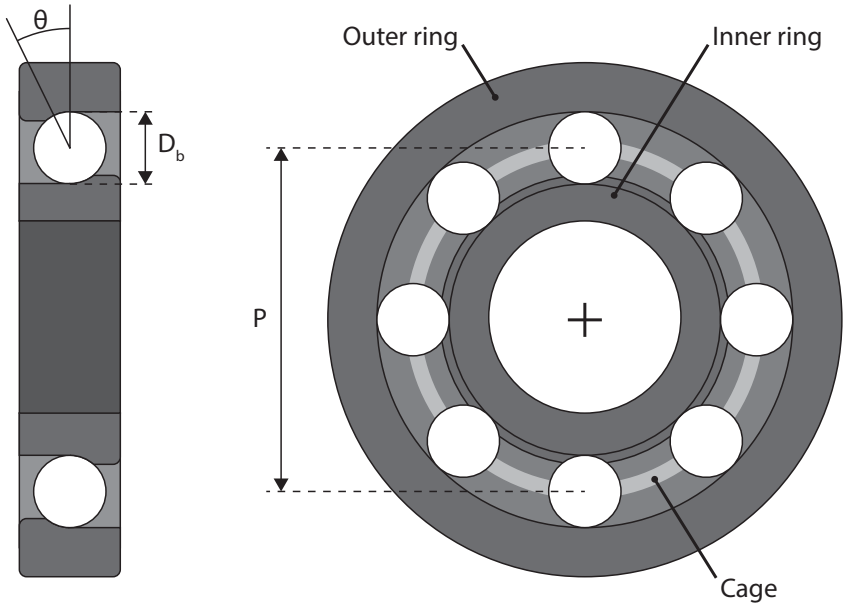

Figure 67: Indication of the geometric parameters used for calculating the characteristic frequencies of the bearings.

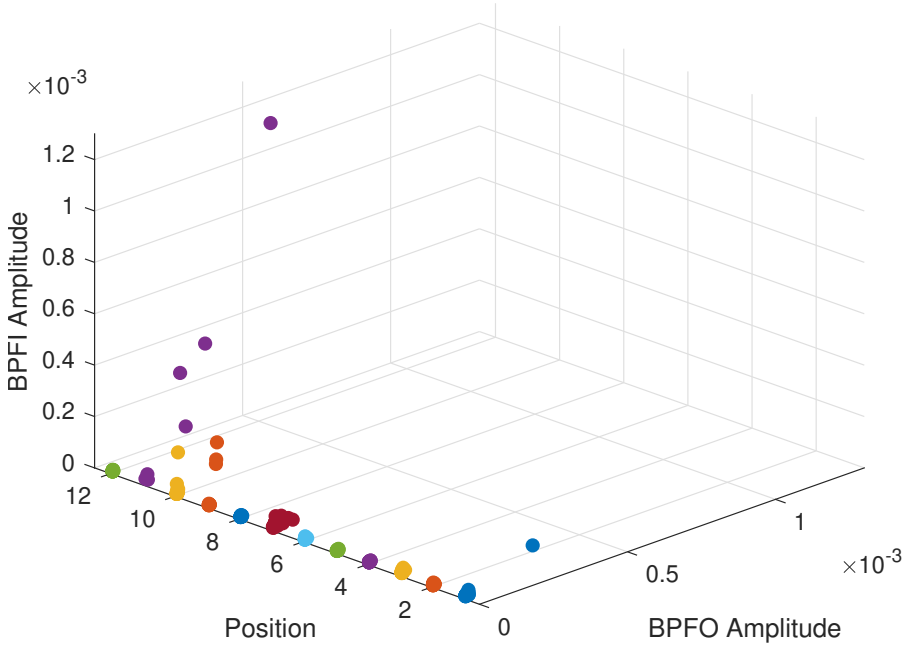

Figure 68: BPFI vs BPFO plot for all the stations of the test rig. Position 11 refers to the bearing that presented the fault due to the crack of the inner ring, while in position 9 there is the bearing that presented the breaking of the lateral seal.

The most significant information for monitoring the status of the samples was obtained from the evaluation of BPFI and BPFO, which were summarised in a single plot, as shown in Figure 68.

This representation allowed not only to identify the damaged components but also to study their behaviour and to highlight the differences between the two bearing models examined.
It was easy to identify the failing bearings during the test campaign, as they showed an increase in the BPFI amplitude. This value was particularly high for the bearing in position 11, the same shown in Figure 65a, which presented a defect on the inner ring to which BPFI referred. The damage exhibited by the bearing shown in Figure 65b was not related to a specific ring, but it was nevertheless possible to note for the position 9 an increase in the BPFI amplitude as the grease leaked out. However, each defect also excited other characteristic frequencies, although only to a limited extent, as was also noted for BPFO.
The behaviour of the two tested bearing models was also interesting. As reported in Table 13, the two samples of model *B1* were mounted respectively in station 1 and station 7. Looking at Figure 68, it was noted that for these samples there was a greater dispersion of the points, with a particular increase in the BPFO coordinate. This behaviour confirmed the significant dependence of these bearings on the periodic greasing maintenance operation, as was already highlighted by the analysis of the waterfall plot in Figure 62.

Thanks to the performed acquisitions, it was possible to define a condition monitoring system that would allow to report the occurrence of a fault based on the limits imposed on BPFI and BPFO values. The visual result of the thresholds proposed for the considered characteristic frequencies is shown in Figure 69, in which the acceptance or warning ranges are represented.

The definition of the limits was adapted to make it functional for both bearing models, thus also taking into account the dispersion of the points of the bearings *B1* due to the need to restore the grease by performing a maintenance operation. Also this last event could be reported defining a further limit of the BPFO value between the standard condition and the alarm region.
This representation also allowed to have an indicator of the severity of the fault based on the position of the points in the alarm region.

Thinking about the implementation of the monitoring system on the real machine, it was important to evaluate a simplified approach that would allow on the one hand to easily represent the evolution of bearing conditions and on the other to contain the computational resources required to extract the information.
As was demonstrated in previous studies, the conditions of the mechanical components could be well defined with reference to the dissipated vibrational energy.
As is well known, the energy content of the vibrational signal can be

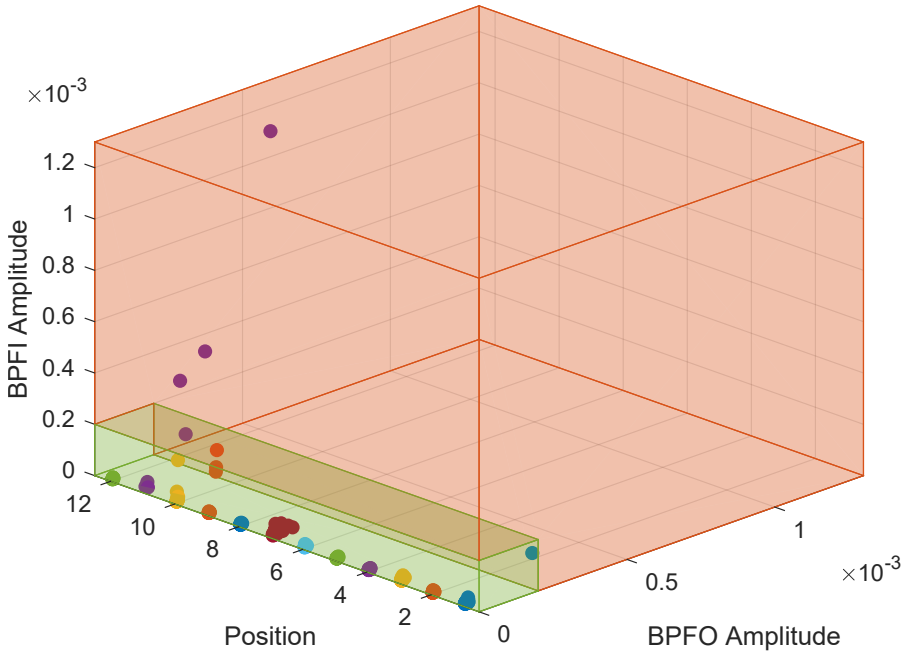

Figure 69: Graphical representation of the defined regions to assess the condition of the bearings in order to monitor fault events. The green region represents a standard bearing condition, while the red region is the alarm region.

evaluated as the area under the squared magnitude of the considered signal, thus summing the contributions calculated by the Equation 5 over the entire acquired time interval. Similar considerations can be made for the evaluation of spectral energy by referring to Equation 6, obtaining:

$$E = \int_{-\infty}^{+\infty} |X(f)|^2 \, df \tag{27}$$

remembering that $X(f)$ is the Fourier transform of the signal acquired in the time domain.
Starting from this idea, an alternative methodology was proposed to filter the acquisitions with a preliminary assessment of the bearing conditions. For each periodic acquisition, the sum of the contributions of each frequency was calculated in order to have an indicative value of the overall energy dissipated during the acquisition time. In this way it was possible to keep track of the evolution of the vibrational signal over time, leading to results consistent with those already highlighted by the previous analyses.
Also in this case, it was possible to define some thresholds that could be indicative of the conditions of the components allowing an easy interpretation to the maintenance staff.
The results obtained from the test campaign are shown in Figure 70.

The reported results refer only to the *B2* bearings since those of the samples of the *B1* model were particularly influenced by the condi-

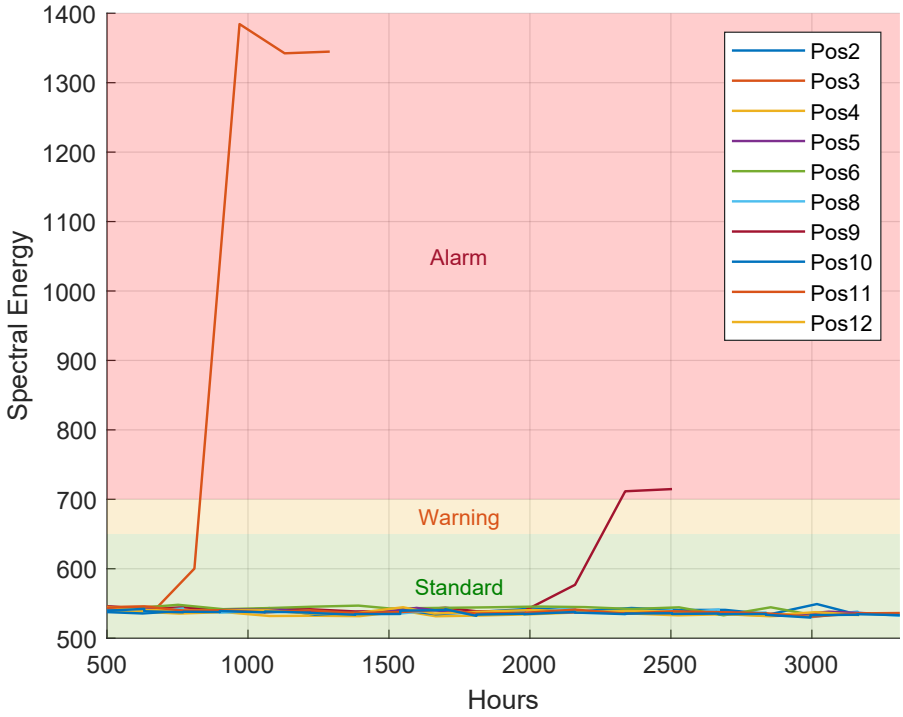

Figure 70: Evolution of the energy content of the signals acquired for the tested *B2* bearings. The defined thresholds made it possible to realise an indicator of the condition of the components.

tions of the grease, presenting peaks of energy for the acquisitions made before the periodic maintenance operation and a drastic reduction immediately after. However, for the bearings already used in the industrial application, it was possible to define suitable thresholds that would also consider this effect allowing a coherent warning.

Looking at Figure 70, the curves for positions 9 and 11 stood out, which were those related to the bearings that reported failures during the test campaign.
It was also easy to understand the severity of the fault based on the amount of energy dissipated: the crack in the inner ring had a greater influence on the operation of the component than the leakage of grease due to the damaged lateral seal of the other sample.

The most interesting result was the progressive increase in measured energy, thanks to which it was possible to implement an effective predictive maintenance approach. As soon as the measured value reached the warning zone, in fact, it was possible to request a maintenance operation. This made it possible to plan maintenance during one of the subsequent events that required the stop of the filling machine, such as changing the product to be packaged or the periodic washing operation, without further affecting productivity.

Also during this phase of the research, the industrial applicability of the condition monitoring system was always taken into consideration. This does not limit its generalisation in order to apply the same techniques for the study of similar applications in which it is necessary to monitor the state of rolling bearings and warn of the occurrence of possible damage.
After checking the effectiveness of the proposed system, it was possible to define the model of the condition monitoring system. In the case examined for the study of bearings used in filling machines, the model shown in Figure 71 was proposed.

Based on what was defined during the study, the accelerometer was fixed in the thread used for the grease fitting already present in the industrial machine. In order to acquire a sufficiently large time interval of the vibrational signal, acquisitions were programmed during the daily automatic cleaning operations. In fact, during these operations, the bearings were in motion and there were also no influences related to the packaging material. This made it possible to replicate the same conditions as the periodic acquisitions performed during the test campaign.
From the proposed model it was possible to notice how the analysis of the acquired vibrational signals was split into two phases: the first assessed the overall energy dispersion, the second the type of fault. This made it possible to reduce the required computational resources, making a preliminary estimate of the bearing conditions. In the event that the result exceeded the warning or alarm thresholds, further analyses would be performed to assess the type of damage that occurred. In this last phase, the evaluation of the characteristic frequencies of the installed bearing model had to be known in order to be compared with those highlighted by the acquisitions.
If no anomaly was detected, the system would keep waiting for the next acquisition to evaluate the evolution of the condition of the components.
This model also allowed to trace a curve of successive points that helped to easily assess the trend of bearing degradation, providing a projection of the subsequent hours of operation.

4.6 CONCLUSIONS AND DELIVERABLES

This research was born from the need to minimise the use of grease for bearings installed in the mechanical system that allowed the forming and separation of the packages in the final part of the filling machines. The new model *B2* was proposed which did not require periodic greasing operations but, before replacing the component *B1* already in use in the industrial application, it had to be compared with the latter. Starting from this request, a method of monitoring the

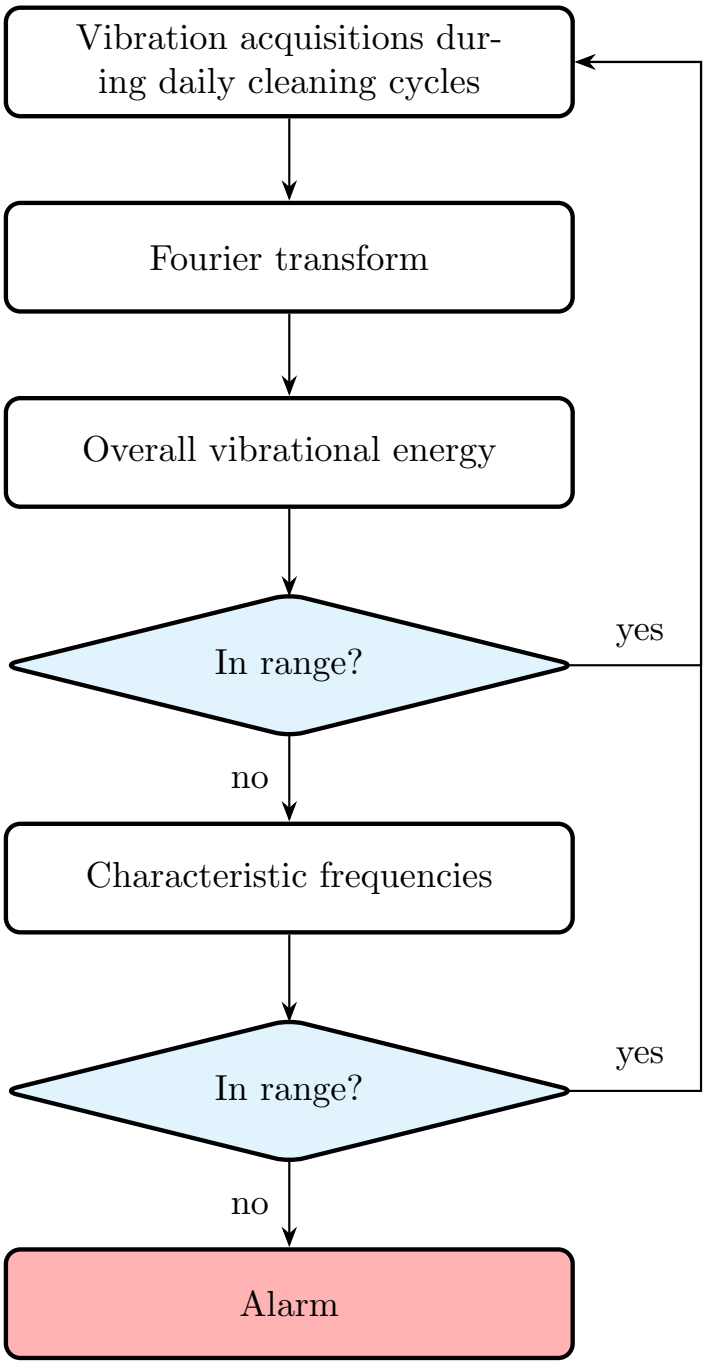

Figure 71: Proposed condition monitoring model to monitor and warn the occurrence of possible damage of the bearings installed on the filling machines.

condition of these components based on vibrational measurements was proposed.
Normally the vibrational acquisitions are carried out by means of an accelerometer fixed on the external housing of the rolling bearing in

a radial direction. For the functionality and the layout of the application considered, an alternative configuration was evaluated with the sensor at the upper end of the shaft that fixed the inner ring of the bearing. Nevertheless, this solution was sufficiently sensitive to allow the assessment of the bearing conditions as the number of operating hours increased.

In order to compare the characteristics of the bearing models under study, a specific test rig was realised to emulate the load cycles and the environmental conditions of the industrial application. During the test campaign, it was therefore possible to periodically acquire the vibrational signals of each station, verifying how the behaviour of each sample evolved.
The comparison of the spectral waterfall plots for the two bearing models showed that the new one had smaller amplitudes in the frequency domain than those of the standard component. This indicated less energy dissipation for the new model even though periodic greasing was not performed to correct the natural deterioration of the lubricant.
Nevertheless, the periodic lubrication to which the *B1* bearings were subjected allowed them to reduce wear while maintaining a rather uniform vibratory response even when working hours increased. The same did not occur for the new bearing model that showed significant degradation, although acceptable, in the last hours of testing, indicated by a progressive increase in amplitudes in the spectral domain.

With the aim of verifying whether the periodic greasing operations led to an improvement in the behaviour of the new bearing model, two of these samples were periodically greased as for the *B1* components. These maintenance operations allowed to preserve the energy dissipation at a low level compared to the progressive degradation identified in the last hours of testing for the same non-greased bearings.

During the test campaign two faults occurred: the first on the inner ring of the bearing, while the second on the lateral seal.
The evaluation of the characteristic frequencies allowed to identify critical bearing conditions thanks to the BPFI vs BPFO plot. The definition of some thresholds made it possible to keep under control and possibly to report the type of component failure.

In order to create a condition monitoring system that would allow an easier interpretation of the evolution of bearing conditions, a vibrational approach was proposed. A greater degradation of the components, in fact, involved an increase in the energy dissipation

that could be estimated by the vibrational signals. For each periodic acquisition, the overall energy content was therefore evaluated, obtaining a trend based on the hours of operation. The bearings that presented the faults were also considered in this approach, as their energy content progressively increased. Observing the trends obtained and imposing the thresholds, it was possible to propose an efficient methodology for assessing the condition of the bearings.

What was noticed by implementing these technologies was the greater stability of *B2* bearing conditions compared to *B1* bearings which had a particular sensitivity to grease degradation. In fact, for the standard model, different threshold values had to be set to take into account the considerable increase in energy dissipation between a greasing operation and the next.

A lower energy dissipation was particularly interesting in terms of the energy required in the industrial application for the movement of the mechanical system, as it allowed to increase the overall efficiency. At the same time, the suppression of periodic greasing operations allowed to save time and costs, minimising the risk of contamination of the packaging material and the product. These assessments would lead to the choice of the *B2* model in the design phase of the filling machines.
However, the two faults that occurred during the test campaign penalised this choice since the survival rate seemed lower than that of the standard model.
It is important to consider that the *B2* model was in the development phase and that the defects found could be the result of the production process and quality control not yet optimised. If after improvement by the supplier the new bearing model achieves survival performance comparable to those of the previous component, *B2* would be better under every functional characteristic.

The research carried out allowed us to study the characteristics of two different bearing models by implementing a tool that helped in the process of choosing the best component for the concerned application, evaluating the dissipated energy and duration in operating conditions as selection parameters. Different methods of investigation were proposed, all based on vibrational acquisitions, allowing on the one hand to measure the performance of the bearings and on the other to define and propose a model for condition monitoring applicable also in the industrial solution.
Furthermore, the methods described can be applied for the study of other bearing models without the limitation due to the installation of the sensor in the radial direction as reported by the most common condition monitoring applications. This offers the possibility in the

development phase to evaluate the performance of the components for design purposes, whereas in the industrial solution to integrate a predictive maintenance solution.

Further studies can be carried out in order to characterise in more detail additional defects that could occur during the operation of rolling bearings, also using already damaged samples and fault injection methods. Moreover, by increasing the number of samples, it will be possible to better define the survival rates and the warning and alarm thresholds for each model.

5

VISION SYSTEM FOR IN-LINE DIGITAL PRINTING CORRECTION

This chapter illustrates the development of a vision system to adjust the position of the graphic to be printed based on the transverse shift of the packaging material. Furthermore, the hardware, the measurement methodology and the tests performed to evaluate the performance of the proposed system are described.
In this case, the research carried out was strongly linked to the industrial need to verify and correct the digital printing process in order to obtain a reliable system that guaranteed the graphic quality requirements for outgoing packages.

5.1 INTRODUCTION

After several studies on subsystems widely used in the food and packaging industry, new research was conducted on a kit developed for the new generation of filling machines. On this occasion it was possible to continue the research moving from the use of condition monitoring methods for the study of the components to that for the study of a process, thus exhausting the typical phases of industrial design, offering new insights and useful information also for other business areas
The objectives of this equipment were the use of in-line digital printing to increase the graphic customisation of the packages and the possibility of adding information on the package, providing the maximum flexibility offered by digital technology.
The idea was to provide an additional kit for filling machines that could be installed between the unwrapper of the packaging material reel and the sterilisation bath. During the intermediate route, the web of material had to undergo numerous processes to allow printing of the graphics from the digital model.
The printing process was divided into three main phases:

- *Corona surface treatment*: it allowed to modify the properties of the surface.
- *Print*: the ink deposition.
- *UV curing*: it allowed the polymerisation and cross-linking of the liquid ink.

The first step was required because the surface tension of the plastic film in the outermost layer of the packaging material was not high

enough to allow good adhesion of the ink. For a better quality of the printing processes, the corona treatment method was used, a technology widely applied today to increase the surface tension of the films.[72]
The next phase involved the actual printing with the deposition of the ink on the web of the packaging material through some printheads. Each of them deposited a single colour among those of the CMYK model, which overlap allowed to obtain the different shades.
Before processing the packaging material in the standard operations provided by the filling machine, the ink must be completely dry. For this purpose, it was cured by exposing it to ultraviolet light which triggered the photochemical process.

The processes described above concerned the operations necessary to guarantee the quality of the interface between the ink and the outer layer of the packaging material. However, the quality of the final result was also influenced by the alignment and repeatability of the position of the graphics on the package.
While the longitudinal alignment was sufficiently accurate thanks to the detection of some graphic elements by means of contrast sensors, the transverse repeatability of the print was difficult to measure by the sensors already provided in the machine.
The lateral displacement was mainly due to the traction system and mechanical vibrations. Indeed, the web of packaging material that ran on multiple rollers could have a slightly variable thickness in the transverse direction causing a different tension between the right and left sides. This resulted in a progressive drift, which in the most serious cases would compromise the position of the graphic printed on the package. This behaviour was also accentuated by the mechanical vibrations that facilitated the progressive lateral movement of the material with respect to the nominal position.

The various models of filling machines had different production rates and, consequently, different speed of the packaging material web, affecting the performance of the printing system. In fact, a lower speed could be the cause of greater transversal shift due to less tensioning of the web, whereas a greater flow of material could lead to printing defects on a greater quantity of packages before the problem could be detected and correct.
In this context, it was necessary to implement a condition monitoring system that would allow on the one hand to correct process errors in order to maintain the imposed quality standards and on the other to assess system performance and its functional limits.
The most appropriate solution for the studied application seemed to be the implementation of a vision system that not only allowed to obtain the essential information for the correction of the print coordi-

nates but also to extract further data from the acquired frames.

Unlike what was done in the studies described in the previous chapters, the monitoring system proposed for this research was an integral part of the filling machine, taking advantage of the assessment of the operating conditions to guarantee the functionality of the printing process.
It is clear that in this last implementation the condition monitoring concept was extended by overcoming the idea of its exclusive use in the field of maintenance, including it in the functional controls of the machine and the process.

5.2 TEST RIG

At the time of the study reported here, the digital in-line printing kit was in prototyping phase. On the only available specimen, it was possible to implement the vision apparatus integrating it with the already assembled systems and frame.
As already explained, the printing process involved several steps and specific components along the route of the packaging material web. In addition to the equipment used to prepare the printing surface, to deposit and to cure the ink, there was also a contrast sensor that allowed the controller that managed the printheads to be synchronised with the web. In fact, for each section of the web with a length equal to the packaging material required for a single package, there was a high contrast graphic mark that could be easily detected by the sensor, drastically reducing the synchronisation error due to variations in the pulling speed.
These data were also useful for implementing the vision system whose hardware was installed just after the contrast sensor and necessarily before the printheads. The space available to capture the characteristics of the packaging material useful for measuring the position of the web was very limited due to the presence of the rollers and the structure. This was problematic not only in terms of the visual field of the optical sensor but also for the obstruction of the lighting system. In order to minimise these limitations, it was necessary to position the vision system in such a way as to obtain an optimal image in terms of focus, brightness and size of the field of view (FOV). The distance between the web and the camera was about 150 mm, thus obtaining a FOV of about 62.5x50 mm.

The prototype used as test rig included several passages of the packaging material web. After being unwrapped from the reel, an input buffer consisting of several rollers allowed to accumulate a few meters of web. Subsequently, the packaging material was subjected

to corona treatment in order to increase the adhesion capacity of the outermost layer with the ink. Following the acquisition of the contrast sensor and the optical sensor, printing was requested from the controller. The latter managed the printheads in order to execute the print in a repeatable and accurate way along the direction of flow of the web. Later the ink was cured by passing through UV lamps. A final buffer, in combination with the inlet one, allowed to amortise the effects due to the speed differences of the web, guaranteeing the stability of the system. Finally, the outgoing packaging material web could continue with the subsequent processes scheduled by the industrial filling machines, first of all the sterilisation bath.
A summary of the components included in the prototype for processing and printing on the packaging material web is shown in Figure 72.

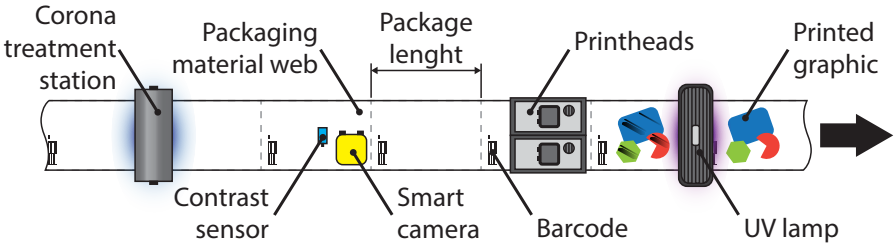

Figure 72: Components used for processing the packaging material web and to perform the print as implemented in the test rig.

5.3 DATA ACQUISITION

In this study, a type of data acquisition completely different from those implemented in the previous chapters was proposed, demonstrating how condition monitoring could deduce the necessary information from innumerable varieties of sources. The measures useful for evaluating the position of the packaging material along the transverse direction were in fact obtained only from the images acquired by the vision system and subsequently communicated to the control system.
In particular, the distance from a known reference to a specific feature that could be an edge of the web or a graphic sign was measured. Based on this parameter it was possible to perceive the correction to be made to the position of the print as the difference from the reference coordinate.

5.3.1 *Data acquisition system*

The essential parts of a vision system are the optical components and the lighting system. The latter is fundamental to guarantee an excel-

lent perception of the first one, allowing to highlight specific features in the field of view and to reduce any disturbing effects such as shadows. Although the importance of well-designed structured lighting is sometimes underestimated, it can be decisive for the success or failure of the implementation of the vision system, in particular to ensure the repeatability of operating conditions over time.
The solution proposed during the study conducted took into account the need for compactness to accommodate the system in the already designed rig, as well as the possibility of creating a system that can already be implemented in the industrial application. The best compromise was therefore to use a smart camera that would allow the creation of an embedded stand-alone vision system with an integrated lighting system.
Table 15 summarised the components of the vision system and their characteristics that can also be found in Figure 73.

Table 15: Components of the vision system. [73]

Component	Model	Technical specifications
Smart camera	In-Sight 7801	• *Image type*: monochrome • *Sensor type*: 1/1.8 in CMOS, global shutter • *Resolution*: 1280 × 1024 pixel • *Bit depth*: 256 grey levels (8 bits/pixel) • *FPS*: 76
Lens	LM12-16-01	• *Focal length*: 16 mm • *Focal ratio*: f/2.5, fixed aperture • *Mount type*: S-mount M12
Lighting system	ISLM-7000-WHI	• *Type*: white LED • *Colour temperature*: 4000 K
Cover	COV-7000-PL-FULL	*Type*: polarising filter

Thanks to the In-Sight Explorer software it was possible to develop an algorithm that would identify and extrapolate specific features from the acquired frames. Once tested, this code could be loaded on the smart camera that would have performed it independently with the possibility of managing I/O signals.
Due to the composition of the outer layer of the packaging mate-

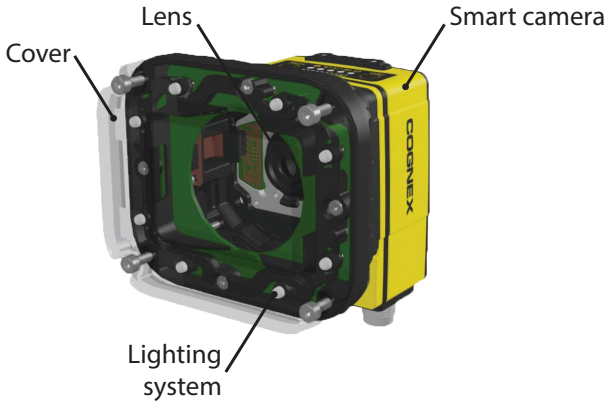

Figure 73: Cognex In-Sight 7801 smart camera with integrated lens, illumination system and polarising filter. [73]

rial, various reflections were created, causing disturbances that could sometimes compromise the identification of the characteristics sought. To overcome this drawback, a polarising filter was used.
Even the integrated lighting system made it possible to improve the image quality in the region of interest by reducing the projection of shadows due to the structure to which the various components were fixed. In fact, the possibility of turning on only specific LEDs allowed to define a structured light with an appropriately oriented light source.

Furthermore, it is also possible to include as a component of the vision system the contrast sensor Sick KTM-WP11182P used to trigger the acquisition, whose characteristics are shown in Table 16.

Table 16: Main characteristics of the contrast sensor Sick KTM-WP11182P. [74]

Sensing distance	12.5 mm
Light source	LED, RGB
Switching output	PNP
Connection type	Cable with M12 male connector, 4-pin

5.4 ACQUISITION

In order to improve the resolution of the measurement, only part of the packaging material web was acquired. The selected region was not only influenced by the references evaluated for the measurement of the transverse shift, but also by the possibility to apply typical algorithms of vision systems.

The reel of the packaging material already had some characteristic graphic elements, used by the filling machines to identify the passage of each section of the web corresponding to a single package. These signs were particularly useful also for the implementation of the vision system. In particular, the edges of the graphic element called barcode could be used as a reference to evaluate the transverse shift. At the same time, it was possible to define an automatic calibration of the system by evaluating the dimensions of this graphic sign in reference to the acquired one: this ploy allowed to reduce the influence of the error in the vertical distance between the smart camera and the web. Indeed, the different tension of the web and the fixing of the camera could lead to variations in height and therefore a different distance than the nominal one. Knowing the nominal size of the barcode it was possible to perform the calibration for each frame, converting the measurements from pixels to real-world units, and improving the accuracy of the system.
In the acquired frame example shown in Figure 74, the reference barcode at the centre of the image appears evident. With the correct setting of the lighting system, the shadows were restricted laterally, guaranteeing uniformity in the central area.

Figure 74: An acquired frame in which the bar code represents the main graphic element.

The accuracy required by the project was ± 0.1 mm, a requirement fully met by the implemented measurement system.

Although the primary purpose of the system studied was to solve the problem related to the transverse shift of the packaging material web, its use was extended to evaluate the performance of the prototype in terms of web deviation during operation.
First of all, it was necessary to define the characteristics of the proposed vision system. The accuracy a was calculable starting from the

technical features and the configuration of the smart camera. The ratio between the FOV and the resolution of the optical sensor in fact gave the accuracy of the vision system which was equal to:

$$\begin{aligned} a &= \frac{FOV_h}{Resolution_h} = \frac{62.5\ mm}{1280\ px} = 0.0488\ mm/px \\ &= \frac{FOV_w}{Resolution_w} = \frac{50\ mm}{1024\ px} = 0.0488\ mm/px \end{aligned} \tag{28}$$

Another essential parameter that had to be evaluated for the proposed measurement system was the repeatability. While accuracy could be improved by a calibration process, repeatability was intrinsically related to the hardware and software used. For this reason specific tests were performed.
Only after defining the characteristics of the vision system, the tests for the evaluation of the prototype performance were carried out.

5.4.1 *Vision system repeatability*

To assess the repeatability value of the vision system it was necessary to provide specific tests. By definition, repeatability is the ability of a system to reproduce a result under unchanged test and sample conditions. According to ISO 3534-2:2006 [75] the repeatability conditions include:

- The same measurement procedure or test procedure;
- The same operator;
- The same measuring or test equipment used under the same conditions;
- The same location;
- Repetition over a short period of time.

For the application evaluated, a specific feature was measured on successive frames of the same region of the packaging material web, therefore in static conditions.
The parameter selected to evaluate the repeatability of the system was the vertical coordinate of the bottom edge of the barcode on the plane of the packaging material web. The coordinate system considered was centred in the upper left corner of the image, the x axis directed as the nominal flow of the web and the y axis downwards, as shown in Figure 75.

By keeping the packaging material web still, 100 consecutive frames were acquired and for each of these the barcode and its lower edge were identified, therefore its coordinates were converted from pixels to millimetres.

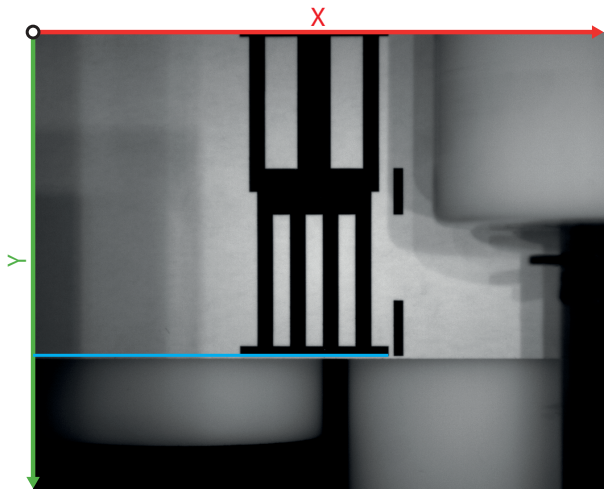

Figure 75: Example of acquired frame for the evaluation of the repeatability of the vision system. The reference system used and the measured coordinate are shown.

The edge identification tool used in the developed algorithm had subpixel accuracy, so it was possible to obtain better measurements than expected from the accuracy value calculated by Equation 28.

The result of the test conducted is shown in Figure 76. In the worst case, considering the difference between the maximum value and the minimum value, the difference was about 0.1 px which corresponded to about 0.005 mm.

Repeatability was around a tenth of the accuracy, and sufficient to guarantee the performance required for the monitoring system.

5.4.2 *Transverse shift acquisition*

Following the verification of the characteristics of the measuring system, the performances relative to the stability of the transverse position of the packaging material web were evaluated. These considerations were essential to understand if the systems provided to guide the web along the kit were sufficient to ensure the continuity of printing operations. The implementation of the vision system, in fact, could guarantee a correction of the transversal position of the graphics limited to the range reachable by the nozzles of the printheads, which was approximately ± 2 mm with respect to the nominal position.

Several tests were carried out using the parameters provided for the standard operation of the machine, of which the most interesting for the purposes of the study was the web speed set to 300 mm/s.

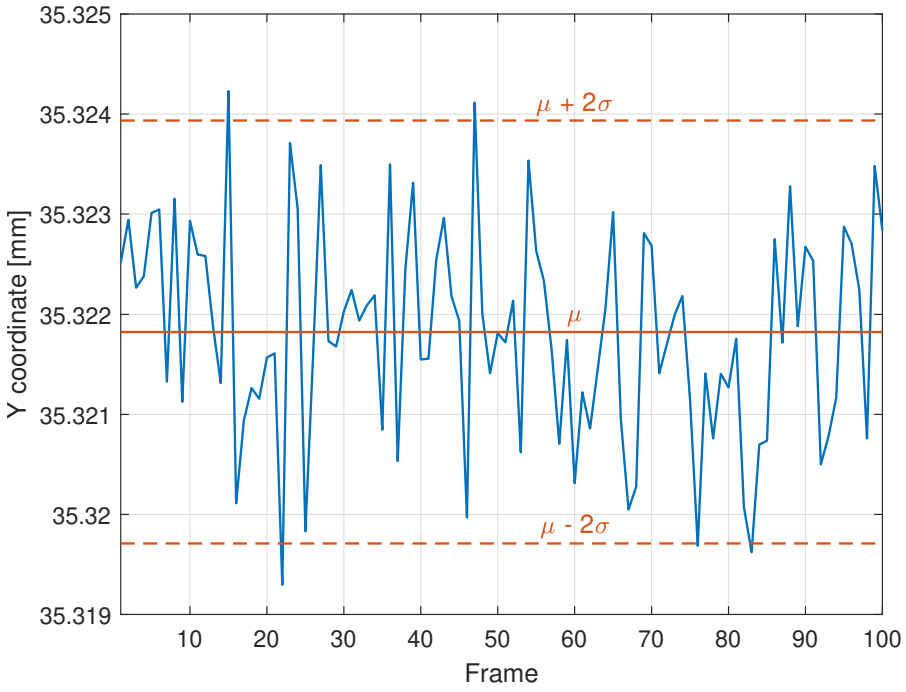

Figure 76: Results of Y coordinate measurements of the bottom edge of the barcode for 100 frames acquired in static conditions in order to evaluate the repeatability of the vision system.

The acquisitions were performed for continuous runs that lasted several minutes. For the sake of flexibility and ease of management, the data was recorded in files of one minute each. Among all, here is reported the worst case also shown in Figure 77, which refers to the coordinates of the bottom edge of the barcode calculated as described above.

The difference between the maximum and minimum value was < 0.39 mm and with respect to the average value, which corresponded approximately to the nominal position of the web, the maximum displacement was about 0.22 mm. Remembering that the graphics could be moved by ± 2 mm, it was clear that the results obtained validate the satisfactory performance of the guidance systems.

The proposed solution for the measurement of the coordinates of the barcode, adjusted to refer to the nominal position, was found to be coherent for the evaluation of the correction that the printing system had to perform in order to guarantee a correct alignment between the graphic elements already present on the packaging material and those of in-line digital printing.

This monitoring can be used as a method of evaluating the performance of the system, appearing as an essential tool in the design of the industrial process, allowing to adjust the functional parameters in order to obtain the best results according to the operating conditions.

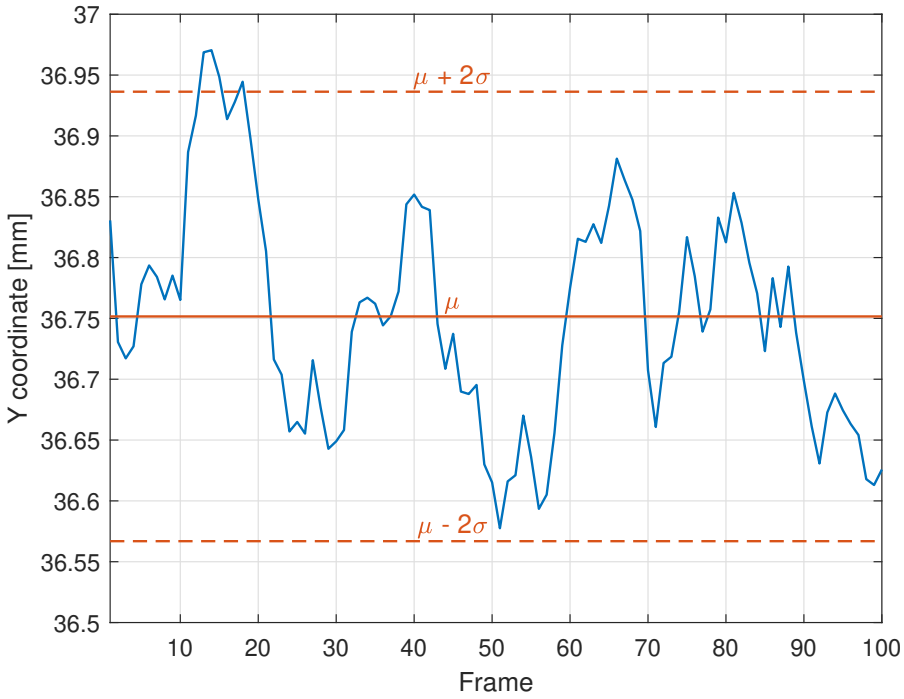

Figure 77: Results of Y coordinate measurements of the bottom edge of the barcode used to evaluate the stability of the packaging material web during standard operation of the prototype.

When the speed varies, for example, it may be useful to evaluate a different tensioning of the packaging material web and/or different towing and guiding systems.

5.5 IMPLEMENTATION OF THE TRANSVERSE SHIFT CORRECTION SYSTEM

After the tests carried out to evaluate the performance of the vision system and the prototype for in-line digital printing, the implementation of the monitoring system for the transverse shift of the packaging material web was finalised. To this end, integrations were required on both the software side and hardware side, so that the readings could be coherently communicated to the controller of the printheads.

The definition of the acquisition settings of the smart camera was fundamental, in particular the exposure time already optimised during the previous tests and set equal to 250 µs. This value allowed to capture a sufficiently clear image, minimising the artefacts due to the moving subject.
It was necessary to define a common reference that could couple the measurements performed by the vision system with the position of the printheads. For this reason, a part of the kit frame mechanically

connected to the printheads was included in the FOV. Thanks to this expedient it was possible to obtain relative measures that allowed to correct the errors due to a not perfect transversal positioning of the smart camera.
As previously described, the correction due to the vertical distance between the smart camera and the packaging material web was allowed by comparing the dimensions of the barcode with the nominal ones, and for this reason the search for this graphic element was the first step of the proposed algorithm.
After that, the edges of main interest were located: the frame reference and the bottom of the barcode. Once the distance between these two features was measured, the data could be sent to the kit control PLC, connected to the printhead controller. The distance between the vision system and the printheads, however, required a buffer to store the information since the smart camera was busy analysing a new frame while the print controller received the previous correction.
Figure 78 shows the output of the algorithm with the already described and other additional features highlighted.

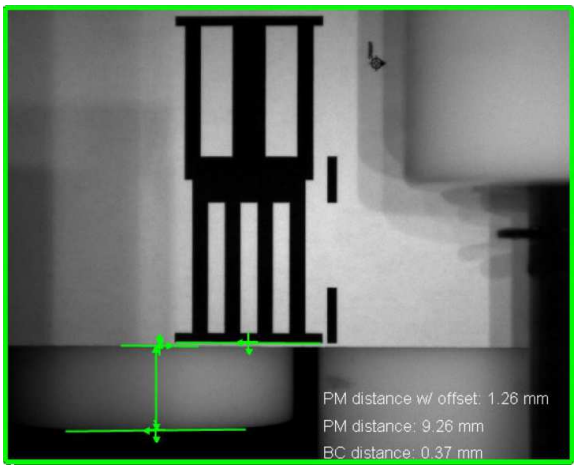

Figure 78: An example of the result obtained from the image analysis algorithm. The bottom edges of the barcode, packaging material web and mechanical reference (in the lower left region) are highlighted.

By optimising the tasks envisaged by the image analysis algorithm, for example by reducing the regions of interest (ROI) in which each graphic element was searched, it was possible to obtain an overall acquisition and analysis time of approximately 60 ms. This value was particularly conservative considering that the expected production capacity for the in-line digital printing application was about 1.75 $packages/s$, therefore with a cycle time > 570 ms. This feature was particularly interesting in view of the implementation of this kit in machines with higher production rates.

The implemented vision system represented the only alternative capable of accurately measuring the transverse shift of the packaging material web while respecting the functional timing of the machine, but it also offered the possibility of analysing further parameters. In fact, as shown also in Figure 78, it was possible to identify both the coordinates of the bottom edge of the barcode and the web. While the alignment of the graphics to be printed with reference to the one already present was interesting for the correction of digital printing, the detection of the edge of the packaging material offered the possibility of integrating a monitoring system for quality control.
In fact, the production of the reels of packaging material initially involved printing graphic elements on much larger sheets, subsequently separated with longitudinal cuts. It is clear that the accuracy of these industrial processes also influenced the relative position of the graphic with respect to the edges of the packaging material web.
From the example shown in Figure 79 related to the monitoring of the distance between the bottom edge of the barcode and that of the packaging material web, it was possible to notice several fluctuations. The deviation from the average value in some cases was > 0.2 mm.

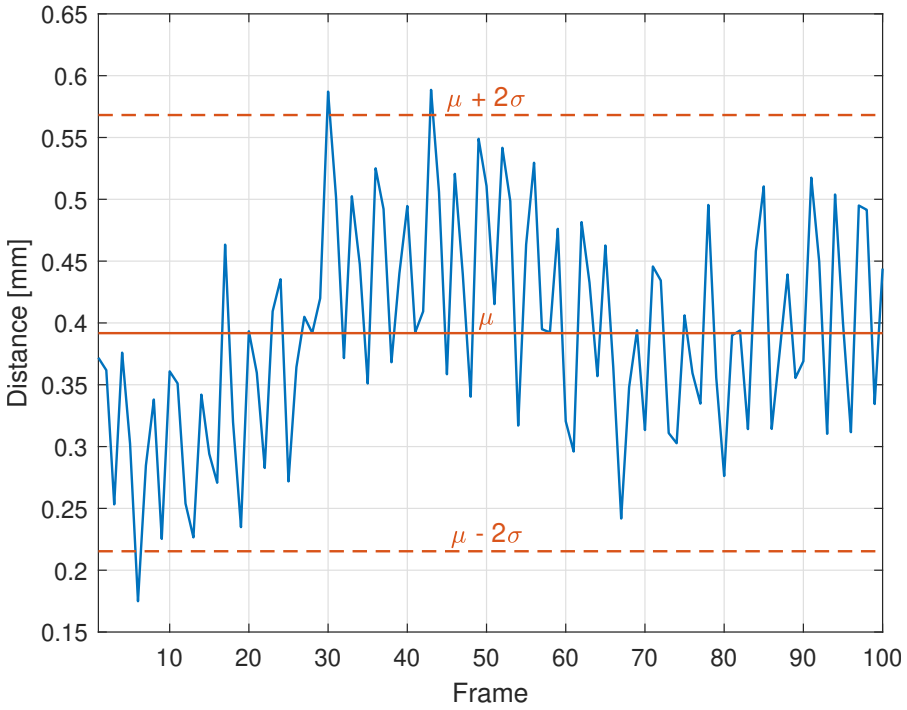

Figure 79: Example of measurements of the distance between the bottom edge of the barcode and that of the packaging material web.

The constant monitoring of the input material of the filling machines could represent a very interesting tool also for the purchasing department that could constantly control the quality of the supply of

packaging material reels based on the accuracy of their production.

It was also interesting to assess which contribution among the transverse displacement of the packaging material web and the distance from the edge of the barcode had a greater influence on the position of the graphic elements with respect to the nominal position. Comparing the vertical coordinate of the bottom edge of the web in Figure 80 with that of the barcode in Figure 77, it was easy to notice that both cases exhibited the same macro-displacement, similar to a carrier signal, that was not noticeable in Figure 79 and that was identified as the actual movement of the web with respect to the nominal position. The higher frequency fluctuations were instead present both in Figure 79 and Figure 80, whereas the trend in Figure 77 was more smoothed, supporting the correlation of these oscillations with the profile of the edges of the packaging material. From these considerations, it emerged how the industrial printing process had a better repeatability and stability compared to those of the cutting of the sheet in different reels which led to greater dimensional uncertainty.

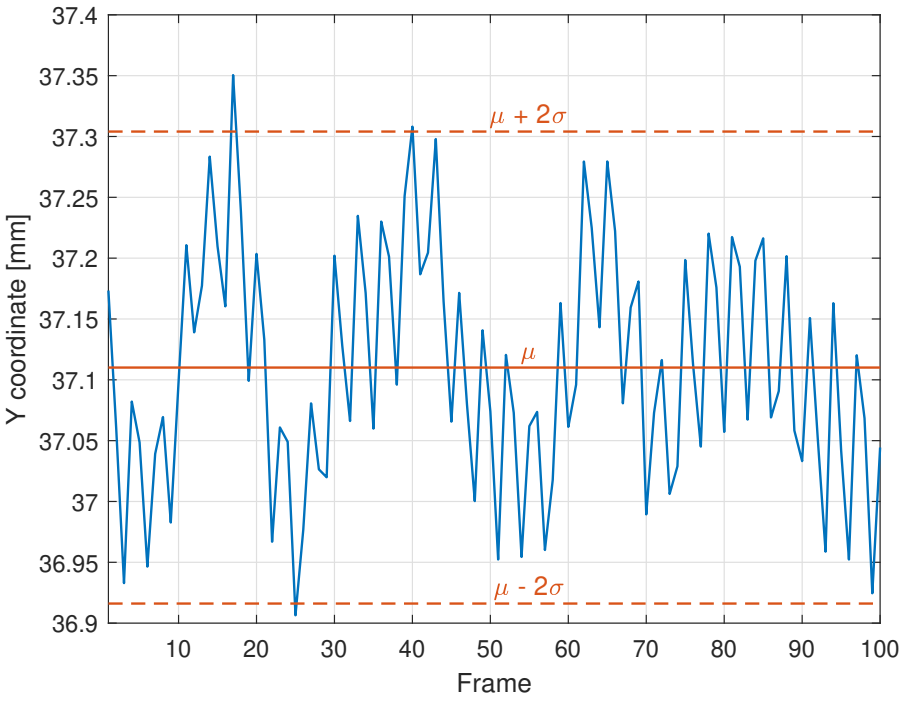

Figure 80: Results of Y coordinate measurements of the bottom edge of the packaging material web.

5.7 CONCLUSIONS AND DELIVERABLES

While in the previous studies the condition monitoring approach concerned already engineered and industrially operational components and processes, in this last study it was possible to demonstrate how

this paradigm could be integrated for the development of a new product, and for the evaluation of its performance.
During the prototyping phase of a kit for the new generation of filling machines, it was requested to study a solution that would allow to correct the position of the graphics that an in-line digital printing system would reproduce on the packaging material web. In fact, the pulling systems and the mechanical vibrations caused a deviation from the nominal position.
The proposed solution evaluated a vision system that allowed monitoring of the transverse position of the graphic elements already present on the packaging material. These measurements were subsequently communicated to the printhead controller in order to correct the coordinates of the graphic to be printed by shifting the range of nozzles used. The integration of the system into the already available prototype required the optimisation of the position of the smart camera and the lighting system, in order to obtain quality images for the extrapolation of useful information.

First of all, the performance of the vision system was evaluated. The accuracy, which depended only on the technical characteristics and the FOV, was about $0.0488\ mm/px$. Repeatability was instead evaluated by taking as a reference the vertical coordinate of the bottom edge of the bar code for subsequent acquisitions in static conditions. The greatest deviation found between the maximum and minimum values was about $0.005\ mm$. From the results obtained, the proposed system was found to be suitable for meeting the requirements of the application.

The measurement of the position of the bar code was sufficient to evaluate the correction of the transverse coordinate of the graph that had to be printed, which in the worst case was found to be about $0.22\ mm$ with respect to the nominal position.
This system can be used to evaluate the performance of the printing system under different functional conditions, such as, for example, the variation of the speed of the packaging material, allowing to optimise the critical parameters of the printing process, such as the tension of the web and the limits of the guidance systems.
This demonstrates how condition monitoring methodologies can be used also in the industrial design of the process, and not only for the evaluation of the current state of operation of the monitored machine.

However, the vision system also allowed to monitor additional parameters useful mainly for quality control of incoming material. In fact, considering the position of the bottom edge of the packaging material web, it was possible to understand how the previous printing process had a greater stability than that of cutting the sheet in

reels. In fact, the coordinate of the edge of the material showed higher frequency fluctuations, not dependent on the simple shift of the web with respect to the nominal position.
This result was also interesting for the printing application, as the greater stability of the position of the graphic elements turned out to be an advantage in terms of requested corrections.

The potential of the proposed system could also be exploited in industrial solutions with higher productivity rates, in fact the cycle time of the entire image acquisition and analysis process was about 60 ms. This solution could also be used for the integration of new tasks, for example to monitor further features of the packaging material.
Another smart camera could be installed downstream of the UV lamps for print quality inspection, collecting further information on the operating status of the process.

Thanks to this study it was possible to extend the scope of applicability of monitoring systems to different business areas, such as the purchasing department and quality control. The method of acquiring information was also peculiar, integrating the vision application in the list of systems used during the research, demonstrating how the condition monitoring paradigms can be applied to any industrial solution.

6

CONCLUSION

The main purpose of this thesis was to demonstrate how the typical methodologies of condition monitoring can be used in innumerable industrial applications offering new knowledge and new investigation tools.
Condition monitoring, understood as an integral part of Industry 4.0, is often interpreted as a method of monitoring specific parameters to define the state of an industrial system for maintenance purposes. During the studies carried out, it was shown that this definition is limiting compared to the potential offered by this approach, which provides essential information for the design and innovation of industrial applications, as well as for other business areas such as the purchasing department and quality control.
In order to demonstrate the efficiency of these approaches, the entire research referred to practical applications generally related to the packaging and food industry thanks to the support provided by the company Ecor International S.p.A.

The research involved various aspects of condition monitoring, starting from the study and implementation of a monitoring system for an industrial process, then moving on to the definition of the degradation status of a component. Subsequently, the monitoring methods were also used for the comparison between two models of the same component in order to innovate it. As a last implementation, instead, it was possible to demonstrate how condition monitoring can become part of the development of a new product, not only acting as a process control, but also providing information for quality control.
The research was then carried out considering the different areas of industrial design, starting from the study of the process and its most significant events, then focusing on the status and performance of critical components, finally integrating condition monitoring in the development of a new process. Condition monitoring was therefore initially used as a diagnostic tool, then moving on to design and functional areas.

For the first case study, the packages separation process performed in the final part of the filling machines was evaluated. Numerous parameters were acquired and analysed, but the most significant of these was the force with which the knife was actuated in order to perform the cutting of the packaging material. Thanks to this it was in fact possible to identify the different components of the cutting

process and define standard operating curves. By monitoring this parameter it was also possible to generate a warning in the event of excessive accumulation of residues in the cutting stations which led to non-conforming packages and premature deterioration of mechanical components.
Another interesting relationship was found between the oil temperature, the hydraulic pressure and the responsiveness of the mechanical system. In particular, with the increase of the oil temperature with the operating hours, there was an increase in the pressure peak and a quicker cutting process.
This first implementation allowed not only to realise a monitoring system of the operating conditions of the cutting process, but it provided information and knowledge that could not be learned by the parameters already implemented in the industrial machine. It is easy to understand how condition monitoring offers an added value compared to the common definition related to process monitoring, giving new prompts to adjust and optimise the functional parameters.

The study then focused on the most critical component of the cutting system: the knife. It was particularly interesting to assess the state of degradation of the tool as the operation hours increased. After clarifying how the cut could be interpreted as a stochastic cyclostationary process, from the pseudo Wigner-Ville time-frequency distribution it was possible to identify different characteristics that allowed to distinguish the behaviour of two models of knife with different bevel angle, and that of components with different wear levels. In fact, it was evident that a greater bevel angle led to an excitation of a wider spectral range. Similarly, it was shown that a higher wear level could be detected by the concentration of dissipated vibrational energy around a specific frequency, which in the case examined was around 5 kHz.
To reduce the required computational resources and facilitate the industrial implementation of the condition monitoring system, an alternative method was proposed by evaluating the zero-order spectral moment. The peak of the cut instant was in fact considerably higher in the case of a degraded knife. Also some features highlighted in practice, such as the worsening of the cutting edges of the packaging material in relation to the irregularity of the profile of the teeth in the case of a worn knife, could be found based on the shape of the curve obtained.
This occasion was useful to demonstrate how some analysis approaches of vibrational signals typically used for rotational systems could be functional also for stochastic cyclostationary processes, furthermore proposing a model of condition monitoring based on dissipated vibrational energy.

Unlike the previous cases which referred to components already used in industrial applications, in the following study the conditions monitoring techniques were used to develop and compare a new model of rolling bearing that did not require periodic greasing operations unlike the one already installed in the mechanical system that formed and separated the packages in some filling machines.
Reconnecting with the dissipated energy approach used in the previous study, also in this case some vibrational signals were acquired, allowing to identify different behaviours and malfunctions during the test hours.
Plotting the Fourier transforms of the periodically acquired signals, it was possible to notice how the new model showed a lower overall amplitude, although symptoms of wear appeared at the end of the test campaign unlike the model already used industrially. However, even subjecting the new generation bearings to the same periodic greasing operations, the effects of wear became completely negligible.
During the test campaign some faults occurred, both on the bearings of the new model. Thanks to the waterfall plots of the vibrational spectrum it was possible to notice a progressive increase in the amplitude before the faults were relevant to the functionality of the components. To improve the identification of faults, the characteristic frequencies of the bearings were considered. In the BPFI vs BPFO plot, the standard and alarm regions were defined to warn when a fault occurred, also identifying its type referring to the prevailing coordinate.
Also in this case an energetic parameter was considered in order to simplify the industrial implementation of the monitoring system. Based on the energy of the signal acquired periodically, in fact, it was possible to evaluate the state of the bearings and, if necessary, carry out a more detailed investigation to assess the type of fault.
In this study it was possible to propose a condition monitoring system that allowed to guide the choice between different models of the same component, assessing their performance and offering ideas for their innovation, realising at the same time a solution that could be also implemented in the industrial application to reduce the required maintenance operations.

Finally, the research involved the application of condition monitoring in the development of a new process, demonstrating how the implementation of a control system could be integrated with the typical methodologies of condition monitoring, providing useful information to different business areas. The application considered required the measurement of the transverse coordinate of the graphic elements already present on the packaging material in order to correct the position of the subsequent in-line digital print. To this end, a vision system was implemented, obtaining accurate and repeatable measure-

ments that could not be achieved by other means.
This solution made it possible to evaluate the performance of the pulling and guiding system of the packaging material web, demonstrating how the condition monitoring system can be used in the design and adjustment of the functional parameters of industrial processes, depending on the working conditions.
Furthermore, the implemented monitoring system opened up the possibility of integrating further analyses particularly interesting to control the production quality of the incoming material. In fact, by evaluating the position of the bar code and the edge of the web, it was possible to highlight how the printing process previously performed had a greater stability compared to the process of cutting the sheets in reels. These parameters could be used to evaluate and compare the performance of different suppliers of reels of packaging material.

During the implementation of the monitoring systems for the various applications, the hardware was chosen and the software was developed so that they could be unified in a single solution in order to simplify its integration in the industrial machine. The only exception was the vision system, which however was able to communicate with the previously mentioned system.

The study conducted allowed to highlight the wide applicability of condition monitoring methods in the industrial field, involving applications of different nature, acquisition systems and heterogeneous data formats, to the advantage of many business areas. It has been demonstrated through the studies conducted how the definition of condition monitoring can often be limiting with respect to the potentialities offered. The development, design and research phases carried out on processes and components, in fact, can benefit from continuous monitoring systems by obtaining periodic data that would not otherwise be available and from which, with appropriate analyses, can be extrapolated information that lead to technological progress, innovative design solutions and optimisation of industrial activities.

The information and potential demonstrated by the implementation of condition monitoring systems can be further expanded to allow even more advanced management of industrial processes. Integration with ERP software, for example, would help to partly automate the management of production and material in the warehouse, reducing the quantity of spare parts and anticipating the need to purchase new ones based on the actual conditions of the plants, with all the associated advantages.

In this thesis the evolution of condition monitoring from in-line maintenance to industrial design has been proposed and validated

with practical cases with the awareness and conviction that the applications considered represent only a small part of the fields in which this approach can be applied, with the possibility of expanding its potential with future research and adapting the models for the specific case studies.

APPENDIX A

During the implementation of the monitoring systems, the visualisation and the management of the acquired data was also considered. In relation to the hardware and software offered in most of the applications examined, two commercial systems supplied by the company National Instruments were tested. Following the assessment of the advantages and disadvantages of these solutions, a parallel project was launched to evaluate the feasibility of an in-house developed software.
A dashboard system for condition monitoring should be able to easily make available the information contained in the big data acquired by the different devices, allowing a flexible integration of the multiple data sources.
To this end, the visualisation software should report significant features that summarise the state of the monitored system, for example by plotting their trends. These concepts are well known in the field of big data management, for which it is often not the raw data that has value, rather their processing to obtain quantities that are easier to interpret and with greater information content.
The following paragraphs describe the software tested during the research work, in order to evaluate its pros and cons.

A.1 NI INSIGHTCM™

This software was initially developed as a condition monitoring solution for power plants. The features offered by this project appeared to be useful also in other industrial realities, which is why National Instrument decided to commercialise this software.
The software offered the possibility to collect the data generated by multiple remote devices in a single platform, linking the channels with the related parameter. During the definition of the properties of each channel, it was possible to choose which features the software should have calculated starting from the raw data, such as the RMS or the peak-to-peak value. Due to the original field of application for which this platform had been developed, by default various parameters related to the study of vibrations and the laws of rotational motion were provided. NI InsightCM™ therefore included a dashboard in which it was possible to observe the evolution of the various parameters obtained from the post-processing of acquisitions, also integrating a warning system based on customisable thresholds.

The entire platform could be installed on a server, while the configuration and display pages could be reached via web from other devices with the necessary access privileges.
An example of what the data display dashboard looked like is shown in Figure 81.

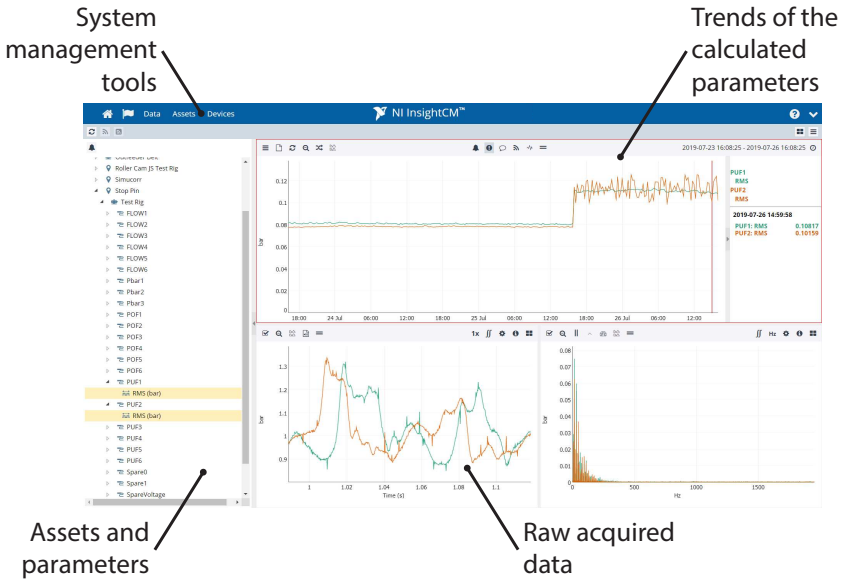

Figure 81: NI InsightCM™ dashboard main screen for data visualisation.

Despite the great potential of the system, some important limitations arose during the testing phase. In fact, it was possible to use only some of the datalogger models commercialised by National Instruments. Furthermore, for applications that had to be integrated into the platform, it was mandatory to choose between specific configurations of modules and layouts. This could be overcome with the use of the NI InsightCM™ Software Development Kit (SDK), which allowed to expand the functionality of the system.
In most of the case studies, the type of application was significantly different from those provided in the standard NI InsightCM™ configurations, requiring a thorough redesign of the projects. This inhibited a fundamental feature of the platform, that is the ability to quickly install and include new monitoring systems in a simple configurable system.

A.2 SystemLink™

Following the difficulties encountered with NI InsightCM™, National Instruments proposed a new platform called SystemLink™, which had been developed to be more flexible than the previous one. Although the basic concept was very similar, maintaining a centralised platform on a server that allowed devices with the appropriate priv-

ileges to access the relative web pages, the acquisition software management and the data visualisation dashboards were more easily adaptable.
Thanks to the SystemLink™ API it was in fact possible to communicate the data acquired by the dataloggers commercialised by National Instruments to the main application running on the server. The latter then made available the information that could be displayed in plots.
Thanks to the *Dashboard Builder* tool, it was easy to create web pages with indicators and controls, implementing simple dashboards that could be easily consulted by users. An example of a dashboard created in SystemLink™ is shown in Figure 82 in which the values in real-time and the trends of their average values are shown on the same web page.
Unlike NI InsightCM™, the acquisition software only required the integration of small sections of code included in the API, giving the possibility to update previously realised projects with minimal modifications.
Also the simplification in the management of user roles turned out to be particularly interesting, providing access to specific pages based on the area of interest.

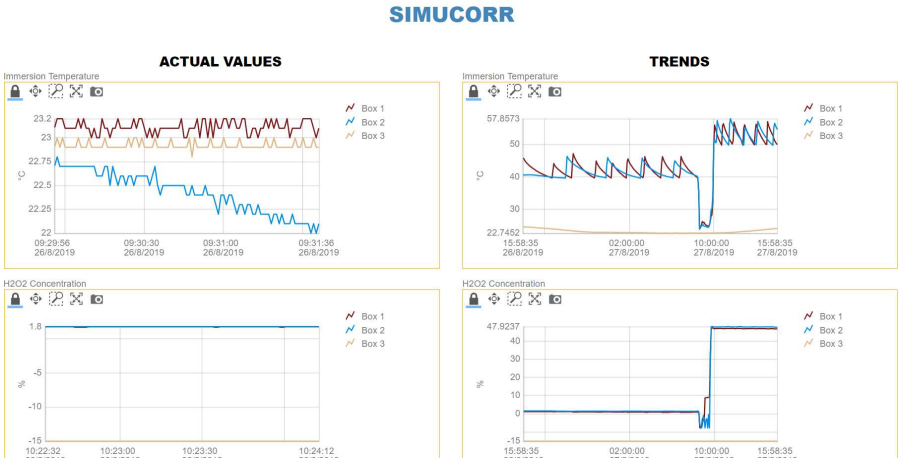

Figure 82: Example of dashboard developed in SystemLink™.

Despite the considerable improvements, this platform did not present significant automatisms to trace trends that would allow to observe the evolution of the state of the monitored system, preferring a real-time visualisation of the acquired data. At the same time, its flexibility, particularly in terms of tools dedicated to data visualisation, failed to satisfy all the applications studied, although it proved to be sufficient for simple monitoring systems.

A.3 CUSTOM PLATFORM FOR CONDITION MONITORING

To satisfy the variety of applications in which it is possible to implement condition monitoring, overcoming the limits of the solutions already tested, Ecor International S.p.A. has launched a new project for the development of an in-house platform.
Although the project is still in the early stages of development, some applications have already been implemented. This system made it possible to satisfy every scenario by offering maximum flexibility both in terms of algorithms for data analysis and information visualisation. It was indeed possible to implement analysis strategies on the main platform or, at a more specific level, in the software executed on the acquisition devices.
The dashboards were developed entirely with web-oriented languages, allowing on the one hand to use many open source resources and on the other to obtain a graphic appearance consistent with the industrial application. These features were particularly interesting in view of future access to the platform by customers, to whom it would be possible to provide customised web pages.
In order to guarantee the recognition of the connected user and the confidentiality of the data, a logging system has been implemented since the early stages of the project.
Figure 83 shows a screen for viewing the acquired channels in real-time. By selecting the relative panel it is also possible to visualise the historical trends of the parameters extrapolated from the raw data to show the evolution of the monitored system. The structure also includes panels to select the files stored in the reference repository and to plot their data, as well as an alarm dashboard.

This solution clearly loses the advantages of a ready-to-use platform as in the case of previously evaluated systems, requiring an important investment of resources for development. From previous experiences, it was however possible to obtain significant ideas for the evaluation of the functionality and structure of the new project.

A.4 PLATFORM COMPARISON

Table 17 lists the advantages and disadvantages for each of the platforms considered.

Table 17: Advantages and disadvantages of the considered platforms.

Platform	Pros	Cons
NI InsightCM™	• Ready-to-use platform • Integrated calculation of the features of the raw signals • Data and trend display dashboard	• Limited range of integrable data logger models • Limited monitoring system layouts • Onerous redesign for non-standard applications
SystemLink™	• Ready-to-use platform • Wide range of integrable datalogger models • Minimum code integrations required for the acquisition software • Simplified tools for creating custom dashboards • Management of user roles	• Calculation of the characteristics of the raw signals not integrated • Layout of dashboards limited to the provided tools
Custom platform	• Maximum flexibility • Theoretically unlimited integration of the devices • Creation of custom dashboards • Management of user roles	• Non-ready-to-use platform • Significant investment of resources for development

Figure 83: Example of dashboard developed for displaying data in real-time. It is possible to notice the panels relating to the display of historical trends, the selection of stored files and the graphing of their data and the alarm dashboard.

BIBLIOGRAPHY

[1] R. K. Mobley, *An introduction to predictive maintenance*. Elsevier, 2002.

[2] V. Roblek, M. Meško, and A. Krapež, "A complex view of industry 4.0," *SAGE Open*, vol. 6, no. 2, 2016.

[3] J. Lee, H.-A. Kao, and S. Yang, "Service innovation and smart analytics for industry 4.0 and big data environment," *Procedia Cirp*, vol. 16, pp. 3–8, 2014.

[4] Y. Liao, F. Deschamps, E. d. F. R. Loures, and L. F. P. Ramos, "Past, present and future of Industry 4.0 - a systematic literature review and research agenda proposal," *International journal of production research*, vol. 55, no. 12, pp. 3609–3629, 2017.

[5] K. Zhou, T. Liu, and L. Zhou, "Industry 4.0: Towards future industrial opportunities and challenges," in *Fuzzy Systems and Knowledge Discovery (FSKD), 2015 12th International Conference on*, pp. 2147–2152, IEEE, 2015.

[6] L. D. Xu, E. L. Xu, and L. Li, "Industry 4.0: state of the art and future trends," *International Journal of Production Research*, vol. 56, no. 8, pp. 2941–2962, 2018.

[7] F. Tao, Y. Wang, Y. Zuo, H. Yang, and M. Zhang, "Internet of Things in product life-cycle energy management," *Journal of Industrial Information Integration*, vol. 1, pp. 26–39, 2016.

[8] Q. Cao, F. Giustozzi, C. Zanni-Merk, F. de Bertrand de Beuvron, and C. Reich, "Smart condition monitoring for industry 4.0 manufacturing processes: An ontology-based approach," *Cybernetics and Systems*, vol. 50, no. 2, pp. 82–96, 2019.

[9] R. Anderl, "Industrie 4.0-advanced engineering of smart products and smart production," in *Proceedings of International Seminar on High Technology*, vol. 19, 2014.

[10] L. Spendla, M. Kebisek, P. Tanuska, and L. Hrcka, "Concept of predictive maintenance of production systems in accordance with industry 4.0," in *2017 IEEE 15th International Symposium on Applied Machine Intelligence and Informatics (SAMI)*, pp. 000405–000410, IEEE, 2017.

[11] CEN, "Maintenance - Maintenance terminology," EN EN 13306, European Committee for Standardization, 2017.

[12] I. P. S. Ahuja and J. S. Khamba, "Total productive maintenance: literature review and directions," *International Journal of Quality & Reliability Management*, vol. 25, no. 7, pp. 709–756, 2008.

[13] J. Moubray, *Reliability-centered maintenance*. Industrial Press Inc., 1997.

[14] J. W. Goodfellow, "Applying reliability centered maintenance (RCM) to overhead electric utility distribution systems," in *Power Engineering Society Summer Meeting, 2000. IEEE*, vol. 1, pp. 566–569, IEEE, 2000.

[15] R. Ahmad and S. Kamaruddin, "An overview of time-based and condition-based maintenance in industrial application," *Computers & Industrial Engineering*, vol. 63, no. 1, pp. 135–149, 2012.

[16] A. K. Jardine, D. Lin, and D. Banjevic, "A review on machinery diagnostics and prognostics implementing condition-based maintenance," *Mechanical systems and signal processing*, vol. 20, no. 7, pp. 1483–1510, 2006.

[17] L. Gehrke, A. Kühn, D. Rule, P. Moore, C. Bellmann, S. Siemes, D. Dawood, S. Lakshmi, J. Kulik, and M. Standley, "A discussion of qualifications and skills in the factory of the future: A german and american perspective," *VDI/ASME Industry*, vol. 4, pp. 1–28, 2015.

[18] J. Lee, E. Lapira, B. Bagheri, and H.-a. Kao, "Recent advances and trends in predictive manufacturing systems in big data environment," *Manufacturing Letters*, vol. 1, no. 1, pp. 38–41, 2013.

[19] Y. Lei, F. Jia, J. Lin, S. Xing, and S. X. Ding, "An intelligent fault diagnosis method using unsupervised feature learning towards mechanical big data," *IEEE Transactions on Industrial Electronics*, vol. 63, no. 5, pp. 3137–3147, 2016.

[20] P. Cheruvu, S. Kapa, and N. P. Mahalik, "Recent advances in food processing and packaging technology," *International Journal of Automation and Control*, vol. 2, no. 4, pp. 418–435, 2008.

[21] N. P. Mahalik and A. N. Nambiar, "Trends in food packaging and manufacturing systems and technology," *Trends in food science & technology*, vol. 21, no. 3, pp. 117–128, 2010.

[22] M. Vanderroost, P. Ragaert, F. Devlieghere, and B. De Meulenaer, "Intelligent food packaging: The next generation," *Trends in Food Science & Technology*, vol. 39, no. 1, pp. 47–62, 2014.

[23] M. Maksimović, V. Vujović, and E. Omanović-Miklić anin, "Application of internet of things in food packaging and transportation," *International Journal of Sustainable Agricultural Management and Informatics*, vol. 1, no. 4, pp. 333–350, 2015.

[24] Rockwell Automation Inc., "https://www.rockwellautomation.com/," 2019.

[25] Greener Corporation, "https://greenercorp.com/," 2019.

[26] Robert Bosch Packaging Technology GmbH, "https://www.boschpackaging.com/," 2019.

[27] G. L. Robertson, *Food packaging: principles and practice*. CRC press, 2005.

[28] S. Ghosh and R. Reddy, "Ultrasonic sealing of polyester and spectra fabrics using thermo plastic properties," *Journal of applied polymer science*, vol. 113, no. 2, pp. 1082–1089, 2009.

[29] R. Coles, D. McDowell, and M. J. Kirwan, *Food packaging technology*, vol. 5. CRC Press, 2003.

[30] TGW International Inc., "https://tgwint.com/," 2019.

[31] I. Ansari and A. Datta, "An overview of sterilization methods for packaging materials used in aseptic packaging systems," *Food and Bioproducts Processing*, vol. 81, no. 1, pp. 57–65, 2003.

[32] burster GmbH & co kg, "https://www.burster.com/," 2019.

[33] Trafag AG, "https://www.trafag.com/," 2019.

[34] Pentronic, "https://www.pentronic.se/," 2019.

[35] National Instruments, "http://www.ni.com/," 2019.

[36] W. Laws and A. Muszynska, "Periodic and continuous vibration monitoring for preventive/predictive maintenance of rotating machinery," *Journal of engineering for gas turbines and power*, vol. 109, no. 2, pp. 159–167, 1987.

[37] E. P. Carden and P. Fanning, "Vibration based condition monitoring: a review," *Structural health monitoring*, vol. 3, no. 4, pp. 355–377, 2004.

[38] R. B. Randall, *Vibration-based condition monitoring: industrial, aerospace and automotive applications*. John Wiley & Sons, 2011.

[39] S. Ebersbach and Z. Peng, "Expert system development for vibration analysis in machine condition monitoring," *Expert systems with applications*, vol. 34, no. 1, pp. 291–299, 2008.

[40] C. Farrar and S. Doebling, "Damage detection and evaluation II," in *Modal analysis and testing*, pp. 345–378, Springer, 1999.

[41] N. Ambhore, D. Kamble, S. Chinchanikar, and V. Wayal, "Tool condition monitoring system: a review," *Materials Today: Proceedings*, vol. 2, no. 4-5, pp. 3419–3428, 2015.

[42] D. E. D. Snr, "Sensor signals for tool-wear monitoring in metal cutting operations – a review of methods," *International Journal of Machine Tools and Manufacture*, vol. 40, no. 8, pp. 1073–1098, 2000.

[43] C. Scheffer and P. Heyns, "Wear monitoring in turning operations using vibration and strain measurements," *Mechanical systems and signal processing*, vol. 15, no. 6, pp. 1185–1202, 2001.

[44] M. Bonifacio and A. Diniz, "Correlating tool wear, tool life, surface roughness and tool vibration in finish turning with coated carbide tools," *Wear*, vol. 173, no. 1-2, pp. 137–144, 1994.

[45] W. Bartelmus and R. Zimroz, "Vibration condition monitoring of planetary gearbox under varying external load," *Mechanical systems and signal processing*, vol. 23, no. 1, pp. 246–257, 2009.

[46] G. Ibrahim and A. Albarbar, "Comparison between Wigner-Ville distribution and empirical mode decomposition vibration-based techniques for helical gearbox monitoring," *Proceedings of the Institution of Mechanical Engineers, Part C: Journal of Mechanical Engineering Science*, vol. 225, no. 8, pp. 1833–1846, 2011.

[47] W. J. Staszewski, K. Worden, and G. R. Tomlinson, "Time-frequency analysis in gearbox fault detection using the Wigner-Ville distribution and pattern recognition," *Mechanical systems and signal processing*, vol. 11, no. 5, pp. 673–692, 1997.

[48] B. Boashash, *Time-frequency signal analysis and processing: a comprehensive reference*. Academic Press, 2015.

[49] B. Boashash and P. Black, "An efficient real-time implementation of the Wigner-Ville distribution," *IEEE transactions on acoustics, speech, and signal processing*, vol. 35, no. 11, pp. 1611–1618, 1987.

[50] K. Sun, T. Jin, and D. Yang, "An improved time-frequency analysis method in interference detection for GNSS receivers," *Sensors*, vol. 15, no. 4, pp. 9404–9426, 2015.

[51] N. Baydar and A. Ball, "A comparative study of acoustic and vibration signals in detection of gear failures using Wigner-Ville distribution," *Mechanical systems and signal processing*, vol. 15, no. 6, pp. 1091–1107, 2001.

[52] S. Rajagopalan, J. A. Restrepo, J. M. Aller, T. Habetler, and R. Harley, "Wigner-Ville distributions for detection of rotor faults in brushless DC (BLDC) motors operating under non-stationary conditions," in *2005 5th IEEE International Symposium on Diagnostics for Electric Machines, Power Electronics and Drives*, pp. 1–7, IEEE, 2005.

[53] L. Cohen, "Time-frequency distributions - A review," *Proceedings of the IEEE*, vol. 77, no. 7, pp. 941–981, 1989.

[54] F. Auger and É. Chassande-Mottin, "Quadratic time-frequency analysis i: Cohen's class," *Time-Frequency Analysis: Concepts and Methods*, pp. 131–163, 2008.

[55] J. Ville, "Théorie et applications de la notion de signal analytique," *Câbles et Transmission*, vol. 2, pp. 61–74, 1948.

[56] J. Antoni, F. Bonnardot, A. Raad, and M. El Badaoui, "Cyclostationary modelling of rotating machine vibration signals," *Mechanical systems and signal processing*, vol. 18, no. 6, pp. 1285–1314, 2004.

[57] PCB Piezotronics, "https://www.pcb.com/," 2019.

[58] J. Antoni, J. Daniere, and F. Guillet, "Effective vibration analysis of ic engines using cyclostationarity. Part I-A methodology for condition monitoring," *Journal of sound and vibration*, vol. 257, no. 5, pp. 815–837, 2002.

[59] F. Vogel, S. Holm, and O. C. Lingjærde, "Spectral moments and time domain representation of photoacoustic signals used for detection of crude oil in produced water," in *Proc. Nordic Symp. on Physical Acoustics, Ustaoset, Norway*, 2001.

[60] B.-S. Yang, T. Han, and J. L. An, "Art–kohonen neural network for fault diagnosis of rotating machinery," *Mechanical Systems and Signal Processing*, vol. 18, no. 3, pp. 645–657, 2004.

[61] J.-D. Wu and C.-K. Huang, "An engine fault diagnosis system using intake manifold pressure signal and Wigner-Ville distribution technique," *Expert Systems with Applications*, vol. 38, no. 1, pp. 536–544, 2011.

[62] B. Jokanovic, M. G. Amin, and F. Ahmad, "Effect of data representations on deep learning in fall detection," in *2016 IEEE Sensor Array and Multichannel Signal Processing Workshop (SAM)*, pp. 1–5, IEEE, 2016.

[63] J. Mathew and R. Alfredson, "The condition monitoring of rolling element bearings using vibration analysis," *Journal of vibration, acoustics, stress, and reliability in design*, vol. 106, no. 3, pp. 447–453, 1984.

[64] P. McFadden and J. Smith, "Vibration monitoring of rolling element bearings by the high-frequency resonance technique - a review," *Tribology international*, vol. 17, no. 1, pp. 3–10, 1984.

[65] N. Tandon and A. Choudhury, "A review of vibration and acoustic measurement methods for the detection of defects in rolling element bearings," *Tribology international*, vol. 32, no. 8, pp. 469–480, 1999.

[66] T. A. Harris and M. N. Kotzalas, *Essential concepts of bearing technology*. CRC press, 2006.

[67] H. Toersen, "Application of an envelope technique in the detection of ball bearing defects in a laboratory experiment," *Tribotest*, vol. 4, no. 3, pp. 297–308, 1998.

[68] R. B. Randall, J. Antoni, and S. Chobsaard, "The relationship between spectral correlation and envelope analysis in the diagnostics of bearing faults and other cyclostationary machine signals," *Mechanical systems and signal processing*, vol. 15, no. 5, pp. 945–962, 2001.

[69] R. B. Randall and J. Antoni, "Rolling element bearing diagnostics - A tutorial," *Mechanical systems and signal processing*, vol. 25, no. 2, pp. 485–520, 2011.

[70] P. Borghesani, R. Ricci, S. Chatterton, and P. Pennacchi, "A new procedure for using envelope analysis for rolling element bearing diagnostics in variable operating conditions," *Mechanical Systems and Signal Processing*, vol. 38, no. 1, pp. 23–35, 2013.

[71] J. Antoni, "Cyclic spectral analysis of rolling-element bearing signals: facts and fictions," *Journal of Sound and vibration*, vol. 304, no. 3-5, pp. 497–529, 2007.

[72] Electro Tech Industries, "https://www.etind.com/," 2019.

[73] Cognex Corporation, "https://www.cognex.com/," 2019.

[74] Sick AG, "https://www.sick.com/," 2019.

[75] ISO, "Statistics. Vocabulary and symbols. Applied statistics," ISO ISO 3534-1, International Organization for Standardization, Geneva, Switzerland, 2006.